

**BIOCHAR EFFECTS ON MYCORRHIZAL SYMBIOSES, PLANT GROWTH, SOIL
PROPERTIES, AND CARBON STABILIZATION MECHANISMS**

By

Chase O'Neil

A THESIS

Submitted to
Michigan State University
in partial fulfillment of requirements
for the degree of

Crop and Soil Sciences – Master of Science

2021

ABSTRACT

BIOCHAR EFFECTS ON MYCORRHIZAL SYMBIOSES, PLANT GROWTH, SOIL PROPERTIES, AND CARBON STABILIZATION MECHANISMS

By

Chase O'Neil

Biochar is a porous charcoal-like material produced from pyrolyzing (or heating without oxygen) organic biomass. It is increasingly being researched for its potential to improve soil fertility and soil health, increase agricultural production, and sequester carbon (C) long-term in soils. However, biochar properties vary depending on feedstock and pyrolysis conditions (e.g., temperature, length of time, etc.) and its effects can also differ across soil habitats. My thesis research examines how biochar amendments can alter soils and the broader impact it may have on agroecosystems. In my first chapter, I sought to understand how different biochar types and nutrient additions could impact plant symbioses with arbuscular mycorrhizal fungi (AMF) through a six-month greenhouse experiment. My results indicated that biochars can mitigate low soil nitrogen (N) and phosphorus (P) levels for plant growth and that N from organic substrates was utilized by AMF more than P from organic substrates. These findings can inform agroecosystem weed management practices when amending soils with nutrients or biochar. In my second chapter, I examined how biochar type and application rates may impact soil C stabilization mechanisms in different soils for one-year and four-year aged samples. Overall, I found the wood-based biochar and the higher application rates to have the greatest effects, which were strongest in the coarsest soil type. Both biochars showed evidence that their recalcitrant structure influenced their stabilization, potentially more than other processes such as aggregation or organo-mineral associations, although this may change over time. Thus, I found biochar can be used to sequester C, improve soil health, and maintain sustainable agroecosystems.

ACKNOWLEDGEMENTS

This thesis was the product of many long days in the lab, nights at my computer, and impromptu pondering sessions; however, it was truly made possible by the people who have guided me along the way.

Firstly, thank you to my academic committee who have been diligent, patient, and informative. Dr. Hui Li provided much needed help on chemistry concepts as well as consistent advice on my search to understand biochar's connection to polyaromatic hydrocarbons. Dr. Lisa Tiemann was kind enough to allow ample usage of her expertise, lab space and helpful staff who introduced me to many of the protocols and techniques presented here. Thank you to Dr. Michelle Quigley who measured all my soil cores via Xray μ CT scanning in addition to generously giving her time to our Zoom meetings where I learned how to analyze this dataset. Thank you to my MS advisor, Dr. Jessica Miesel, who has shown flexibility and patience when I needed it and has challenged me to think creatively and analytically on all aspects of this experience. Her constructive feedback has improved both the content of this thesis and my ability as a researcher.

I also would like to thank the post-docs, graduate students, technicians, and undergraduates who have provided advice, helped with protocols, or lifted my spirits during this tumultuous time. Specifically, thank you to Midhun Gelder, Jaron Adkins, Faisal Sherif, Camryn Brent, Maxwell Oerther, Sarah Ruth, Mary "Cait" Llyod, Andrea Gatchell, Cheristy Jones, Brian Liang, Andrew Curtright, Jake Nash, Violeta Matus Acuna and Daniel Hoffman. Thank you also to my funding sources: MSU Plant Soil and Microbial Sciences department, Project GREEN, and Michigan Department of Agricultural Rural Development.

Finally, a giant thank you to my parents, Conn and Virginia, my wonderful sisters, Riley and Quinn, and my best friend Anna who have not only put up with my soil carbon talk but inspire me daily with their stories and go above and beyond to support me. Thank you to my partner Matthew, for your constant attention whether on statistical advice or how to dice a pepper, your amazing presence was unquantifiable, even if you used an integrated model.

TABLE OF CONTENTS

LIST OF TABLES	vii
LIST OF FIGURES	viii
CHAPTER 1: MYCORRHIZAL SYMBIOSES ENHANCE COMPETITIVE WEED GROWTH IN BIOCHAR AND NUTRIENT-AMENDED SOILS	1
1.1 ABSTRACT.....	1
1.2 INTRODUCTION	2
1.3 METHODS	4
1.3.1 Biochar.....	4
1.3.2 Experimental design and establishment period.....	4
1.3.3 Nutrient treatment period.....	6
1.3.4 Sample collection and processing.....	8
1.3.5 Laboratory analysis and calculations.....	8
1.3.6 Statistical approach	10
1.4 RESULTS	10
1.4.1 Plants.....	10
1.4.2 Mycorrhizae	14
1.4.3 Media nutrient availability.....	15
1.5 DISCUSSION	15
APPENDIX.....	19
REFERENCES	26
CHAPTER 2: BIOCHAR TYPE, APPLICATION RATE AND AGE ALTER CARBON STABILIZATION MECHANISMS IN THREE SOIL TYPES	33
2.1 ABSTRACT.....	33
2.2 INTRODUCTION	34
2.3 METHODS	38
2.3.1 Biochars	38
2.3.2 Soils.....	39
2.3.3 Mesocosm experiment	39
2.3.4 Field experiment	41
2.3.5 Sample collection.....	41
2.3.6 Lab processing and analysis.....	42
2.3.7 Statistical analysis.....	48
2.4 RESULTS	49
2.4.1 CO ₂ flux & N mineralization rates.....	49
2.4.2 Enzyme assays	51
2.4.3 DOC & TDN.....	56
2.4.4 pH.....	58
2.4.5 Root biomass.....	59
2.4.6 Water-stable aggregates	59
2.4.7 EDX	61

2.4.8 Soil porosity + POM	62
2.4.9 Total soil C & N.....	62
2.4.10 Soil fractions C	64
2.4.11 FTIR-DRIFT	66
2.5 DISCUSSION.....	67
2.5.1 Priming effect.....	68
2.5.2 Biochar sorption & leaching	70
2.5.3 N sorption & immobilization.....	71
2.5.4 Aggregation.....	73
2.5.5 Organo-mineral associations + biochar recalcitrance	75
2.6 CONCLUSIONS.....	77
APPENDIX.....	79
REFERENCES	89

LIST OF TABLES

Table S1.1 ANOVA results for all response variables.....	23
Table S1.2 Tukey post-hoc test results.....	24
Table 2.1 Means \pm (SE) of FTIR-DRIFT peak area ratios of aromatic to aliphatic C compounds for POM fractions	67
Table S2.1 FTIR-DRIFT spectral regions.....	88

LIST OF FIGURES

Figure 1.1 Diagram depicting the two experimental phases before harvest	7
Figure 1.2 Means (\pm SE) of plant biomass.....	12
Figure 1.3 Means (\pm SE) of plant tissue concentrations	14
Figure 1.4 Means (\pm SE) of AMF colonization and activity rates.....	15
Figure S1.1 Means (\pm SE) of media (A) nitrate (NO_3^-) (B) ammonium (NH_4^+)	20
Figure S1.2 Means (\pm SE) of media phosphate (PO_4^-)	21
Figure S1.3 Means (\pm SE) of plant tissue nutrient ratios	22
Figure 2.1 Means (\pm SE) of CO_2 flux rates.....	50
Figure 2.2 Means \pm (SE) of nitrification (A), ammonification (B), and mineralization rates (C)	51
Figure 2.3 Means \pm (SE) of potential enzyme activity rates related to C acquisition	53
Figure 2.4 Means \pm (SE) of potential enzyme activity rates related to C acquisition	54
Figure 2.5 Means \pm (SE) of potential enzyme activity rates related to N acquisition	55
Figure 2.6 Means \pm (SE) of potential enzyme activity rates related to N acquisition	56
Figure 2.7 Means \pm (SE) of dissolved organic carbon (DOC) (A, B) and total dissolved nitrogen (TDN) (C, D)	58
Figure 2.8 Means \pm (SE) of water stable aggregate proportions (%) for one-year samples compared across soil textures	60
Figure 2.9 Means \pm (SE) of water stable aggregate proportions (%) for one-year (1Y) versus four-year (4Y) samples for USB treatments in the sandy loam.....	61
Figure 2.10 Means \pm (SE) of calculated soil C (A) and N (C) when mesocosms were constructed and total C (B) and N concentrations (D) in mesocosm soils after one-year	63

Figure 2.11 Means of soil C concentrations, total and by soil fractions, across different soil textures in one-year samples (A) and one-year (1Y) versus four-year (4Y) field exposure of USB biochar in sandy loam soils (B) or C proportions (%) by soil fractions, across different soil textures in one-year samples (C) and one-year (1Y) versus four-years (4Y) field exposure of USB biochar in sandy loam soils (D).	65
Figure S2.1 Means \pm (SE) of nitrification (A), ammonification (B), and mineralization rates (C)	80
Figure S2.2 Means \pm (SE) of potential enzyme activity rates related to P acquisition.....	81
Figure S2.3 Means \pm (SE) of soil pH.....	82
Figure S2.4 Means \pm (SE) of root biomass	83
Figure S2.5 Means \pm (SE) of aggregate mean weight diameter (mm) (MWD).....	84
Figure S2.6 Means \pm (SE) of total C (%) (A) and total O (%) (B) on aggregate (> 2 mm) surfaces	85
Figure S2.7 Poly-aromatic hydrocarbons present in CMS, USB and two other biochars	86
Figure S2.8 Effect size (\pm SE) of application rate on soil porosity (A) and total soil POM (B) for intact four-year samples (preliminary data).....	87

CHAPTER 1:

MYCORRHIZAL SYMBIOSES ENHANCE COMPETITIVE WEED GROWTH IN BIOCHAR AND NUTRIENT-AMENDED SOILS¹

1.1 ABSTRACT

Velvetleaf (*Abutilon theophrasti*) is a highly competitive weed in agroecosystems that is well-studied for its efficient nitrogen (N) acquisition, yet research on its phosphorus (P) uptake is lacking. One pathway may be through symbioses with arbuscular mycorrhizal fungi (AMF) which increase nutrient acquisition. These AMF benefits can be further enhanced by soil amendment with biochar, although effects may vary with different biochar production characteristics. We implemented a fully factorial nutrient and biochar addition experiment in a greenhouse for six months to determine how AMF nutrient uptake impacts plant growth and how these effects vary between two biochar types. We measured total above- and belowground biomass, plant tissue concentration (N and P), AMF colonization and activity rates, and soil media N and P availability. Overall, we observed few statistically significant results, however AMF N uptake may have been more beneficial to velvetleaf than AMF P uptake as evidenced by increased biomass and tissue N concentrations in treatments where N was only accessible by AMF. Additionally, by maintaining root to shoot ratios biochar may have provided plants with N and P (through sorption of nutrients to surfaces or its inherent properties) when nutrients were more difficult to access. We also found variable plant responses across the two biochar types used. Understanding how nutrient and biochar additions can influence weed competition is

¹ Originally published as: O'Neil, C. M., Nash, J., Tiemann, L. K., and Miesel, J. R. (2021). Mycorrhizal Symbioses Enhance Competitive Weed Growth in Biochar and Nutrient-Amended Soils. *Front. Agron.* 3. doi:10.3389/fagro.2021.731184.

important for anticipating potential undesirable consequences of novel soil amendments such as biochar.

1.2 INTRODUCTION

Velvetleaf (*Abutilon theophrasti*) is a financially devastating weed in the upper Midwest and Eastern United States (Spencer, 1984). While velvetleaf primarily reduces crop yield by shading out other plants (Akey, 1989; Lindquist and Mortensen, 1999), aboveground biomass increases may be due to successful competition for nutrients belowground (Bonifas et al., 2005; Barker et al., 2006; Vitousek et al., 2010). For example, velvetleaf has a higher nitrogen (N) uptake efficiency than corn (Bonifas and Lindquist, 2006) likely because it can maintain its total root system length with less root biomass (Bonifas and Lindquist, 2009). Although belowground competition for N is well-documented between velvetleaf and crops (Bonifas et al., 2005; Barker et al., 2006; Lindquist et al., 2007; Bonifas and Lindquist, 2009), competition for phosphorus (P) acquisition is less studied. One potentially advantageous way to compete for P may be through symbioses with arbuscular mycorrhizal fungi (AMF) (Smith and Read, 2008).

Arbuscular mycorrhizal fungi (AMF) colonize plant root systems and increase nutrient uptake through hyphal networks that grow outside the root depletion zone (Sanders and Tinker, 1971; Smith and Read, 2008). Velvetleaf is a “strong” AMF host with higher colonization rates compared to other agronomic weed species (Vatovec et al., 2005); both biomass and nutrient shoot tissue concentrations increase when colonized by AMF in the field (Stanley et al., 1993). Therefore, AMF symbioses could enhance velvetleaf P uptake and help the weed outcompete weak (< 10% colonized) or non-mycorrhizal (e.g., sugar beets, cabbage, or kale) crops (Ocampo et al., 1980; Li et al., 2016). Furthermore, symbioses may also allow mycorrhizae to access P from plant-inaccessible sources, such as organic or insoluble nutrients (Jayachandran, K;

Schwab, A.P.; Hetrick, 1992; Tarafdar and Marschner, 1994; Feng et al., 2003). Research has traditionally focused on P uptake because its slow recycling and low solubility in soil reduces plant uptake (Sanders and Tinker, 1971; Mosse, 1973; Holford, 1997). However, recent work has showcased the importance of AMF N transport and its potential benefits for plant growth (Hodge and Fitter, 2010; Smith and Smith, 2011; Hodge and Storer, 2014). Therefore, additional research examining how AMF-colonized velvetleaf respond to both N and P sources is needed. Such information is vital to understanding velvetleaf competitive abilities, especially for agroecosystems that apply N and P amendments to soils.

AMF benefits may be further amplified by biochar, a soil amendment that is increasingly being applied in agroecosystems. Produced from pyrolyzed biomass (Lehmann and Joseph, 2009), biochar is proposed for augmenting soil health (Glaser et al., 2001) and sequestering carbon (Smith, 2016; Du et al., 2017), but has also been found to increase AMF colonization (Warnock et al., 2007; Lehmann et al., 2011) and crop yield (Jeffery et al., 2011). Unfortunately, because biochar generally promotes plant growth (Biederman and Harpole, 2013) it may also increase weed biomass (Major et al., 2005; Nash et al., 2021). Thus, strong AMF weed hosts such as velvetleaf may become more competitive when colonized in biochar-amended soils. However, these effects can also vary greatly among biochar production methods, biomass feedstock types, and different soil conditions (Keiluweit et al., 2010; Jeffery et al., 2011; Cantrell et al., 2012; Clark et al., 2019). Therefore, while some studies suggest biochar can enhance AMF effects (Warnock et al., 2007; Gujre et al., 2021), there is a lack of information quantifying how different biochar types impact weed growth and potential for increased weed-crop competition.

We conducted a six-month greenhouse study to assess how nutrient additions and biochar affect weed competitive abilities, using velvetleaf as a model weed species. We tested

three hypotheses: (1) P uptake by AMF will increase weed growth and nutrient tissue concentrations more than N uptake; (2) biochar will enhance AMF colonization and therefore nutrient acquisition and plant growth; and (3) biochar's effects on plant growth will vary across nutrient treatments (interactive effects). Understanding how nutrient and biochar additions may enhance weed-crop competition will ultimately inform biochar application practices and help ensure agricultural producers avoid undesirable consequences of these novel soil amendments, especially in areas with strong AMF weed species.

1.3 METHODS

1.3.1 Biochar

We used two pyrolysis biochars (hereafter: BGR, USB) to assess differences between biochar types. The BGR biochar was produced from forest harvesting residues (*Pinus resinosa* and *P. banksiana*) from the Upper Peninsula of Michigan, USA, and pyrolyzed in a rotary reactor system at 650°C for 30 minutes. The USB biochar was produced from waste wood pallets (southern yellow pine species), pyrolyzed in a continuous carbonizer at 550°C for 18 minutes. To eliminate mineral ash effects from fresh biochar, we soaked biochars with 0.1 M HCl for 72 hours and thoroughly rinsed with water. After this weathering treatment, biochar pH was 7.26 ± 0.15 and 7.14 ± 0.01 , and density was 0.19 g/cm^3 and 0.30 g/cm^3 for BGR and USB, respectively.

1.3.2 Experimental design and establishment period

We implemented a factorial mesocosm experiment in a greenhouse, using three biochar treatments (BGR, USB and No Biochar control) and four nutrient addition treatments, with five replicates per treatment (60 total mesocosms). We created biochar treatments by mixing each type of biochar with a commercially washed and screened sand (3% silt) at 12% volume, which

equates to a field application rate of biochar at 50 Mg ha⁻¹. We chose this high rate to help determine upper thresholds where carbon sequestration is maximized, and plant health is maintained. Biochar and sand mixtures were combined in a cement mixer to ensure even mixing and then steam-sterilized overnight.

We created mesocosms using 12.7 cm × 12.7 cm × 30.5 cm square pots that we divided into three compartments: two side “plant” compartments and a center “nutrient” compartment. The compartments were separated with plastic sheeting, into which we established a 10 cm × 10 cm window comprised of 50 μm nylon mesh (Elko Filtering Company) secured with silicon caulk. The mesh window allowed fungal hyphae to pass through but excluded plant roots. We filled each mesocosm compartment with the appropriate biochar + sand treatment (all compartments within a given pot received the same biochar + sand treatment). We then placed AMF whole inoculum (1.2 g per mesocosm, International Culture Collection of Vesicular Arbuscular Mycorrhizal Fungi, West Virginia University) in 7.5 cm deep holes in each plant compartment and filled the holes leaving a shallow indentation (~0.75 cm deep) for seeds. The whole inoculum included roots, spores, hyphae, and growth medium of AMF species *Gigaspora rosea* (120-150 spores per g), *Rhizophagus clarus* (220-250 spores per g), and *R. irregularis* (250-300 spores per g). Velvetleaf seeds (collected from MSU’s Agriculture Research Farm, 42°42’38.2”N, 84°28’16.6”W) were planted on May 3rd in each shallow hole on top of the inoculum to ensure contact with seedling roots and covered with media. We planted additional seeds in compartments that had not germinated on May 10th and May 16th, with all germination occurring by May 20th. Then, we thinned seedlings to two plants per mesocosm, one in each plant compartment. Germination did not occur in some plant compartments (~11%), so we transplanted the extra seedlings from other mesocosms within the same biochar treatment.

Mesocosm treatments were placed randomly on the greenhouse table and maintained under supplemental lighting (16 h:8 h L:D) at ~20°C, with daily watering through an automated sprinkler system. To ensure all plants had access to basic nutrient supply needed to establish initial growth, we fertilized mesocosms with 200 ml of 0.5X Hoagland solution (Hoagland and Arnon, 1950) twice a week from May 3, 2019 to July 23, 2019 (12 weeks). Because carbonates in the sand led to a media pH ~ 9, we acidified the Hoagland solution to pH 5.5 with HCl to create conditions more favorable to plant growth.

1.3.3 Nutrient treatment period

On July 23, 2019 we stopped regular Hoagland applications and initiated four nutrient addition treatments to test how N and P uptake by mycorrhizae influences velvetleaf competitiveness. Each nutrient treatment combined (a) a weekly application (100 mL) of a modified Hoagland's solution with soluble N and/or P, accessible to both AMF hyphae and plants, and (b) an insoluble, organic N and/or P substrate tube added to each mesocosm's central compartment, accessible to AMF hyphae but not plant roots. This was designed to ensure that plants could only utilize the organic substrates if AMF proliferated through the mesh windows into the central compartment, where they could then solubilize the organic nutrient sources (e.g., excreting extra-cellular enzymes or stimulating other microbes to do so) and then transport the resulting inorganic ions to the plant (Frey, 2019). By limiting nutrient acquisition to AMF only, we can better quantify symbiosis impact on plants. Treatments were: (1) Soluble NP (Sol NP),

(2) Insoluble N and Soluble P (Insol N + Sol P), (3) Insoluble P and Soluble N (Insol P + Sol N), and (4) Insoluble NP (Insol NP) (**Figure 1.1**).

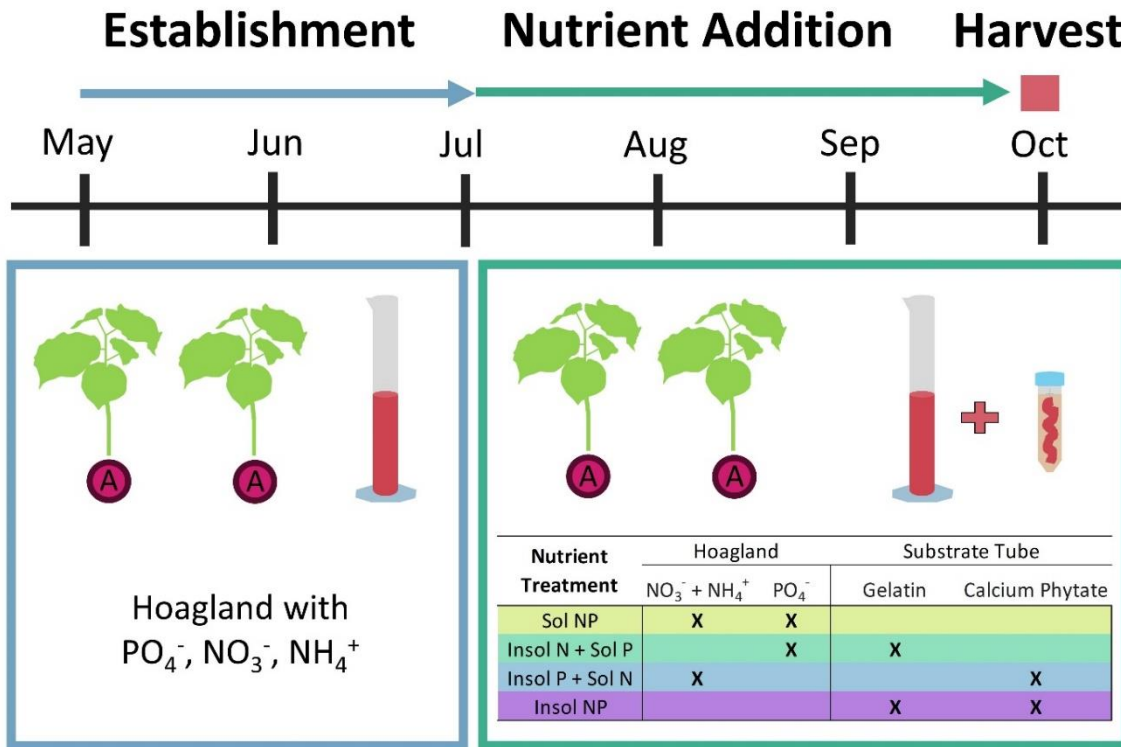


Figure 1.1 Diagram depicting the two experimental phases before harvest. Each mesocosm is represented by two AMF-colonized velvetleaf plants. During the establishment period, we applied Hoagland’s solution (which contained both soluble N and P sources) to encourage plant establishment: adjusting to mesocosm and greenhouse conditions and forming relationships with mycorrhizal populations. In the nutrient addition period, we applied different combinations of modified Hoagland solutions (see table) and substrate tubes with insoluble N and/or P sources to better quantify mycorrhizal nutrient uptake benefits.

To create the organic substrate tubes, we constructed 50 μm fine nylon mesh windows (Elko Filtering Company) on 50 mL centrifuge tubes (polypropylene, Fisher Scientific). We then used a blender to homogenize organic N (gelatin, 3 g per tube, 0.06 g/ml) and/or P (calcium phytate, 0.3 g per tube, 0.006 g/ml) with biochar + sand media and filled the tubes with these mixtures. Organic substrate concentrations were calculated to equal the total amount of soluble N or P applied via modified Hoagland solutions over the course of the experiment. We deployed

the substrate tubes (top of tube flush with soil surface) in the center mesocosm compartment. We modified Hoagland solutions by excluding soluble N and/or P, depending on treatment.

1.3.4 Sample collection and processing

After 11 weeks of nutrient treatments, we harvested the plants and separated shoots from roots at the root collar. We collected media samples from each mesocosm by shaking the residual biochar + sand media from the roots of both mesocosm plants into 50 mL tubes. We then clipped five 1.0 cm samples of fine roots from each of the two plants in the mesocosm and stored at 4°C. Plant samples were rinsed with water, dried at 60°C for 48 hours and weighed before grinding (Wiley mill, 1.0 mm mesh screen).

1.3.5 Laboratory analysis and calculations

Ground plant samples were analyzed for total P concentration by ashing samples at 500°C for 5 hours and then digesting with 3N nitric acid. Samples were then diluted (1:9 with 0.3N sodium hydroxide) before analysis via the ascorbic acid method (John, 1970). We pulverized ground plant tissues using a roller-mill and determined total C and N concentrations (Costech ECS 4010 CN analyzer, Valencia, CA USA). We calculated above- and belowground biomass values by weighing both mesocosm plants and dividing by two to get average biomass per mesocosm. We then added above- and belowground biomass values to get total net primary production (NPP).

We measured AMF colonization of plant roots to interpret AMF benefits on nutrient uptake and plant response (Treseder, 2013). Although colonization rates can vary across AMF species (Treseder, 2013), our plants were inoculated with the same three species. We rehydrated roots (from 4°C storage) 24 hours before staining and colonization counting procedures (Phillips and Hayman, 1970; McGonigle et al., 1990). Root tissues were cleared with 10% KOH, stained

with 0.05% Trypan Blue, de-stained with 5% acetic acid, and mounted on microscope slides. Each slide contained five 1.0 cm roots from each mesocosm. We examined slides under a compound microscope at 400x magnification, with 20 fields-of-view per root. For each field-of-view, we scored presence or absence of mycorrhizal hyphae, vesicles, and/or arbuscules as colonized or not colonized, respectively. We calculated colonization percentage as the total number of colonized views divided by total field-of-views multiplied by 100. We did not differentiate between AMF species and assumed that steam sterilization removed most all other mycorrhizae in the sand-biochar mixtures besides those in our inoculum (Brito et al., 2009).

We also measured extraradical hyphal length density (ERH) in organic substrate tubes as a proxy for AMF activity (Jakobsen et al., 1992; Staddon et al., 1999). We rinsed each organic substrate tube contents with H₂O and decanted through a sieve stack (top: 500 μm, bottom: 212 μm). We then stained residues on the 212 μm sieve with 0.05% Trypan blue stain (lactoglycerol) and incubated for 30 minutes. The stained residue was rinsed and mixed with 200 ml of H₂O, and 20 mL was collected and vacuum-filtered (0.45 μm nylon filter). Two filters for each mesocosm were mounted on microscope slides and scored with 25 random fields-of-view at 10x objective magnification, 100x total magnification. For each field-of-view, we counted the number of times an AMF hypha crossed any gridline present in the reticle (1 cm per side, 10 × 10). We then used the average hyphal intersection counts per filter to calculate average hyphal densities (calculations in Appendix).

We extracted inorganic N in media from each mesocosm using 25 mL of 0.5 M K₂SO₄ and 5 g media, and measured nitrate (NO₃⁻) via an enzyme reduction method (Patton and Kryskalla, 2011) and a microplate protocol for ammonium (NH₄⁺) (Sinsabaugh et al., 2000) (Biotek synergy H1, Winooski, VT, USA). We extracted phosphate (PO₄⁻) using 40 mL of 0.5 M

NaHCO₃ and 8 g of media, and analyzed concentrations using the molybdenum blue-ascorbic acid protocol (John, 1970) adapted for a microplate assay (Song et al., 2019). We oven-dried media subsamples at 105°C for 48 hours to calculate gravimetric soil moisture and reported nutrient concentrations as a dry mass basis ($\mu\text{g g}^{-1}$). We measured media pH as 1:2 w:v in H₂O.

1.3.6 Statistical approach

For all response variables, we performed general linear models with interactions (multiple two-way analysis of variance) with biochar type and nutrient treatment as explanatory variables. Because of the unbalanced design (due to plant mortality, etc.), we used type III sum of squares. Statistical significance was determined when $p < 0.05$. We performed pairwise comparisons using Tukey's tests, adjusted for multiple comparisons. For AMF colonization comparisons, we used a beta-distributed (response bounded by 0,1) mixed-effects linear model with a random effect of mesocosm ID to account for variation between the root replicates collected per mesocosm. For ERH comparisons, we used a normally-distributed mixed-effects linear model with a random effect of mesocosm ID to account for the variation between the two filters processed per mesocosm. We checked model assumptions visually by plotting residuals and predicted values and log-transformed any response variables that did not conform to normality assumptions. All analyses were performed using R statistical software version 3.5.3.

1.4 RESULTS

1.4.1 Plants

Belowground biomass was significantly affected by nutrient treatment (ANOVA, $p = 1.07 \times 10^{-4}$). For treatments without biochar, belowground biomass in Insol NP treatments was 63% higher than Sol NP treatments ($p = 4.48 \times 10^{-3}$), 29% higher than Insol N + Sol P treatments ($p \geq 0.05$), and 69% higher than Insol P + Sol N treatments ($p = 2.35 \times 10^{-3}$) (**Figure 1.2B**).

However, this relationship was not significant across biochar treatments (all $p \geq 0.05$).

Additionally, there were no significant effects of nutrient treatment, biochar, or the nutrient \times biochar interaction on aboveground biomass or total NPP (**Figure 1.2A, 1.2C**).

Nutrient treatment also significantly affected root:shoot biomass ratio (ANOVA, $p = 7.85 \times 10^{-7}$) with similar trends to belowground biomass. For example, without biochar, root:shoot ratios were the highest in Insol NP treatments (**Figure 1.2D**). Root:shoot ratios in Insol NP treatments were 60% larger than ratios in Sol NP ($p = 1.43 \times 10^{-4}$), 38% larger than ratios in Insol N + Sol P ($p = 0.04$), and 61% larger than ratios in Insol P + Sol N ($p = 1.24 \times 10^{-4}$). Additionally, compared to No Biochar treatments, BGR and USB decreased the root:shoot ratio in Insol NP treatments by 42% and 27% respectively ($p = 1.66 \times 10^{-3}$, 0.05), but had no significant effects in other nutrient treatments (all $p \geq 0.05$).

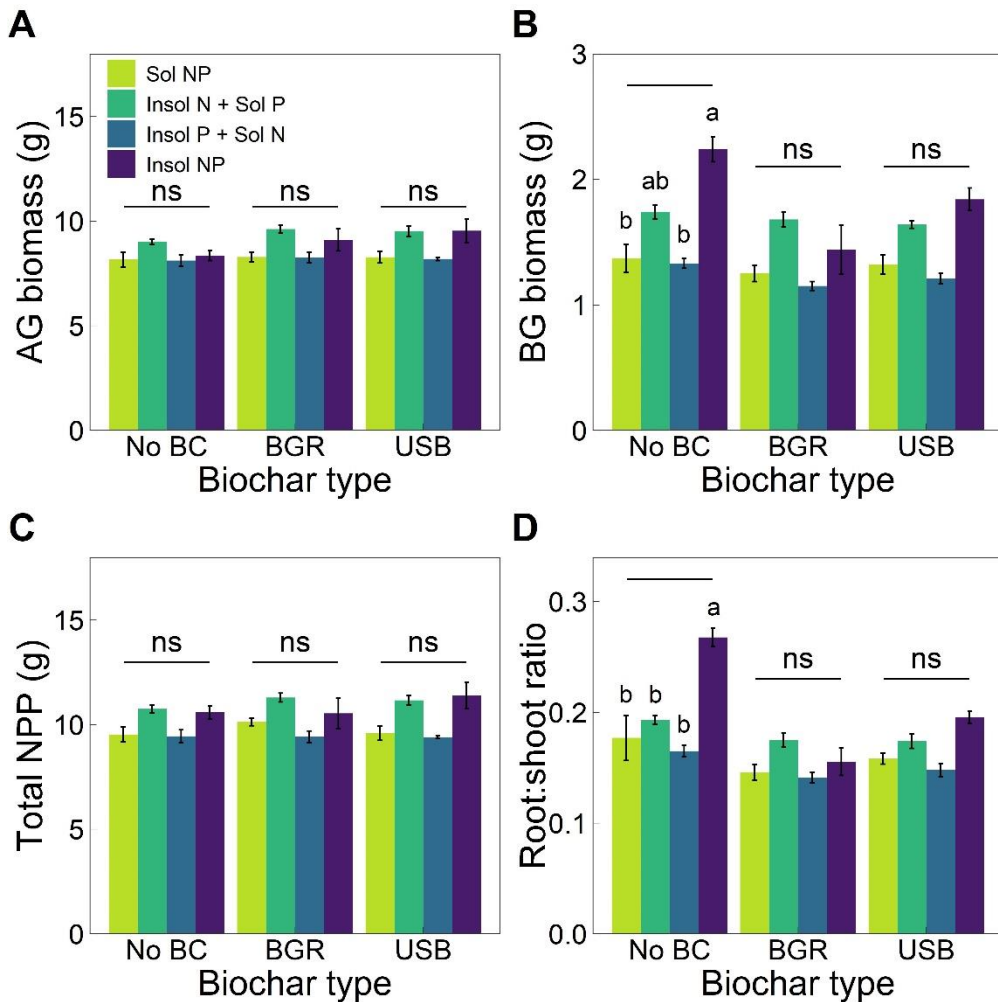


Figure 1.2 Means (\pm SE) of plant biomass (A) aboveground (AG) and (B) belowground (BG) biomass, (C) total NPP (AG + BG biomass) and (D) root:shoot ratios for biochar (x-axis) and nutrient treatments (varied colors). Lowercase letters indicate significant differences (Tukey post-hoc tests, $p < 0.05$) among nutrient treatments within biochar type and “ns” indicates no significant differences. Significant differences among biochar types within nutrient treatments are displayed in Table 1.S2. The x-axis label “No BC” stands for No Biochar treatments.

Nutrient treatment significantly affected aboveground plant tissue N (ANOVA, $p = 0.04$); however, post-hoc testing did not reveal statistically significant differences between treatments (all $p \geq 0.05$). Nutrient treatments had significant effects on belowground plant tissue N (ANOVA, $p = 1.22 \times 10^{-3}$) that were similar to aboveground N tissue, but did not vary across biochar treatments (interaction, $p \geq 0.05$). Therefore, regardless of biochar treatment, tissue N concentrations were the highest in Insol N + Sol P treatments compared to all other nutrient

treatments in both above- and belowground tissue (**Figure 1.3A, 1.3C**); although, this relationship was only significant for BGR treatments in belowground tissue. In BGR, belowground N tissue in Insol N + Sol P treatments was 37% higher than Sol NP ($p = 0.07$) and 52% higher than both Insol P + Sol N ($p = 1.99 \times 10^{-3}$) and Insol NP treatments ($p = 0.05$).

Biochar, nutrient, and biochar \times nutrient interaction (ANOVA, $p = 4.21 \times 10^{-8}$, 6.7×10^{-4} , 9.26×10^{-7}) all significantly affected belowground tissue P concentrations. Overall, BGR biochar decreased belowground tissue P compared to No Biochar treatments (**Figure 1.3D**). For example, BGR significantly decreased belowground plant tissue P by 38% for both Sol NP treatments ($p = 9.71 \times 10^{-6}$) and Insol NP ($p = 6.6 \times 10^{-4}$). Additionally, plant tissue P was 31% lower in BGR compared to USB Sol NP treatments ($p = 5.85 \times 10^{-3}$). For USB, belowground plant tissue P was 33% lower in Insol P + Sol N treatments when compared to No Biochar ($p = 1.51 \times 10^{-3}$), although USB Sol NP treatments did not significantly differ from No Biochar Sol NP treatments (11% difference, $p \geq 0.05$). Nutrient treatments had different effects on belowground tissue P within biochar types (**Figure 1.3D**). Within BGR, belowground plant tissue P was 53% higher in Insol N + Sol P compared to Sol NP treatments ($p = 3.43 \times 10^{-4}$), however this relationship was reversed in No Biochar treatments ($p \geq 0.05$). In USB biochar, plant tissue P was generally lower in Insol P + Sol N treatments with 32% less than Sol NP ($p = 2.41 \times 10^{-3}$) and 37% less than Insol NP ($p = 6.86 \times 10^{-5}$). Aboveground tissue P concentrations were significantly affected by biochar \times nutrient interaction (ANOVA, $p = 0.03$), however post-hoc tests did not reveal differences between treatments (all $p \geq 0.05$, **Figure 1.3B**).

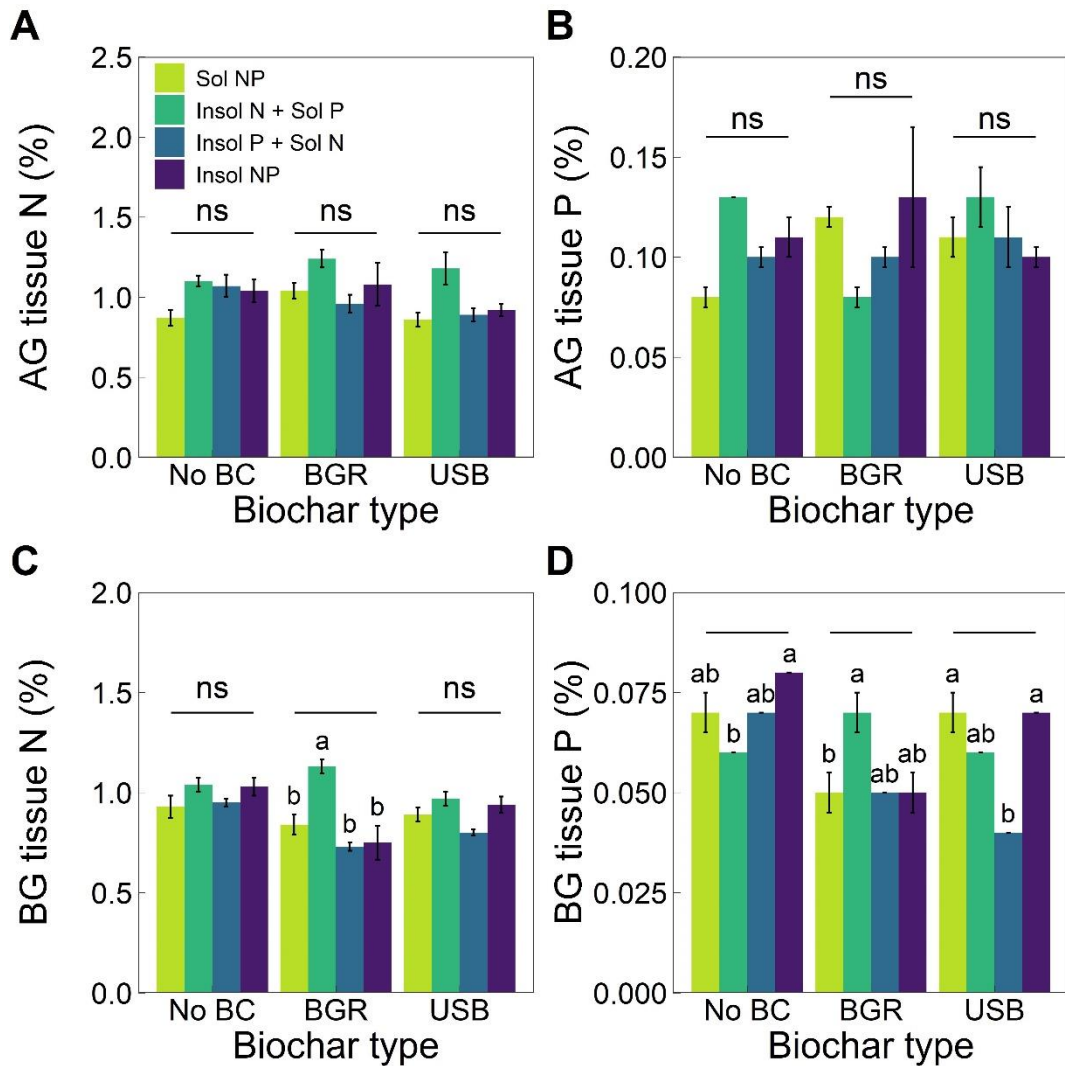


Figure 1.3 Means (\pm SE) of plant tissue concentrations (A) aboveground (AG) total plant tissue N, (B) AG total plant tissue P, (C) belowground (BG) total plant tissue N and (D) BG total plant tissue P for biochar (x-axis) and nutrient treatments (varied colors). Lowercase letters indicate significant differences (Tukey post-hoc tests, $p < 0.05$) among nutrient treatments within biochar type and “ns” indicates no significant differences. Significant differences among biochar types within nutrient treatments are displayed in Table 1.S2. The x-axis label “No BC” stands for No Biochar treatments.

1.4.2 Mycorrhizae

Nutrient treatment significantly affected AMF root colonization (ANOVA, $p = 7.31 \times 10^{-5}$) with rates generally highest in Insol NP or Insol N + Sol P treatments and lowest in Insol P + Sol N treatments (Figure 1.4A). In No Biochar treatments, root colonization was on average

161% higher in Insol NP treatments than Insol P + Sol N ($p = 1.51 \times 10^{-3}$). There were no significant effects of any treatment on AMF ERH (**Figure 1.4B**).

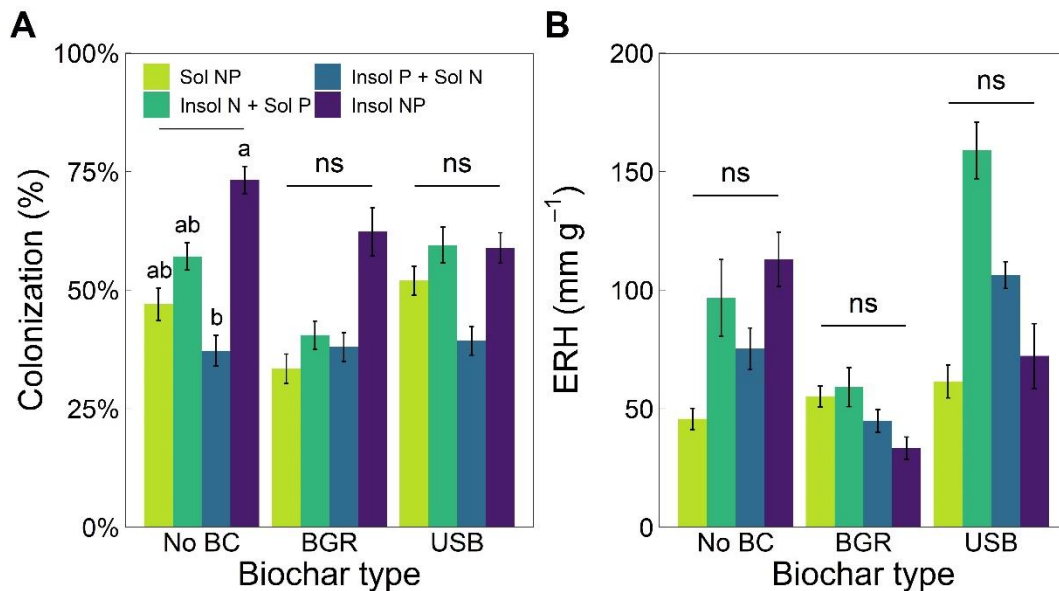


Figure 1.4 Means (\pm SE) AMF colonization and activity rates (A) AMF colonization and (B) extraradical hyphal length density (ERH) for biochar (x-axis) and nutrient treatments (varied colors). Lowercase letters indicate significant differences (Tukey post-hoc tests, $p < 0.05$) among nutrient treatments within biochar type and “ns” indicates no significant differences. Significant differences among biochar types within nutrient treatments are displayed in Table 1.S2. The x-axis label “No BC” stands for No Biochar treatments.

1.4.3 Media nutrient availability

Inorganic N and P media concentrations were low (NO_3^- and $\text{NH}_4^+ < 4 \mu\text{g g}^{-1}$; $\text{PO}_4^- < 1 \mu\text{g g}^{-1}$) but were generally higher in treatments with soluble N and soluble P, for NO_3^- and PO_4^- respectively (**Figure S1.1, S1.2**). Despite this, none of our treatments significantly affected media NO_3^- , NH_4^+ , total inorganic N ($\text{NO}_3^- + \text{NH}_4^+$) nor PO_4^- (**Table S1.1**).

1.5 DISCUSSION

After a six-month greenhouse experiment, AMF-colonized velvetleaf grew and accumulated nutrients the most when AMF accessed insoluble N, contrary to our original hypothesis on P uptake. Biochar altered and potentially improved weed root biomass growth,

however, many biochar effects were neutral or non-significant, including impact on AMF colonization or activity rates. We also found some evidence for interactive effects between biochar and nutrient treatments (e.g., plant tissue P), and our two similarly produced biochars caused variable plant responses.

Our results suggest that nutrient type and form may influence velvetleaf performance. Specifically, velvetleaf may have benefited more from AMF access to insoluble N versus P sources. Plants in treatments with insoluble N substrate consistently (although not significantly) had higher NPP and above- and belowground N tissue concentrations compared to treatments with insoluble P and soluble N or soluble N and P. This also suggests that plants grew more and accumulated more N from AMF uptake of insoluble N rather than plant and AMF uptake of soluble N. Instead, soluble N may have leached from our sandy media before plants/AMF could acquire it and thus AMF N uptake from insoluble N was a more efficient pathway (Sexton et al., 1998). Other studies have also found AMF to utilize organic N sources (Hodge et al., 2001; Atul-Nayyar et al., 2009; Whiteside et al., 2012), with one reporting that organic patch N was responsible for 31% of fungal N and 3% of plant N (Hodge and Fitter, 2010) while another found one third of the patch's N to be transported to the plant by AMF (Leigh et al., 2009). Furthermore, AMF N uptake may be more valuable than P because some weeds respond more to high N availability (Blackshaw and Brandt, 2008), including velvetleaf which typically outcompetes corn in high N soils (Barker et al., 2006). AMF symbioses could therefore amplify velvetleaf competitiveness by increasing N acquisition from harder to access (or insoluble) nutrient sources. This also suggests that agricultural practices which apply these nutrients (e.g., slow-release organic N fertilizers, manure or crop residues) to promote soil fertility (Diacono and Montemurro, 2010) could actually promote AMF-colonized velvetleaf populations.

Low N availability may have increased insoluble N benefits, but also may have caused the neutral and non-significant biochar effects (**Table S1.2**). Decreases in soil N availability, often caused by biochar (Gao et al., 2019), could potentially trigger neutral or negative responses for plants sensitive to N limitation (Gale et al., 2017; Liao and Thomas, 2019). Though our biochars did not significantly affect nutrient media availability (**Figure S1.1, S1.2**), our media appeared nutrient-limited (e.g., pH ~ 9, low $\text{NO}_3^- + \text{NH}_4^+$), especially for N (**Figure S1.3**, low N:P ratios). Thus, under N-limited conditions, velvetleaf may have responded minimally to biochar. Neutral biochar effects could also be because our experiment was too short to observe biochar's more long-term beneficial effects (Liu et al., 2013; Lone et al., 2015). A longer-term experiment could reveal clearer differences between biochar types, as our variable plant and mycorrhizae responses make it difficult for managers to make informed decisions on what biochar to apply.

Both biochars did appear to alter weed biomass allocation strategies. In the No Biochar control, root:shoot ratios increased in Insol NP treatments when compared to Sol NP treatments, suggesting that velvetleaf increased root biomass when nutrients were harder to access. However, this relationship did not exist in biochar treatments. Biochar did not suppress plant growth, as aboveground biomass and NPP were unaffected, but may instead have acted as a nutrient source, either through its inherent properties (Yamato et al., 2006) or by retaining available nutrients through sorption (Schofield et al., 2019). Wood-based biochars typically release less N and P compared to other biochar feedstocks (e.g., poultry manure) (Piash et al., 2021), however they have been found to absorb available N (Fidel et al., 2018) and P (Zhang et al., 2016; Gao and DeLuca, 2018). Additionally, biochar pore sizes may prevent plant root access, however AMF hyphae are smaller than plant roots and can harvest P from biochar

surfaces (Hammer et al., 2014). Thus, our biochars seemed to enhance weed growth belowground and could increase competition with crops in agroecosystems.

In conclusion, although our results did not support our original hypotheses, they suggest that insoluble N decomposition may play a more vital role than P decomposition in AMF-velvetleaf symbioses. Biochar may impact nutrient dynamics and consequent biomass allocation strategies for AMF-colonized plants. Biochar type also caused variable results, despite similar starting feedstocks. Thus, we found biochar and nutrient additions can enhance velvetleaf's competitive abilities in agroecosystems, although additional competition experiments in greenhouses and the field should be conducted. Further research should examine mechanisms of N and P access by AMF (Wang et al., 2017), especially insoluble sources, as well as how these processes interact with biochar. Such results can help guide agricultural management decisions that must consider velvetleaf (or other strong AMF weed hosts) when amending soils with nutrients and/or novel amendments such as biochar.

APPENDIX

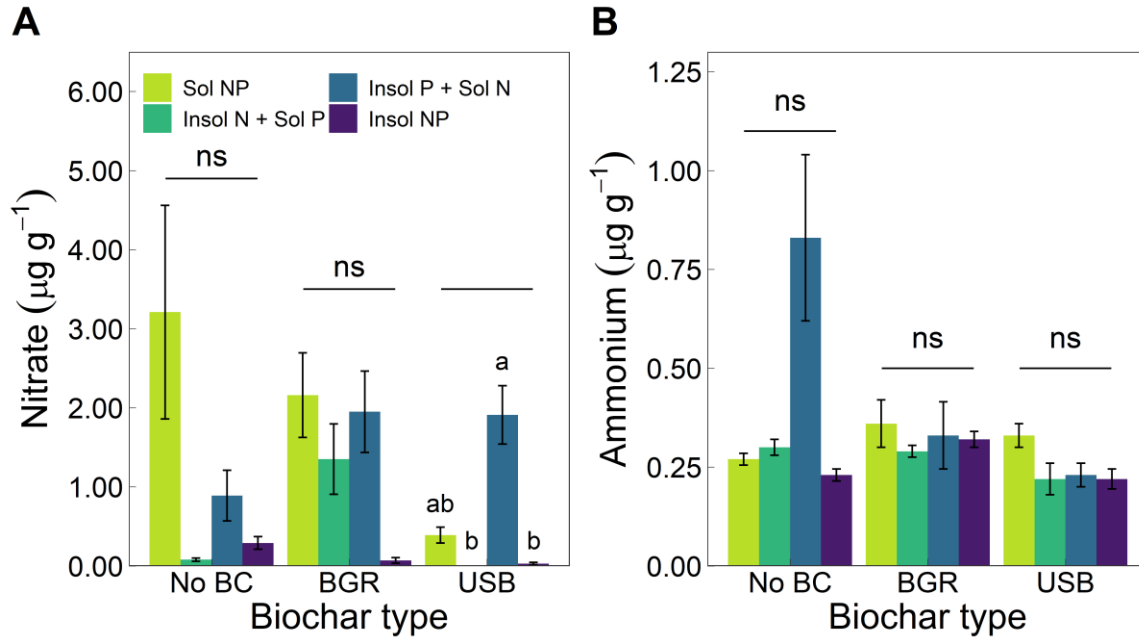


Figure S1.1 Means (\pm SE) of media (A) nitrate (NO_3^-) (B) ammonium (NH_4^+) for biochar (x-axis) and nutrient treatments (varied colors). Lowercase letters indicate significant differences (Tukey post-hoc tests, $p < 0.05$) among nutrient treatments within biochar type and “ns” indicates no significant differences. Significant differences among biochar types within nutrient treatments are displayed in Table S2. The x-axis label “No BC” stands for No Biochar treatments.

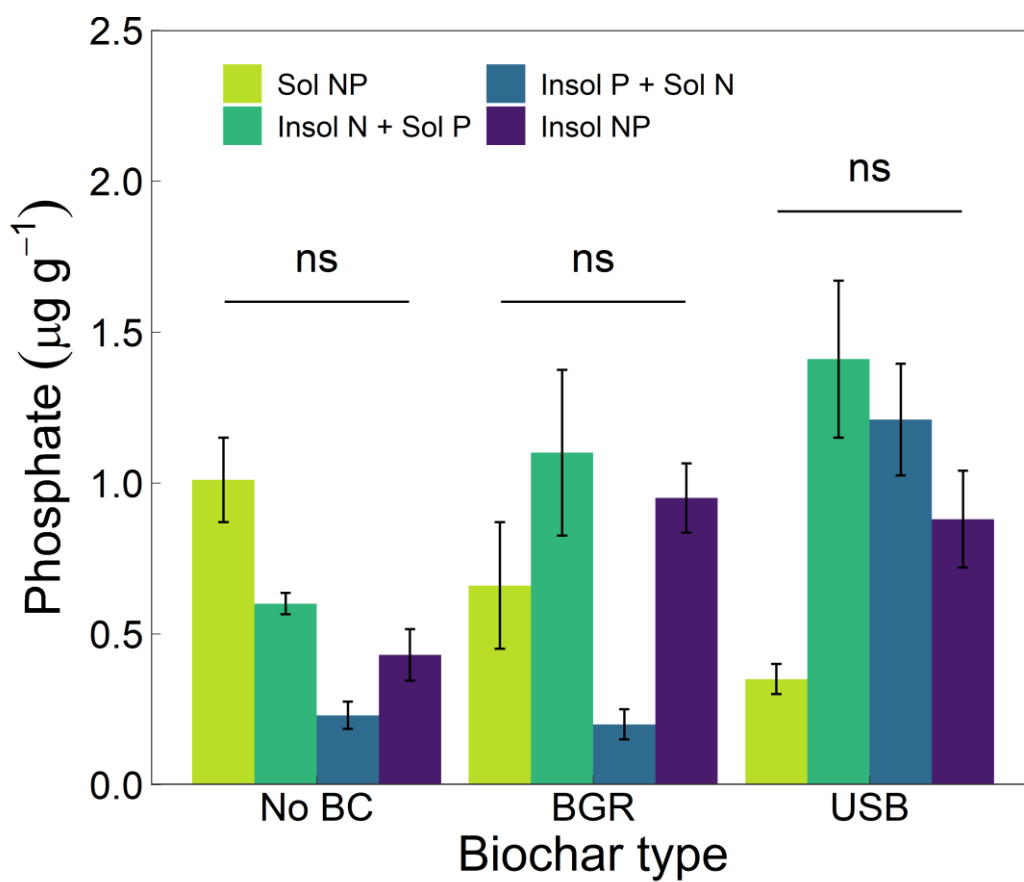


Figure S1.2 Means (\pm SE) of media phosphate (PO_4^-) for biochar (x-axis) and nutrient treatments (varied colors). There were no significant differences (Tukey post-hoc tests, $p < 0.05$) among nutrient treatments within biochar type, indicated by “ns”. Significant differences among biochar types within nutrient treatments are displayed in Table S2. The x-axis label “No BC” stands for No Biochar treatments.

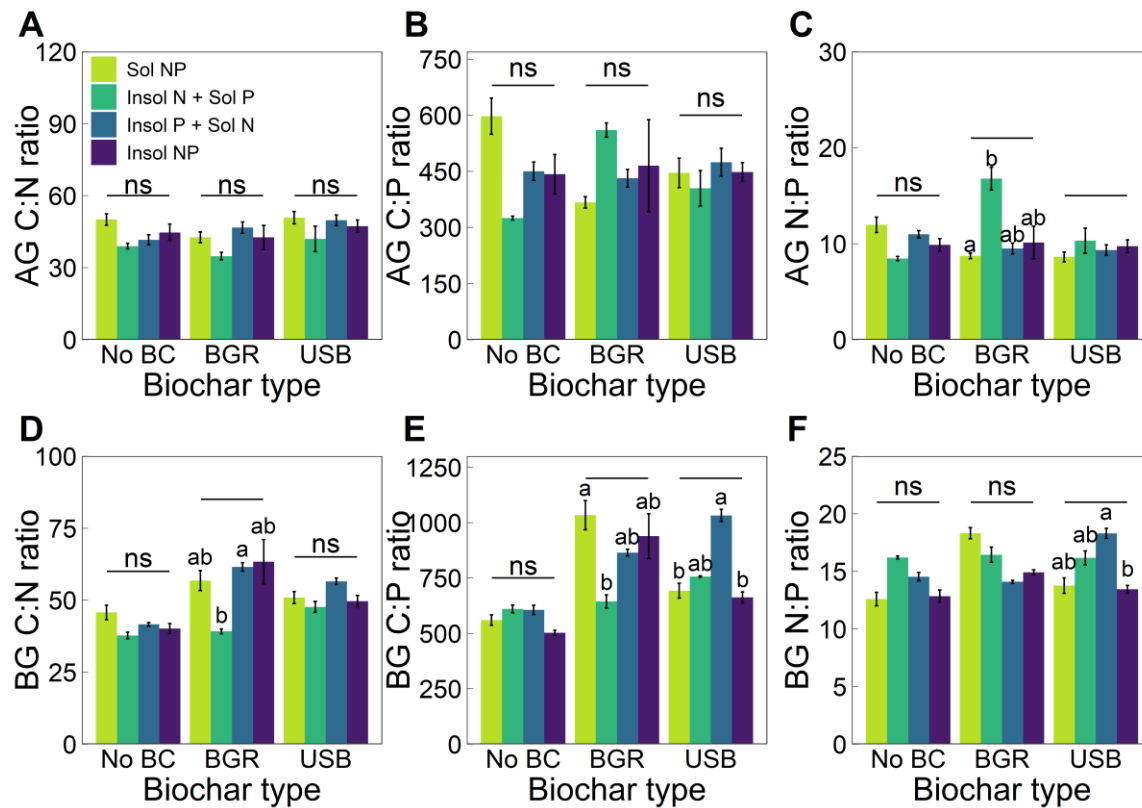


Figure S1.3 Means (\pm SE) of plant tissue nutrient ratios (A-C) aboveground carbon to nitrogen ratios (C:N), carbon to phosphorus ratios, nitrogen to phosphorus ratios, (D-F) belowground carbon to nitrogen ratios, carbon to phosphorus ratios, and nitrogen to phosphorus ratios for biochar (x-axis) and nutrient treatments (varied colors). Lowercase letters indicate significant differences (Tukey post-hoc tests, $p < 0.05$) among nutrient treatments within biochar type and “ns” indicates no significant differences. The x-axis label “No BC” stands for No Biochar treatments.

Table S1.1 ANOVA results for all response variables showing degrees of freedom (df), F-values and p-values for all response variables.

Response Variable	Effect	df	F	p
Total NPP	<i>Biochar</i>	2	0.18	0.83
	<i>Nutrient</i>	3	1.14	0.34
	<i>Biochar × Nutrient</i>	6	0.18	0.98
Aboveground biomass	<i>Biochar</i>	2	0.04	0.96
	<i>Nutrient</i>	3	0.69	0.56
	<i>Biochar × Nutrient</i>	6	0.14	0.99
Belowground biomass	<i>Biochar</i>	2	0.19	0.83
	<i>Nutrient</i>	3	8.83	1.07E-04
	<i>Biochar × Nutrient</i>	6	0.98	0.45
Root:shoot ratio	<i>Biochar</i>	2	0.81	0.67
	<i>Nutrient</i>	3	31.16	7.85E-07
	<i>Biochar × Nutrient</i>	6	8.84	0.18
Aboveground tissue N	<i>Biochar</i>	2	1.32	0.27
	<i>Nutrient</i>	3	2.76	0.04
	<i>Biochar × Nutrient</i>	6	0.40	0.88
Belowground tissue N	<i>Biochar</i>	2	3.33	0.04
	<i>Nutrient</i>	3	5.28	1.22E-03
	<i>Biochar × Nutrient</i>	6	1.53	0.16
Aboveground tissue P	<i>Biochar</i>	2	4.00E-03	1.00
	<i>Nutrient</i>	3	0.29	0.83
	<i>Biochar × Nutrient</i>	6	2.27	0.03
Belowground tissue P	<i>Biochar</i>	2	16.98	4.21E-08
	<i>Nutrient</i>	3	5.71	6.70E-04
	<i>Biochar × Nutrient</i>	6	6.41	9.26E-07
Root colonization	<i>Biochar</i>	2	3.16	0.42
	<i>Nutrient</i>	3	7.55	7.31E-05
	<i>Biochar × Nutrient</i>	6	0.702	0.65
ERH	<i>Biochar</i>	2	0.17	0.92
	<i>Nutrient</i>	3	3.47	0.32
	<i>Biochar × Nutrient</i>	6	6.05	0.42
Media - nitrate	<i>Biochar</i>	2	0.22	0.81
	<i>Nutrient</i>	3	2.73	0.06
	<i>Biochar × Nutrient</i>	6	1.40	0.24
Media - ammonium	<i>Biochar</i>	2	0.08	0.92
	<i>Nutrient</i>	3	1.69	0.18
	<i>Biochar × Nutrient</i>	6	1.31	0.27
Media - phosphate	<i>Biochar</i>	2	0.97	0.39
	<i>Nutrient</i>	3	1.04	0.38
	<i>Biochar × Nutrient</i>	6	1.59	0.18

Table S1.2 Tukey post-hoc test results showing comparisons among biochar types within each nutrient treatment. Lowercase letters indicate significant differences ($p < 0.05$) between biochar types within each nutrient treatment (also bolded).

Response Variable	<u>Sol NP</u>			<u>Insol N + Sol P</u>			<u>Insol P + Sol N</u>			<u>Insol NP</u>		
	No BC	BGR	USB	No BC	BGR	USB	No BC	BGR	USB	No BC	BGR	USB
Total NPP (g)	a	a	a	a	a	a	a	a	a	a	a	a
Aboveground biomass (g)	a	a	a	a	a	a	a	a	a	a	a	a
Belowground biomass (g)	a	a	a	a	a	a	a	a	a	a	a	a
Root:shoot ratio	a	a	a	a	a	a	a	a	a	a	b	b
Aboveground tissue N (%)	a	a	a	a	a	a	a	a	a	a	a	a
Belowground tissue N (%)	a	a	a	a	a	a	a	a	a	a	a	a
Aboveground tissue P (%)	a	a	a	a	a	a	a	a	a	a	a	a
Belowground tissue P (%)	a	b	a	a	a	a	a	ab	b	a	b	ab
Root colonization (%)	a	a	a	a	a	a	a	a	a	a	a	a
ERH (mm g ⁻¹)	a	a	a	a	a	a	a	a	a	a	a	a
Media - nitrate (µg g ⁻¹)	a	a	a	a	a	a	a	a	a	a	a	a
Media - ammonium (µg g ⁻¹)	a	a	a	a	a	a	a	a	a	a	a	a
Media - phosphate (µg g ⁻¹)	a	a	a	a	a	a	a	a	a	a	a	a

Equation for hyphal density (mm g⁻¹ per media dry weight) from hyphal counts:

$$\left(\frac{\text{Filter paper area (mm}^2\text{)}}{\left[\frac{\text{Recticle length (mm)}}{\text{Magnification (objective)}} \right]^2} \times \frac{\text{Recticle segment length (mm)}}{\text{Mag(obj)}} \times \frac{\text{Hyphal Count}}{25 \text{ fields of view}} \right) / 2$$

Example calculation:

Sample ID: CVC-1, filter A → $\left(\frac{490 \text{ mm}^2}{\left[\frac{12 \text{ mm}}{10} \right]^2} \times \frac{1.2 \text{ mm}}{10} \times \frac{47}{25 \text{ fields of view}} \right) / 2 = 38.383 \text{ mm g}^{-1}$

REFERENCES

REFERENCES

- Akey, W. C. (1989). The role of competition for light in interference between velvetleaf (*Abutilon theophrasti*) and soybean (*Glycine max*). Dissertation. Ames (IA): Iowa State University.
- Atul-Nayyar, A., Hamel, C., Hanson, K., and Germida, J. (2009). The arbuscular mycorrhizal symbiosis links N mineralization to plant demand. *Mycorrhiza* 19, 239–246. doi:10.1007/s00572-008-0215-0.
- Barker, D. C., Knezevic, S. Z., Martin, A. R., Walters, D. T., Lindquist, J. L., Barker, D. C., *et al.* (2006). Effect of Nitrogen Addition on the Comparative Productivity of Corn and Velvetleaf (*Abutilon theophrasti*). *Weed Sci.* 54, 354–363. doi:10.1614/WS-05-127R.1.
- Biederman, L. A., and Harpole, W. S. (2013). Biochar and its effects on plant productivity and nutrient cycling: A meta-analysis. *GCB Bioenergy* 5, 202–214. doi:10.1111/gcbb.12037.
- Blackshaw, R. E., and Brandt, R. N. (2008). Nitrogen fertilizer rate effects on weed competitiveness is species dependent. *Weed Sci.* 56, 743–747. doi:10.1614/ws-08-065.1.
- Bonifas, K. D., and Lindquist, J. L. (2006). Predicting biomass partitioning to root versus shoot in corn and velvetleaf (*Abutilon theophrasti*). *Weed Sci.* 54, 133–137. doi: 10.1614/WS-05-079R1.1
- Bonifas, K. D., and Lindquist, J. L. (2009). Effects of nitrogen supply on the root morphology of corn and velvetleaf. *J. Plant Nutr.* 32, 1371–1382. doi:10.1080/01904160903007893.
- Bonifas, K. D., Walters, D. T., Cassman, K. G., John, L., Walters, D. T., and Cassman, K. G. (2005). Nitrogen supply affects root:shoot ratio in corn and velvetleaf (*Abutilon theophrasti*). *Weed Sci.* 53, 670–675. doi:10.1614/WS-05-002R.1
- Brito, I., de Carvalho, M., and Goss, M. J. (2009). “Techniques for Arbuscular Mycorrhiza Inoculum Reduction,” in *Symbiotic Fungi: Principles and Practice*, eds. A. Varma and A. C. Kharkwal (Berlin, Heidelberg: Springer Berlin Heidelberg), 307–318. doi:10.1007/978-3-540-95894-9_19.
- Cantrell, K. B., Hunt, P. G., Uchimiya, M., Novak, J. M., and Ro, K. S. (2012). Impact of pyrolysis temperature and manure source on physicochemical characteristics of biochar. *Bioresour. Technol.* 107, 419–428. doi:10.1016/j.biortech.2011.11.084.
- Clark, M., Hastings, M. G., and Ryals, R. (2019). Soil carbon and nitrogen dynamics in two agricultural soils amended with manure-derived biochar. *J. Environ. Qual.* 48, 727–734. doi:10.2134/jeq2018.10.0384.

- Diacono, M., and Montemurro, F. (2010). Long-term effects of organic amendments on soil fertility. A review. *Agron. Sustain. Dev.* 30, 401–422. doi:10.1051/agro/2009040.
- Du, Z. L., Zhao, J. K., Wang, Y. D., and Zhang, Q. Z. (2017). Biochar addition drives soil aggregation and carbon sequestration in aggregate fractions from an intensive agricultural system. *J. Soils Sediments* 17, 581–589. doi:10.1007/s11368-015-1349-2.
- Feng, G., Song, Y. C., Li, X. L., and Christie, P. (2003). Contribution of arbuscular mycorrhizal fungi to utilization of organic sources of phosphorus by red clover in a calcareous soil. *Appl. Soil Ecol.* 22, 139–148. doi:10.1016/S0929-1393(02)00133-6.
- Fidel, R. B., Laird, D. A., and Spokas, K. A. (2018). Sorption of ammonium and nitrate to biochars is electrostatic and pH-dependent. *Sci. Rep.* 8, 1–10. doi:10.1038/s41598-018-35534-w.
- Frey, S. D. (2019). Mycorrhizal Fungi as Mediators of Soil Organic Matter Dynamics. *Annu. Rev. Ecol. Evol. Syst.* 50, 237–259. doi:10.1146/annurev-ecolsys-110617-062331.
- Gale, N., Halim, A., Horsburgh, M., and Thomas, S. C. (2017). Comparative responses of early-successional plants to charcoal soil amendments. *Ecosphere* 8, 1–18. doi:10.1002/ecs2.1933.
- Gao, S., and DeLuca, T. H. (2018). Wood biochar impacts soil phosphorus dynamics and microbial communities in organically-managed croplands. *Soil Biol. Biochem.* 126, 144–150. doi:10.1016/j.soilbio.2018.09.002.
- Gao, S., DeLuca, T. H., and Cleveland, C. C. (2019). Biochar additions alter phosphorus and nitrogen availability in agricultural ecosystems: A meta-analysis. *Sci. Total Environ.* 654, 463–472. doi:10.1016/j.scitotenv.2018.11.124.
- Glaser, B., Haumaier, L., Guggenberger, G., and Zech, W. (2001). The “Terra Preta” phenomenon: A model for sustainable agriculture in the humid tropics. *Naturwissenschaften* 88, 37–41. doi:10.1007/s001140000193.
- Gujre, N., Soni, A., Rangan, L., Tsang, D. C. W., and Mitra, S. (2021). Sustainable improvement of soil health utilizing biochar and arbuscular mycorrhizal fungi: A review. *Environ. Pollut.* 268, 1-17. doi:10.1016/j.envpol.2020.115549.
- Hammer, E. C., Balogh-Brunstad, Z., Jakobsen, I., Olsson, P. A., Stipp, S. L. S., and Rillig, M. C. (2014). A mycorrhizal fungus grows on biochar and captures phosphorus from its surfaces. *Soil Biol. Biochem.* 77, 252–260. doi:10.1016/j.soilbio.2014.06.012.
- Hoagland, D. R., and Arnon, D. I. (1950). Preparing the nutrient solution. *Water-Culture Method Grow Plants without Soil*. Berkley, CA: College of Agriculture, University of California.

- Hodge, A., Campbell, C. D., and Fitter, A. H. (2001). An arbuscular mycorrhizal fungus accelerates decomposition and acquires nitrogen directly from organic material. *Nature* 413, 297–299. doi:10.1038/35095041.
- Hodge, A., and Fitter, A. H. (2010). Substantial nitrogen acquisition by arbuscular mycorrhizal fungi from organic material has implications for N cycling. *Proc. Natl. Acad. Sci. U. S. A.* 107, 13754–13759. doi:10.1073/pnas.1005874107.
- Hodge, A., and Storer, K. (2014). Arbuscular mycorrhiza and nitrogen: Implications for individual plants through to ecosystems. *Plant Soil* 386, 1–19. doi:10.1007/s11104-014-2162-1.
- Holford, I. C. R. (1997). Soil phosphorus: its measurement, and its uptake by plants. *Aust. J. Soil Res.* 35, 227–239. doi:10.1071/S96047.
- Jakobsen, I., Abbott, L. K., and Robson, A. D. (1992). External hyphae of vesicular-arbuscular mycorrhizal fungi associated with *Trifolium subterraneum* L. 1. Spread of hyphae and phosphorus inflow into roots. *New Phytol.* 120, 371–380. doi:10.1111/j.1469-8137.1992.tb01077.x.
- Jayachandran, K.; Schwab, A.P.; Hetrick, B. A. D. (1992). Mineralization of organic phosphorus by vesicular-arbuscular mycorrhizal fungi. *Soil Biol. Biochem.* 24, 897–903. doi: 10.1016/0038-0717(92)90012-M.
- Jeffery, S., Verheijen, F. G. A., van der Velde, M., and Bastos, A. C. (2011). A quantitative review of the effects of biochar application to soils on crop productivity using meta-analysis. *Agric. Ecosyst. Environ.* 144, 175–187. doi:10.1016/j.agee.2011.08.015.
- John, M. K. (1970). Colorimetric determination of phosphorus in soil and plant materials with ascorbic acid. *Soil Sci.* 109, 214–220. doi: 10.1097/00010694-197004000-00002.
- Keiluweit, M., Nico, P. S., Johnson, M., and Kleber, M. (2010). Dynamic molecular structure of plant biomass-derived black carbon (biochar). *Environ. Sci. Technol.* 44, 1247–1253. doi:10.1021/es9031419.
- Lehmann, J., and Joseph, S. (2009). *Biochar for Environmental Management*. London: Earthscan Dunstan House. doi:10.4324/9780203762264.
- Lehmann, J., Rillig, M. C., Thies, J., Masiello, C. A., Hockaday, W. C., and Crowley, D. (2011). Biochar effects on soil biota - A review. *Soil Biol. Biochem.* 43, 1812–1836. doi:10.1016/j.soilbio.2011.04.022.
- Leigh, J., Hodge, A., and Fitter, A. H. (2009). Arbuscular mycorrhizal fungi can transfer substantial amounts of nitrogen to their host plant from organic material. *New Phytol.* 181, 199–207. doi:10.1111/j.1469-8137.2008.02630.x.

- Li, M., Jordan, N. R., Koide, R. T., Yannarell, A. C., and Davis, A. S. (2016). Meta-Analysis of Crop and Weed Growth Responses to Arbuscular Mycorrhizal Fungi: Implications for Integrated Weed Management. *Weed Sci.* 64, 642–652. doi:10.1614/ws-d-16-00050.1.
- Liao, W., and Thomas, S. (2019). Biochar Particle Size and Post-Pyrolysis Mechanical Processing Affect Soil pH, Water Retention Capacity, and Plant Performance. *Soil Syst.* 3, 1–16. doi:10.3390/soilsystems3010014.
- Lindquist, J. L., Barker, D. C., Knezevic, S. Z., Martin, A. R., and Walters, D. T. (2007). Comparative Nitrogen Uptake and Distribution in Corn and Velvetleaf (*Abutilon theophrasti*). *Weed Sci.* 55, 102–110. doi:10.1614/ws-06-141.1.
- Lindquist, J. L., and Mortensen, D. A. (1999). Ecophysiological characteristics of four maize hybrids and *Abutilon theophrasti*. *Weed Res.* 39, 271–285. doi: 10.1046/j.1365-3180.1999.00143.x.
- Liu, X., Zhang, A., Ji, C., Joseph, S., Bian, R., Li, L., et al. (2013). Biochar's effect on crop productivity and the dependence on experimental conditions—a meta-analysis of literature data. *Plant Soil* 373, 583–594. doi:10.1007/s11104-013-1806-x.
- Lone, A. H., Najar, G. R., Ganie, M. A., Sofi, J. A., and Ali, T. (2015). Biochar for Sustainable Soil Health: A Review of Prospects and Concerns. *Pedosphere* 25, 639–653. doi:10.1016/S1002-0160(15)30045-X.
- Nash, J., Miesel, J., Bonito, G., Sakalidis, M., Ren, H., Warnock, D., et al. (2021). Biochar alters soil properties, microbial community diversity, and enzyme activities, while decreasing conifer performance. *bioRxiv* [Preprint]. doi: 10.1101/2021.05.17.444392.
- Major, J., DiTommaso, A., Lehmann, J., and Falcão, N. P. S. (2005). Weed dynamics on Amazonian Dark Earth and adjacent soils of Brazil. *Agric. Ecosyst. Environ.* 111, 1–12. doi:10.1016/j.agee.2005.04.019.
- McGonigle, T. P., Miller, M. H., Evans, D. G., Fairchild, G. L., and Swan, J. A. (1990). A new method which gives an objective measure of colonization of roots by vesicular—arbuscular mycorrhizal fungi. *New Phytol.* 115, 495–501. doi:10.1111/j.1469-8137.1990.tb00476.x.
- Mosse, B. (1973). Advances in the study of vesicular-arbuscular mycorrhiza. *Annu. Rev. Phytopathol.* 11, 171–196. doi: 10.1146/annurev.py.11.090173.001131.
- Ocampo, J. A., Martin, J., and Hayman, D. S. (1980). Influence of Plant Interactions on Vesicular-Arbuscular Mycorrhizal Infections. I. Host and Non-Host Plants Grown Together. *New Phytol.* 84, 27–35. doi:10.1111/j.1469-8137.1980.tb00746.x.

- Patton, C. J., and Kryskalla, J. R. (2011). Colorimetric Determination of Nitrate Plus Nitrite in Water by Enzymatic Reduction, Automated Discrete Analyzer Methods. U.S. Geol. Surv. Tech. Methods, B. 5, 1–34. doi: 10.3133/tm5B8.
- Phillips, J. M., and Hayman, D. S. (1970). Improved procedures for clearing roots and staining parasitic and vesicular-arbuscular mycorrhizal fungi for rapid assessment of infection. Trans. Br. Mycol. Soc. 55, 158–161. doi:10.1016/s0007-1536(70)80110-3.
- Piash, M. I., Iwabuchi, K., Itoh, T., and Uemura, K. (2021). Release of essential plant nutrients from manure- and wood-based biochars. Geoderma 397, 1–12. doi:10.1016/j.geoderma.2021.115100.
- Sanders, F. E., and Tinker, P. B. (1971). Mechanism of Absorption of Phosphate from Soil by Endogone Mycorrhizas. Nature 233, 278–279. doi: 10.1038/233278c0.
- Schofield, H. K., Pettitt, T. R., Tappin, A. D., Rollinson, G. K., and Fitzsimons, M. F. (2019). Biochar incorporation increased nitrogen and carbon retention in a waste-derived soil. Sci. Total Environ. 690, 1228–1236. doi:10.1016/j.scitotenv.2019.07.116.
- Sexton, B. T., Moncrief, J. F., Rosen, C. J., Gupta, S. C., and Cheng, H. H. (1998). Optimizing Nitrogen and Irrigation Inputs for Corn Based on Nitrate Leaching and Yield on a Coarse-Textured Soil. J. Environ. Qual. 27, 247–247. doi:10.2134/jeq1998.00472425002700010040x.
- Sinsabaugh, R. L., Reynolds, H., and Long, T. M. (2000). Rapid assay for amidohydrolase (urease) activity in environmental samples. Soil Biol. Biochem. 32, 2095–2097. doi:10.1016/S0038-0717(00)00102-4.
- Smith, P. (2016). Soil carbon sequestration and biochar as negative emission technologies. Glob. Chang. Biol. 22, 1315–1324. doi:10.1111/gcb.13178.
- Smith, S. E., and Read, D. (2008). Mycorrhizal Symbiosis. Amsterdam (NL): Elsevier Ltd. doi:10.1016/b978-012370526-6.50007-6.
- Smith, S. E., and Smith, F. A. (2011). Roles of arbuscular mycorrhizas in plant nutrition and growth: New paradigms from cellular to ecosystem scales. Annu. Rev. Plant Biol. 62, 227–250. doi:10.1146/annurev-arplant-042110-103846.
- Song, S., Wen, Y., Zhang, J., and Wang, H. (2019). Rapid spectrophotometric measurement with a microplate reader for determining phosphorus in NaHCO₃ soil extracts. Microchem. J. 146, 210–213. doi: 10.1016/j.microc.2019.01.002.
- Spencer, N. R. (1984). Velvetleaf, *Abutilon theophrasti* (malvaceae), history and economic impact in the United States. Econ. Bot. 38, 407–416. doi:10.1007/BF02859079.

- Staddon, P. L., Fitter, A. H., and Graves, J. D. (1999). Effect of elevated atmospheric CO₂ on mycorrhizal colonization, external mycorrhizal hyphal production and phosphorus inflow in *Plantago lanceolata* and *Trifolium repens* in association with the arbuscular mycorrhizal fungus *Glomus mosseae*. *Glob. Chang. Biol.* 5, 347–358. doi:10.1046/j.1365-2486.1999.00230.x.
- Stanley, M. R., Koide, R. T., and Shumway, D. L. (1993). Mycorrhizal symbiosis increases growth, reproduction and recruitment of *Abutilon theophrasti Medic.* in the field. *Oecologia* 94, 30–35. doi:10.1007/BF00317297.
- Tarafdar, J. C., and Marschner, H. (1994). Phosphatase activity in the rhizosphere and hyphosphere of VA mycorrhizal wheat supplied with inorganic and organic phosphorus. *Soil Biol. Biochem.* 26, 387–395. doi:10.1016/0038-0717(94)90288-7.
- Treseder, K. K. (2013). The extent of mycorrhizal colonization of roots and its influence on plant growth and phosphorus content. *Plant Soil* 371, 1–13. doi:10.1007/s11104-013-1681-5.
- Vatovec, C., Jordan, N., and Huerd, S. (2005). Responsiveness of certain agronomic weed species to arbuscular mycorrhizal fungi. *Renew. Agric. Food Syst.* 20, 181–189. doi:10.1079/raf2005115.
- Vitousek, P. M., Porder, S., Houlton, B. Z., and Chadwick, O. A. (2010). Terrestrial phosphorus limitation: Mechanisms, implications, and nitrogen-phosphorus interactions. *Ecol. Appl.* 20, 5–15. doi:10.1890/08-0127.1.
- Wang, W., Shi, J., Xie, Q., Jiang, Y., Yu, N., and Wang, E. (2017). Nutrient Exchange and Regulation in Arbuscular Mycorrhizal Symbiosis. *Mol. Plant* 10, 1147–1158. doi:10.1016/j.molp.2017.07.012.
- Warnock, D. D., Lehmann, J., Kuyper, T. W., and Rillig, M. C. (2007). Mycorrhizal responses to biochar in soil - concepts and mechanisms. *Plant Soil* 300, 9–20. doi:10.1007/s11104-007-9391-5.
- Whiteside, M. D., Garcia, M. O., and Treseder, K. K. (2012). Amino Acid Uptake in Arbuscular Mycorrhizal Plants. *PLoS One* 7, 8–11. doi:10.1371/journal.pone.0047643.
- Yamato, M., Okimori, Y., Wibowo, I. F., Anshori, S., and Ogawa, M. (2006). Effects of the application of charred bark of *Acacia mangium* on the yield of maize, cowpea and peanut, and soil chemical properties in South Sumatra, Indonesia. *Soil Sci. Plant Nutr.* 52, 489–495. doi:10.1111/j.1747-0765.2006.00065.x.
- Zhang, H., Chen, C., Gray, E. M., Boyd, S. E., Yang, H., and Zhang, D. (2016). Roles of biochar in improving phosphorus availability in soils: A phosphate adsorbent and a source of available phosphorus. *Geoderma* 276, 1–6. doi:10.1016/j.geoderma.2016.04.020.

CHAPTER 2:

BIOCHAR TYPE, APPLICATION RATE AND AGE ALTER CARBON STABILIZATION MECHANISMS IN THREE SOIL TYPES

2.1 ABSTRACT

Stabilizing organic matter in agroecosystem soils is one way to reduce carbon (C) emissions and, consequently, impact climate change. However, these processes are highly controlled by soil properties and thus can vary greatly across soil habitats and management practices. One such management practice is applying biochar, a soil amendment made from pyrolyzed organic biomass/wastes. Biochar is a unique amendment to study stabilization processes because its decomposition is constrained by both its recalcitrant structure and its ability to alter soil properties and underlying stabilization mechanisms. However, soil responses to biochar can be complicated depending on its production characteristics (e.g., feedstock and pyrolysis temperatures), application rates, and/or age (i.e., time deployed). Thus, we implemented a one-year field-incubated mesocosm experiment with two biochars and two application rates in three soil types and measured biological, chemical and physical soil properties response. We also collected samples from our field site amended with biochar four years previously to assess longer-term effects of aging. Overall, we found our wood-based and greater C content biochar (USB) and the higher application rate (75 Mg ha^{-1}) to have greater effects on soil properties than our municipal waste-based and lower C content biochar (CMS) or lower application rate (25 Mg ha^{-1}). Additionally, these effects were most prominent in the coarser-textured and lower pH soil type (i.e., a loamy sand). However, higher soil C loss in USB treatments after one year suggests CMS treatments may have stabilized more C possibly through negative soil priming and its recalcitrant chemical structure. In fact, after one year, biochar

decomposition may be most controlled by its recalcitrant chemical structure as biochar-induced aggregation changes were minimal and C in organo-mineral associations increased only after four years. Our work shows how biochar may fit into contemporary SOM stabilization concepts whilst also presenting soil response variability depending on biochar type, application rate, and soil habitat. By increasing soil C stocks, biochar can decrease climate change impacts and improve soil health, therefore contributing to agroecosystem sustainability and human well-being.

2.2 INTRODUCTION

Soil organic matter (SOM) is a large source of terrestrial carbon (C), containing up to three times the amount present in all the world's plants (Weil and Brady, 2016). Protecting or stabilizing this C may therefore be a viable option to reduce emission and mitigate climate change, especially in highly-degraded habitats like agroecosystems (Goh, 2004; Lal, 2009). Agroecosystems can easily increase soil C concentrations through various strategies (e.g., incorporating crop residues or applying organic amendments) (Lal, 2009; Diacono and Montemurro, 2010), however, this does not necessarily lead to protection as added sources vary in chemical composition and soil conditions dictate stabilization processes (Schmidt et al., 2011). Thus, untangling soil processes and how they vary across habitats is highly valuable to understanding SOM protection.

Biological, chemical, and physical processes stabilize organic matter within the soil. Specifically, SOM is biologically altered and decomposed by soil organisms, chemically bound via organo-mineral associations, and/or physically incorporated within aggregates (Six et al., 2002; Schimel and Schaeffer, 2012; Plaza et al., 2013). Biological breakdown was originally thought to be controlled by SOM chemical structure, its resistance to decomposition (i.e.,

recalcitrance) and microbial capability, however current research directions suggest microbial accessibility is a larger determinant (Schmidt et al., 2011; Dungait et al., 2012; Kravchenko et al., 2019). In fact, Lehmann et al. (2020) proposed that in some cases, distance between decomposer and C substrates limits SOM breakdown more than aggregate formation. Other work suggests recalcitrant organic matter inputs can have similar stability as other more labile forms (Cotrufo et al., 2015; Angst et al., 2017). For example, Angst et al. (2017) observed little difference between accumulation of lignin, an organic polymer long classified as chemically recalcitrant, and other biomolecules in the less protected particulate organic matter (POM) fractions. Thus, these shifts in scientific understanding advocate for a larger research focus on how soil properties influence stabilization processes (Schmidt et al., 2011; Lehmann and Kleber, 2015) as well as continued work on how soil management may alter these properties and therefore SOM persistence (Six et al., 2000).

Biochar is a soil amendment that can impact SOM stabilization both through its unique chemical structure and by altering soil properties. Produced from pyrolysis (i.e., heating in oxygen-limited conditions), biochar is often promoted in agroecosystems to improve nutrient retention, soil moisture, and pH (Glaser et al., 2002; Jeffery et al., 2011); however, it may be most beneficial as a negative-emission tool, sequestering C long-term in the soil (Lehmann et al., 2006; Smith, 2016). In fact, biochar's carbon-rich and highly aromatic chemical structure may strongly influence its stabilization (Sohi et al., 2009), despite current thinking on other mechanisms' importance. For example, Lavallee et al. (2019) concluded that chemical recalcitrance was more important for protecting pyrogenic carbon (i.e., biochar) than mineral association in three agricultural soils, as they found no evidence for additional preservation of pyrogenic carbon in mineral soil fractions compared to the light and POM fractions. Biochar can

also alter the underlying soil properties, such as cation exchange capacity (Liang et al., 2006), soil porosity and bulk density (Obia et al., 2016), and/or enzyme activity (Wang et al., 2015, Nash et al., 2021), which can affect the mechanisms that dictate C stabilization (Lehmann et al., 2006; Gul et al., 2015; Plaza et al., 2016). For example, almost ten years after biochar was applied, Weng et al. (2017) found decreased microbial C mineralization rates and increased formation of organo-mineral complexes with plant-derived C in biochar-amended soil. Thus, C persistence in this system was aided by biochar's ability to stabilize other C sources (i.e., plant-derived C) not just recalcitrant C from its structure (Weng et al., 2017).

Despite its potential for long-term benefits, some studies have found biochar effects to diminish over time. For instance, de la Rosa et al. (2018) found decreased biochar pH and aromatic composition as well as a physically fragmented structure after only two years deployed in the field. Other work using a two-pool (fast and slow cycling) modeling approach contends that estimated pyrogenic carbon soil residence times (millennia timescale) are overinflated by hundreds of years (Singh et al., 2012). Furthermore, biochar can be physically removed from soils when rain transports lightweight biochar particles off-site, thereby decreasing its overall impact (Major et al., 2010). Nonetheless, Anthrosols in Brazil reinforce assumptions about biochar longevity as they contain pyrogenic carbon estimated to be 7,000 years old, show reduced C mineralization rates compared to adjacent, unamended soils and have slower SOC turnover (Liang et al., 2008). Further work on field-aging is needed to examine how biochar may fit into the theories of SOM stabilization, especially if it is to be used as a carbon sequestration strategy. Additionally, many biochar studies are short-term, with one meta-analysis reporting the average experimental length for field studies to be 1.3 years and < 1 year for pot experiments (Jeffery et

al., 2011). Longer-term experiments are necessary to understand biochar's lasting impact on soil properties and C storage.

Biochar effects can also vary greatly because diverse production strategies (e.g., different bioenergy feedstocks and pyrolysis temperatures) and application methods (e.g., rates) create variable soil responses (Sohi et al., 2009; Hernandez-Soriano et al., 2016; Antonangelo et al., 2019). For example, in a 12-month incubation experiment, there was greater C mineralization in soils amended with a biochar produced under 450°C pyrolysis temperature than with a biochar of the same feedstock but 550°C pyrolysis temperature, likely due to differences in recalcitrant C compositions (Fang et al., 2014). Manure-based biochars can release more nitrogen (N) which can aid crop nutrient requirements (Piash et al., 2021), although wood-based biochars can adsorb more N to surfaces, acting as a longer-term N sink (de la Rosa et al., 2018). Higher application rates should simply amplify biochar effects; however, in some examples, biochar's positive effect on soil extracellular enzyme activity rates (Wang et al., 2015) and crop growth (Laghari et al., 2015) decreased or became negative at certain thresholds. Furthermore, biochar impact often varies across soil types (Fang et al., 2014), with more dramatic effects in low-nutrient and low-pH soils (Jeffery et al., 2011; Pandit et al., 2018). Thus, despite some generalities that have emerged from biochar research, many factors like biochar type, application rate, and soil type continue to create uncertainty for practical use.

In our study, we asked how different types of biochar (i.e., different feedstock and production procedures) and application rate can affect SOM stabilization mechanisms. To understand how biochar alters the underlying processes that drive SOM stabilization, we measured biological (e.g., N mineralization, CO₂ flux rates, potential enzyme activity rates), chemical (e.g., pH, dissolved organic C and total N, total bulk C and N) and physical (e.g., root

biomass, water stable aggregates) soil properties. We also fractionated our samples by particle size and measured C concentration and SOM composition. We used three soil types in a one-year field-incubated mesocosm experiment, and in a longer-term field site amended four years previously to evaluate how mechanisms may change over an extended (four-year) time span. We evaluated three main hypotheses: (1) biochars will enhance soil C stabilization by altering underlying soil properties and mechanisms; (2) biochar changes will vary across (i) biochar type, with stronger effects in the biochar with greater C; (ii) application rate, with stronger effects in the higher application rates; and (iii) soil environments, with stronger effects in the coarser-textured soil; and (3) biochar's impact on soil properties will dissipate over time, thus biochar effects will be larger in one-year samples than four-year samples.

2.3 METHODS

2.3.1 Biochars

To assess variation across production methods and bioenergy feedstocks, we used two pyrolysis biochars (hereafter: CMS and USB). CMS is a class-A agricultural amendment made from Detroit, MI municipal waste, which was then pyrolyzed at 650°C. USB was made from southern yellow pine waste wood pallets that were pyrolyzed in a continuous carbonizer at 550°C for 18 minutes. CMS and USB had dry densities of 0.52 g/cm³ and 0.30 g/cm³ and pHs of 9.27 ± 0.15 and 9.33 ± 0.03 (mean ± s.d., 1:5 w:v in H₂O, n = 3), respectively. Total C and N (via combustion) for CMS was 29.5 ± 2.57% and 2.76 ± 0.18% for C and N, respectively and 84.2 ± 1.9% and 0.26 ± 0.01% for USB (mean ± s.d., n = 3). Biochars were also analyzed for the 16-priority pollutant poly-aromatic hydrocarbons (EPA method 8310, Phoslab Environmental Services, FL, USA) with results shown in appendix.

2.3.2 Soils

To investigate carbon stabilization mechanisms in different soil conditions, we collected three Michigan soils. We obtained a well-drained Rousseau fine loamy sand (89.3% sand, 1.9% silt, 8.8% clay; 2.59% C, 0.05% N) collected from the MSU Upper Peninsula Forestry Innovation Center in Escanaba, MI (NRCS, 2021). We also collected a well-drained Marlette fine sandy loam (59.6% sand, 20.9% silt, 19.5% clay; 1.77% C, 0.12% N) at the MSU Tree Research Center in East Lansing, MI (NRCS, 2021). Our third soil was a poorly-drained Colwood-Brookston clay loam (36.6% sand, 33.9% silt, 29.5% clay; 2.52% C, 0.19% N) that we collected at the MSU Agricultural Research Farm in East Lansing, MI (NRCS, 2021).

2.3.3 Mesocosm experiment

We created a factorial mesocosm experiment which used the three soil types (loamy sand, sandy loam, and clay loam), three biochar additions (CMS, USB, and No Biochar) and two biochar application rates (25 Mg ha⁻¹ and 75 Mg ha⁻¹). The 25 Mg ha⁻¹ biochar treatment represents a common application rate (Lehmann and Joseph, 2009), and we chose the higher rate (75 Mg ha⁻¹) to determine where biochar effects may either reach an upper threshold or reveal negative consequences. Because the No Biochar treatment cannot have biochar application rates 25 and 75 Mg ha⁻¹, biochar and application rate treatments were combined as the following: No Biochar, CMS-25, CMS-75, USB-25, USB-75. In total, we had 15 treatments (3 soils × 5 biochar application treatments) with 9 mesocosms in each treatment giving us a total of 135 mesocosms. We will refer to No Biochar treatments as the control treatments.

Using shovels, we collected 40 L of soil from each site from the 0-15 cm layer. We then sieved the soils through a 4 mm screen and homogenized each type separately using a small cement mixer. Soils were air-dried until further processing. To create each soil + biochar

application treatment, we first determined total grams of soil per mesocosm (using soil bulk densities without biochar), converted biochar application rates (Mg ha^{-1}) to a volume concentration (g Mg^{-1}), calculated biochar weight for mesocosm volume, and then calculated total biochar weight and total soil weight for all 9 mesocosms per treatment. Biochar and soil were then combined in a small cement mixer. We constructed cylindrical mesocosms (11 cm height \times 5 cm diameter) from 4 mm plastic mesh (Darice company, Strongsville, OH, USA) and secured with staples. Plastic caps (1 cm height \times 5 cm diameter) were attached to cylinder bottoms to produce a 10 cm interior height. We then packed the soil + biochar mixtures into labeled mesocosms with similar bulk densities within soil types: the loamy sand was $1.36 \pm 0.02 \text{ g cm}^{-3}$, the sandy loam was $1.43 \pm 0.02 \text{ g cm}^{-3}$, and the clay loam was 1.37 ± 0.02 (mean \pm s.d., $n = 45$), although these may not represent natural conditions as we did not have this data. To prevent soil moisture loss, mesocosms were wrapped in aluminum foil until deployment.

We deployed mesocosms on July 22, 2019 at our field experiment site (MSU Tree Research Center, see description below) between the two experimental units, in a randomized complete block. We also deployed a second, identical block of 135 mesocosms on July 24, 2019 that will be collected in five years to assess longer-term change. Each block consisted of 15 units with each unit containing 9 mesocosms (3 soil + biochar application treatments with 3 replicates per treatment). Units measured 50 cm \times 50 cm, with mesocosms separated by 10 cm. To deploy mesocosms, we used rubber mallets and beveled PVC pipes (\sim 5 cm diameter) to core holes 11 cm deep and then we discarded extracted soil. Once all the holes within a unit were cored, we deployed the unit's mesocosms by carefully lowering each into a hole and adding or removing soil to ensure the top of the mesocosm was level with the ground and its sides were touching the

surrounding soil profile. After we deployed all mesocosms, we covered the grid in thatch to protect the disturbed soil from drying out.

2.3.4 Field experiment

We established our experimental Christmas tree farm in 2016 at the MSU Tree Research Center (see Ren et al., 2021 for full description) to examine long-term effects (i.e., within a typical 10-year rotation) of biochar amendments on tree growth. We used a factorial design with three USB application rates (0 Mg ha⁻¹, 25 Mg ha⁻¹, and 75 Mg ha⁻¹) and two common landscaping and Christmas tree species: balsam fir (*Abies balsamea*) and Colorado Blue Spruce (*Picea pungens*). However, as there was high tree mortality (Nash et al., 2021) and remaining trees have yet to grow large enough to have any expected effects on the whole plot, we pooled these samples across tree species such that we only used the biochar application rate as a single factor. The field experiment is arranged in two units (17 m × 30 m) with three biochar treatment columns (2 m × 30 m) separated by 2 m alleys. USB biochar was applied (broadcast spreader and discing) in the top 15 cm of the soil and tree seedlings were planted. The site has an average summer temperature of 15°C and 4°C in the winter with about 80.6 cm of annual rainfall and 130 cm winter snowfall (U.S. Weather Service, 2018). The field site is enclosed in an electrical fence to prevent disturbance such as deer browsing.

2.3.5 Sample collection

We collected three types of soil cores: 1) a set of mesocosms (135 constructed mesh cores) after one year of field aging, referred to as “one-year samples”, 2) soil cores from the long-term field experiment after four years of field aging, referred to as “four-year samples”, and 3) intact soil cores collected from the long-term field experiment in 2020 for Xray μ CT scanning analysis, referred to as “intact four-year samples.” On August 6, 2020 we collected all 135

mesocosms or one-year samples from Block 1 using trowels and serrated garden knives (horis). We placed mesocosms in polyethylene bags in groups of three (the three treatment replicates within a unit) and stored on ice packs in a cooler until returning to the lab where they were refrigerated (4°C) until further processing. On August 18, 2020, we collected four-year samples from the three biochar application rate treatments from our field experiment using 5 cm diameter beveled PVC pipes. We collected four replicate samples from each of the three biochar treatments to account for the greater variation associated with a less-controlled field experiment. For each field replicate, we collected three 5 cm diameter cores within 15 cm of one another and composited in the field. We chose random sampling locations within each treatment that had not been sampled in the past two years to avoid collecting disturbed soil.

To assess biochar's effect on soil porosity and organic matter via Xray μ CT scanning, we collected five replicate intact soil cores (15 cm height \times 5 cm diameter) from each of the field experiment's three biochar treatments in October 2020 ($3 \times 5 = 15$ total intact cores). Soil core locations were randomly selected (within a treatment) and intact cores were stored in plastic sheets at 4°C until scanning.

2.3.6 Lab processing and analysis

For one-year samples, we first removed protruding roots and soil from the mesocosms exteriors, measured total soil height to determine actual soil volume, and recorded field-moist mass. Next, we combined the soil from the three replicate mesocosms within a collection group (i.e., the three treatment replicates from a unit) into one lab sample in order to have enough mass for all protocols. Therefore, we had three combined samples, or replicates, per soil + biochar application treatment (9 mesocosms per treatment / 3 combinations = 3 replicates) and 45 total soil samples for lab analyses (3 replicates \times 15 treatments = 45 soil samples).

All lab procedures described below were carried out on both one-year and four-year samples. For each soil sample, we sieved half through an 8-mm particle size sieve and the other half through a 2-mm particle sieve. Soil sieved at 8-mm was air-dried and used for water stable aggregates and aggregate surface elemental analysis. Soil sieved at 2-mm was first subsampled when field-moist for gravimetric soil moisture, potential enzyme activity, DOC/TDN, pre-incubated nitrate/ammonium, and lab incubation protocols. Then, the remaining 2-mm sieved soil was air-dried and used for soil fractionation procedures. We also collected root biomass on the 2-mm sieve. For one-year samples, we added roots on the sieve to the root biomass we had collected by hand (before sieving) when extracting and combining soil from the mesocosms. We then floated both one-year and four-year root biomass samples in tubs of water, shaking and rinsing soil particles off, and used tweezers and plastic mesh screens (size: 1 mm) to collect floating roots (Thibault and Stewart, 2018).

We measured gravimetric soil moisture by oven-drying 10 g subsamples (2-mm sieved, field-moist) for 24 hours at 105°C to calculate water-filled pore space (WFPS) for the incubation and to report soil nutrients and enzyme activity rates on a dry mass basis ($\mu\text{g g}^{-1}$). To determine respiration rates and N mineralization, we weighed 50 g of soil (2-mm sieved, field-moist) at 60% WFPS (calculated using bulk density and soil moisture) in specimen cups and incubated in loosely capped 1 L glass jars in the dark for 16-days (Robertson et al., 1999). We checked soil moisture biweekly, adjusting to 60% WFPS with DI water as needed. We took our first measurement on day 9 when we assumed microbial populations had adjusted to lab conditions. On day 9, we flushed jar airspace by uncapping and placing in front of an oscillating fan for 30 minutes. We then capped the jars tightly and incubated in the dark for 2 hours after which we used a syringe to take 1 mL gas aliquots from the jars and measured CO_2 on a LI-820 CO_2 gas

analyzer (LICOR Inc., Lincoln, NE, USA). We used standards with known CO₂ concentrations to create a calibration curve and calculate the CO₂ in our samples. After sampling, sealed jars were placed back in the dark, and we repeated flushing and gas measurements for 24-hour (day 10) and 48-hour (day 11) measurements. After 48 hours, jars were flushed, capped loosely, and placed in the dark again. On day 14, we implemented the same measuring scheme: 2-hours, 24-hours (day 15), and 48-hours (day 16). We processed pre-incubated soils (2-mm sieved, field-moist) for nitrate, ammonium, dissolved organic carbon (DOC), and total dissolved nitrogen (TDN) and post-incubated soil samples (2-mm sieved, field-moist) for nitrate and ammonium by first extracting 8.0 ± 0.05 g soil in 0.5 M K₂SO₄ (shaking at 200 rpm for one hour and filtering through a Whatman Qualitative filter #5). Extracts were frozen at -20°C till further analysis. We obtained DOC/TDN by diluting samples ($\times 1.25$) and processing on a TOC/TN Vario Select analyzer (Elementar, Americas, Ronkonkoma, NY, USA). For nitrate, we used a modified enzyme reduction method (Wittbrodt et al., 2015) on extracts in a 96-well microplate and read absorbance at 540 nm using spectroscopy (BioTek Synergy HT1, BioTek Instruments Inc., Winuski, VT, USA). For ammonium, we reacted extracts with ammonia salicylate and ammonia cyanurate in a 96-well microplate (Sinsabaugh et al., 2000) and read absorbance at 610 nm using spectroscopy (BioTek Elx800, BioTek Instruments Inc., Winuski, VT, USA). We converted absorbance to $\mu\text{g g}^{-1}$ and calculated average daily ammonification, nitrification and N mineralization rates ($\mu\text{g g}^{-1} \text{d}^{-1}$) by subtracting the initial ammonium, nitrate, or total inorganic N (ammonium + nitrate) from their respective final measurement and dividing by total incubation days (16). Due to different collection dates, we did separate incubations and extractions for one-year and four-year soils, however procedures were the same.

We determined potential soil extracellular enzyme activities (EEA) from 1 g soil aliquots (2-mm sieved, field-moist) that were frozen at -20°C within 5 days of one-year sample collection and 1 day of four-year sample collection. We performed colorimetric and fluorometric assays in 96-well microplates using seven substrates: β -Glucosidase (BG), cellobiohydrolase (CBH), phenyl oxidase (PHEN), peroxidase (PER), leucine aminopeptidates (LAP), β -N-acetyl glucosaminidase (NAG), and acid phosphatase (PHOS) (Saiya-Cork et al., 2002; Sinsabaugh et al., 2000). These substrates allow us to quantify how microbes obtain more labile C forms (BG and CBH) and recalcitrant C forms (PHEN and PER). Other substrates indicate N (LAP and NAG), and phosphorus (PHOS) acquisition potential. Absorbance was measured on a Biotek synergy H1 microplate reader (Winooski, VT, USA). We used soil slurry blanks, substrate blanks and buffer blanks to calculate EEA rates ($\text{nmol activity h}^{-1} \text{ g}^{-1} \text{ dry soil}$).

We determined water stable aggregates through a modified rotary sieve shaker method (Tiemann et al., 2015). We weighed 100 g of soil (8-mm sieved, air-dried) on a wet filter (Whatman Grade 1 Qualitative) and used DI water to slowly saturate soil through capillary action. Then we placed saturated soil on a mechanical sieve stack (Restsch AS200 basic, Haan, Germany) with sieve sizes 2 mm, 250 μm , 53 μm . With an amplitude of 30, we applied water at a pressure of 10 psi for 2 minutes. Soil remaining on each sieve was rinsed into labeled containers, dried at 60°C for 48 hours and weighed. We calculated mean weight diameter (MWD) by summing the products of each sieve size weight proportion (e.g., if we obtained 77 grams on the 250 sieve, it would be 77 grams / 100 total grams = 0.77) and the average aggregate size per sieve: 5.0, 1.125, and 0.1515 for sieves 2 mm, 250 μm , and 53 μm , respectively.

To investigate how biochar affected C in soil aggregates over time we used scanning electron microscopy (SEM) imaging and energy-dispersive X-ray analysis (EDX) to quantify C

concentrations on aggregate surfaces. We used soil aggregates (8-mm sieved, air-dried) from a subset of one-year and four-year samples in the control and USB-25 treatments (2 biochars \times 3 replicates \times 2 time periods = 12 samples). Because we were financially constrained, we chose to test the application rate (25 Mg ha⁻¹) more commonly used in the field. For each sample, we took an SEM image at 30x magnification, selected three random locations in this image for further magnification at 300x, and measured elemental concentrations (%) via EDX. Out of these three locations, we chose the one that appeared the flattest morphologically to spatially map C concentrations. An area with high C percent may indicate biochar presence, therefore we also further magnified (x6000) and imaged these potential biochar pieces.

We used a North Star Imaging (NSI) X3000 system (Rogers, MN, USA) to analyze the intact four-year samples collected for Xray μ CT scanning. Each scan took 11 minutes with the following settings: voltage = 75 kV, amperage = 450 μ A, and frame rate = 12.5 frames per second. We also used the Vortex Scan settings with total projections at 7200, no frame averages, and a total scan height of 15 cm. We used North Star Imaging efX software to reconstruct the final 3D images, which had a resolution of 36.5 μ m. Then with ImageJ, we transformed images from 16-bit into 8-bit, filtered with 3D median filter (x, y, z = 2 pixels), and segmented manually to separate air, POM, and biochar.

Using a time-efficient and highly-reproducible method (Balesdent et al., 1987, 1991; Poeplau et al., 2018), we separated soils (2-mm sieved, air-dried) into five particle-size fractions: coarse sand (CS), fine sand (FS), coarse POM (CPOM), fine POM (FPOM), and a clay + silt fraction. To break up soil aggregates, we shook 25 g of soil (2-mm sieved, air-dried) with 7 glass beads in 150 mL of 0.5% sodium hexametaphosphate for 16 hours at 200 rpm. After shaking, we poured soil slurries through a sieve stack with two sizes: 250 μ m to catch coarse sand and POM

and 53 μm to catch fine sand and POM. Soil that passed through both sieves was the silt + clay fraction. Soil contained on each sieve (250 μm and 53 μm) was rinsed thoroughly with DI water (until rinsate became clear) and the remaining soil on the sieve was then transferred into a 250 mL beaker. From there, we employed a flotation-panning technique with DI water to separate the lighter POM fraction, which floated, and the heavier sand fraction that sank. We weighed all fractions after drying at 60°C for 48 hours to assess recovery (all above 98% recovery) and mass of each fraction. We then dried fractions and bulk soil subsamples at 105°C for 24 hours and pulverized them before determining total C and N concentrations via dry combustion elemental analysis (Costech Analytical Technologies Inc., Valencia, CA, USA) for all fractions except the sand fractions (250 μm and 53 μm) which were below detection limits and were therefore analyzed on a Thermo Flash 2000 EA (ThermoFisher, Finnigan, Germany). All sand fractions were less than 0.2% C and only used in **Figure 2.11**. Starting (pre-field deployment of one-year samples) soil + biochar treatments C and N concentrations were estimated using application rates and total C and N concentrations (%) of soils and biochars.

We characterized SOM composition in POM fractions using Fourier-transform mid-infrared spectroscopy (Vertex, 70 Bruker Scientific LLC, Bellerica, MD, USA) operating in the 4500-600 cm^{-1} range, equipped with a PIKE Easy-Diff diffuse reflectance accessory (FTIR-DRIFT). We used a 4 cm^{-1} resolution with 60 scans per sample. Background spectra from an empty sample cup were collected every hour. All samples were measured neat to avoid challenges introduced by diluting samples into KBr which is hygroscopic. Mean spectra were background-subtracted and baseline-corrected (concave rubber band method) in OPUS 7.5 (Bruker) before quantifying peak areas for absorbance regions associated with organic bonds characteristic of key types of organic compounds (Calderón et al., 2013) (**Table S2.1**). The

biochar treatments consistently had lower peak areas for all organic bond regions, suggesting potential absorbance issues. Instead, we present ratios of aromatic C region peak areas to aliphatic C peak areas to show potential differences in decomposition processes (Demyan et al., 2012). We therefore assume that absorbance issues affected the biochar treatment samples the same across the organic bond regions.

2.3.7 Statistical analysis

To quantify how our treatments influenced response variables, we ran fully interactive general linear models (two-way analyses of variance). For all one-year responses, we used soil type and biochar treatment as predictor variables. We performed 18 specific post-hoc pairwise comparisons assessing difference between each biochar treatment and the control as well as differences between application rates within each biochar type. These post-hoc tests were corrected using the Bonferroni-Holm method and statistical significance determined at $p < 0.05$. Although we originally ran general mixed-effects linear models with a random effect of starting mixture to acknowledge that all mesocosms within a biochar treatment came from the same starting mixture, most of these models did not converge. For four-year samples, we compared the one-year treatments control, USB-25 and USB-75 in the sandy loam to the corresponding field-collected, four-year treatments using an interactive general linear model with time (one-year or four-year) and biochar treatments (control, USB-25, and USB-75) as predictor variables. Due to the different number of replicates per biochar treatment in one-year and four-year samples (one-year: 3 replicates per biochar treatment, four-year: 4 replicates), we used type III sum of squares for an unbalanced design. We performed 6 post-hoc pairwise comparisons assessing differences between one-year and four-year corresponding biochar treatments (e.g., one-year USB-25 vs four-year USB-25) as well as between the two four-year biochar application rates and the four-

year control. These post-hoc tests were also corrected using the Bonferroni-Holm method and statistical significance determined at $p < 0.05$. For water stable aggregates and Xray μ CT scanning data (porosity and organic matter content) where models were bounded by (0, 1) (percent), we used a beta-distributed linear model. For Xray μ CT scanning data, we ran a one-way analysis of variance with biochar application rate as the predictor variable. For EDX data, we ran a fully interactive two-way analysis of variance with time (one-year versus four-year) and biochar (control versus USB-25) as predictor variables. During the lab incubation, two lab replicates contained standing water throughout the 16 days and thus may have been overwatered when adjusting soil conditions to 60% WFPS. These replicates generally differed by over 50% from others within the same treatment and were therefore dropped from CO₂ flux rates and N rates datasets. We checked all models for normality of error and homogeneity of variance. Response variables that did not conform to normality were log-transformed before analysis. Log transformation did not fix the unequal variance for the LAP enzyme activity data (four-year samples); thus, we used a weighted least squares model with different variance for each treatment (i.e., USB-75 one-year versus USB-75 four-year). All statistical analyses were performed in the R statistical software version 3.5.3.

2.4 RESULTS

2.4.1 CO₂ flux & N mineralization rates

CO₂ flux rates increased with finer soil textures in one-year samples, however few biochar treatments were significantly different from the controls (**Figure 2.1**). For example, USB-75 increased C flux in the loamy sand treatments by 54% ($p = 0.03$) and CMS-75 decreased CO₂ rates by 23% in clay loam treatments ($p = 3.31 \times 10^{-3}$). Four-year USB-25 treatments

decreased CO₂ daily rates compared to both the four-year control (23% decrease, $p = 0.06$) and the four-year USB-75 treatments (32% decrease, $p = 5.26 \times 10^{-3}$).

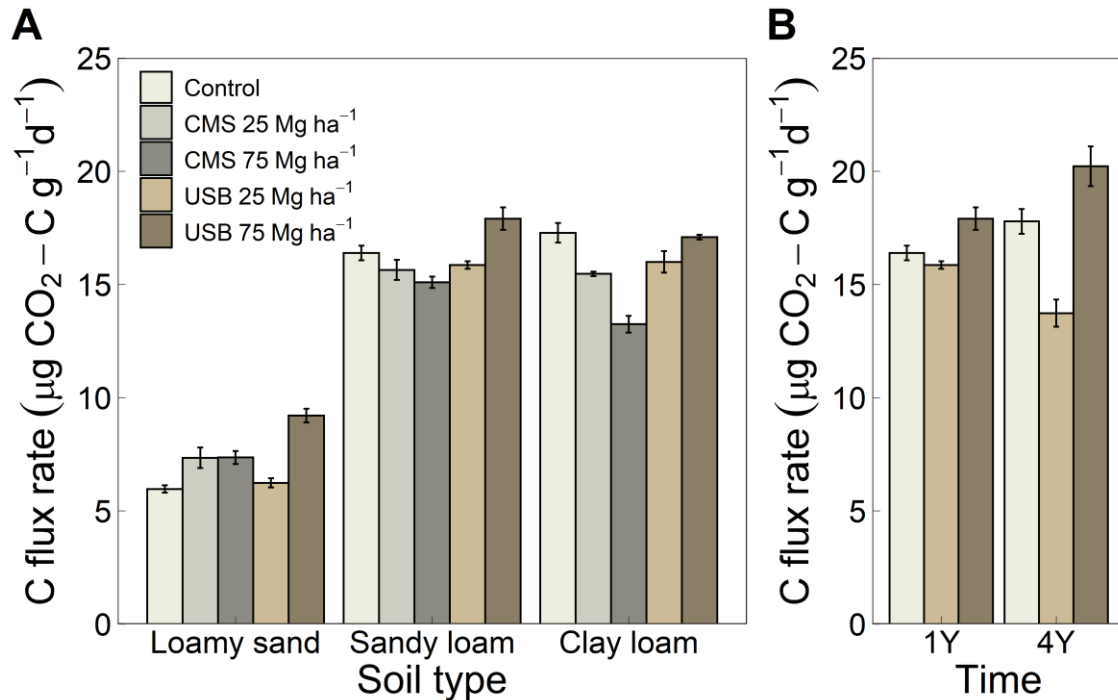


Figure 2.1 Means \pm (SE) of CO₂ flux rates from our 16-day lab incubation comparing different soil textures in our one-year samples (A) and one-year (1Y) versus four-year (4Y) field exposure of USB biochar in sandy loam soils (B) with different biochar treatments indicated by varied colors.

N mineralization rates decreased in biochar treatments across soil textures (**Figure 2.2**).

Biochar treatments in loamy sands decreased the most, with CMS-75 treatments exhibiting N mineralization rates 2 times lower than control ($p = 1.72 \times 10^{-5}$). In both sandy loam and clay loam textures, higher biochar application rates had a larger negative effect on N mineralization rates. For example, within sandy loam textures, N mineralization rates were 61% lower for CMS-25 compared to control treatments ($p = 2.1 \times 10^{-6}$) while CMS-75 treatments were 89% lower ($p = 6.23 \times 10^{-9}$). Additionally, N mineralization rates in treatment USB-75 were 79% less than USB-25 ($p = 8.81 \times 10^{-5}$). In clay loams, N mineralization rates decreased more in the 75 Mg ha⁻¹ biochar treatments than the 25 Mg ha⁻¹ rate (all $p < 0.001$). Time aging did not appear to

affect N mineralization rates, however rates in four-year USB-25 treatments were 77% greater than one-year USB-25 ($p = 1.57 \times 10^{-4}$, **Figure S2.1**). Nitrogen mineralization rates were primarily driven by nitrification; although they were diminished by negative ammonification rates, especially in clay loam biochar treatments. In clay loam textures, all ammonification rates for treatments CMS-75, USB-25 and USB-75 were over 6 times lower than that in control treatments (all $p < 0.001$). Similar to N mineralization results, four-year USB-25 treatments had greater nitrification rates compared to one-year USB-25 treatments ($p = 7.69 \times 10^{-5}$), however did not significantly impact ammonification rates.

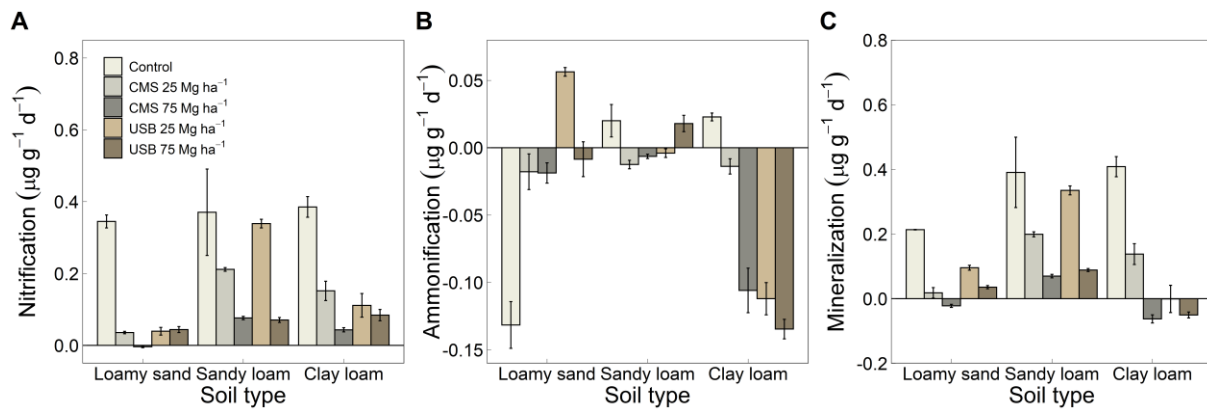


Figure 2.2 Means ± (SE) of nitrification (A), ammonification (B), and mineralization rates (C) from our 16-day lab incubation comparing different soil textures in one-year treatments with different biochar treatments indicated by varied colors.

2.4.2 Enzyme assays

BG activity in all three soils was elevated in the USB-75 treatment compared to both the control and USB-25 (**Figure 2.3A**, all $p < 0.05$). The sandy loam had the largest effect size with BG activity 117% greater in USB-75 compared to the control ($p = 8.35 \times 10^{-8}$) and the clay loam had the lowest effect size (60% greater, $p = 4.4 \times 10^{-4}$). However, the greatest difference between USB application rates occurred in the loamy sand where BG activity in USB-75 was double that in USB-25 ($p = 7.9 \times 10^{-7}$). Four-year USB-75 treatments were similar; BG activity was 71% greater than the four-year control (**Figure 2.4A**, $p = 6.32 \times 10^{-3}$), even though activity was 34%

lower in four-year USB-75 treatments compared to one-year USB-75 treatments ($p = 2.41 \times 10^{-3}$).

CBH activity was also elevated in USB-75 treatments but was only statistically significant in the sandy loam and clay loam treatments (**Figure 2.3B**). In the sandy loam, CBH activity was 118% greater in USB-75 compared to control ($p = 6.58 \times 10^{-10}$) and 45% greater than USB-25 ($p = 3.49 \times 10^{-8}$). In the clay loam, CBH activity in USB-75 was 39% greater than control ($p = 5.82 \times 10^{-4}$) and 35% greater than USB-25 ($p = 1.52 \times 10^{-3}$). However, CBH activity in the clay loam was affected differently by CMS biochar with the 75 Mg ha⁻¹ concentration decreasing activity levels by 26% compared to the control ($p = 0.05$). Over time, CBH activity in four-year USB-75 treatments did not significantly differ from control or USB-25 (both $p > 0.05$), but activity rates were 53% lower than one-year USB-75 (**Figure 2.4B**, $p = 2.48 \times 10^{-4}$).

PHEN activity differed across soil types, although biochar treatments only had significant effects in the loamy sand (**Figure 2.3C**). Specifically, PHEN activity in USB-75 had the highest increase, being 97% greater than the control ($p = 4.93 \times 10^{-6}$) and CMS-75 was second, increasing by 79% ($p = 6.07 \times 10^{-5}$). There were no significant effects with time (**Figure 2.4C**). On the other hand, PER activity generally decreased in biochar treatments in the loamy sand and sandy loam (**Figure 2.3D**). Specifically, in the loamy sand PER activity was 23% lower in CMS-75 treatments compared to the control ($p = 0.04$). Conversely, PER activity in the clay loam increased in biochar treatments, with 34% greater activity in USB-75 treatments than the control ($p = 0.02$). Over time, biochar decreased activity levels by 54% in control treatments (**Figure**

2.4D, $p = 2.72 \times 10^{-5}$) and 49% in USB-25 treatments ($p = 1.48 \times 10^{-4}$), however four-year treatments did not significantly differ from one another (all $p \geq 0.05$).

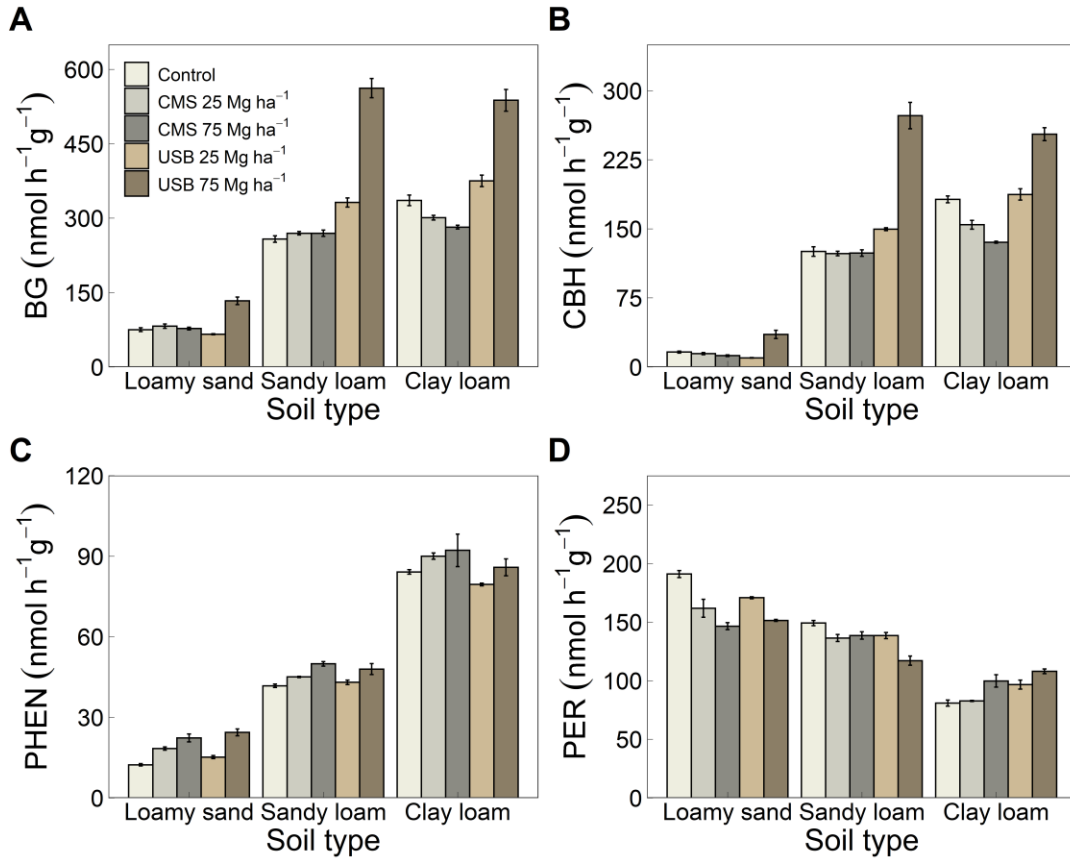


Figure 2.3 Means \pm (SE) of potential enzyme activity rates related to C acquisition from labile C sources such as cellulose (BG, A and CBH, B) or recalcitrant C sources such as lignin (PHEN, C and PER, D) across different soil textures in one-year samples. Different biochar treatments are indicated by varied colors.

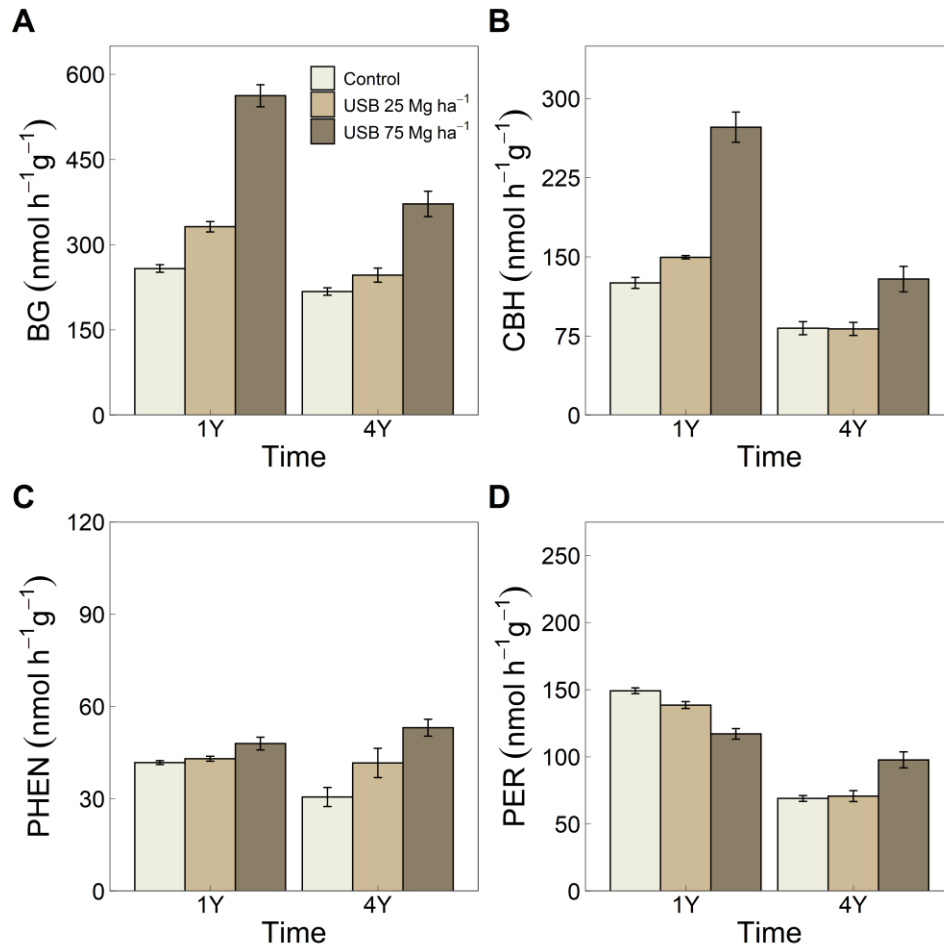


Figure 2.4 Means ± (SE) of potential enzyme activity rates related to C acquisition from labile C sources such as cellulose (BG, A and CBH, B) or recalcitrant C sources such as lignin (PHEN, C and PER, D) across one-year (1Y) and four-year (4Y) samples for USB treatments in the sandy loam soil. Different biochar treatments are indicated by varied colors.

LAP activity was affected by biochar treatments in all three soil types, with USB-75 having the largest effect sizes (**Figure 2.5A**). In the loamy sand, all biochar treatments significantly increased LAP activity compared to the control with greater increases in the 75 Mg ha⁻¹ application rate ($p = 6.01 \times 10^{-6}$ and 3.96×10^{-18} , for CMS and USB respectively). Additionally, LAP activity increased to a greater extent in USB treatments compared to CMS. For example, LAP activity in USB-75 was over 20 times greater than activity in control treatments ($p = 7.69 \times 10^{-20}$) while activity in CMS-75 was only about 2 times greater than

control treatments ($p = 3.41 \times 10^{-15}$). Out of all the treatments, LAP activity was the highest in USB-75 in the sandy loam. However, compared to the control, the effect size was not as large as in the loamy sand with LAP activity in USB-75 increasing by 272% ($p = 4.58 \times 10^{-9}$). The clay loam had the smallest increases with LAP activity increasing by 140% in USB-75 compared to the control ($p = 2.16 \times 10^{-6}$). Over time, biochar treatments significantly affected NAG activity in the sandy loam (**Figure 2.5B**). Four-year NAG activity was 108% greater in USB-75 compared to control ($p = 3.31 \times 10^{-6}$) and 45% greater than USB-25 treatments ($p = 1.0 \times 10^{-4}$). Four-year USB-75 treatments were also 59% greater in NAG activity compared to four-year USB-25 treatments (**Figure 2.6B**, $p = 6.0 \times 10^{-4}$).

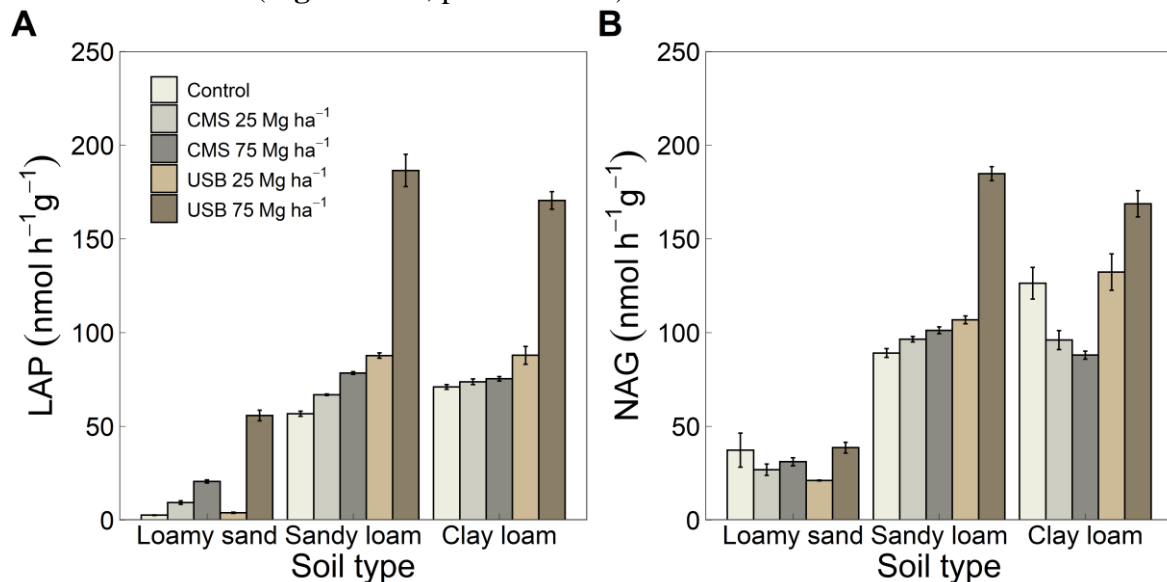


Figure 2.5 Means \pm (SE) of potential enzyme activity rates related to N acquisition from N sources such as protein (LAP, A) or chitin (NAG, B) across soil textures in one-year samples. Different biochar treatments are indicated by varied colors.

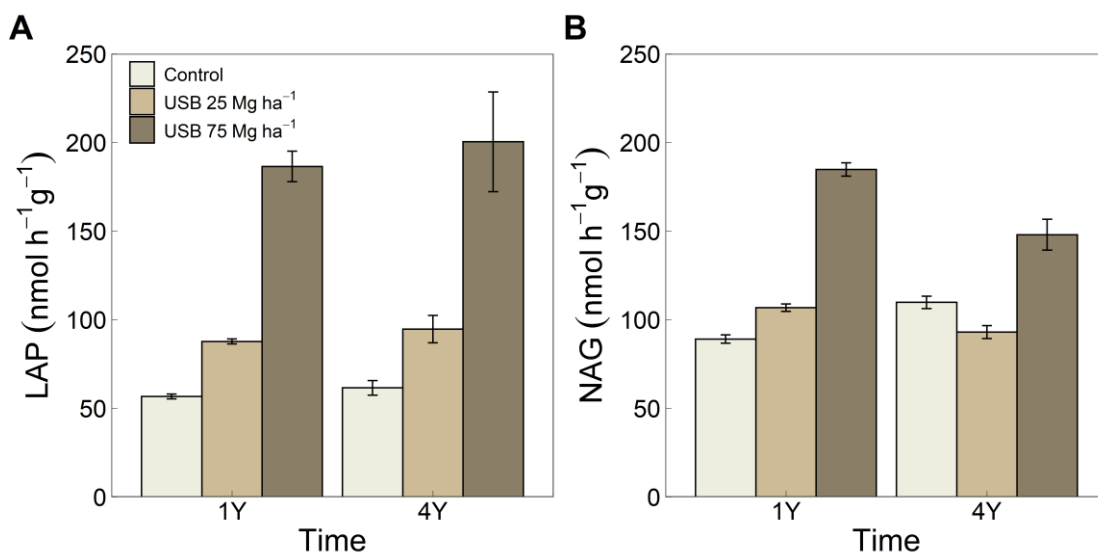


Figure 2.6 Means ± (SE) of potential enzyme activity rates related to N acquisition from N sources such as protein (LAP, A) or chitin (NAG, B) across one-year (1Y) and four-year (4Y) samples for USB treatments in the sandy loam. Different biochar treatments are indicated by varied colors.

All biochar treatments significantly affected PHOS activity in the sandy loam, but only USB-75 appeared to affect PHOS in the clay loam (**Figure S2.2**). In the sandy loam, CMS and USB biochar both increased PHOS activity compared to the control, with greater increases in the 75 Mg ha⁻¹ application rate ($p = 0.05$, 2.28×10^{-5}). In fact, PHOS activity in CMS-75 and USB-75 was 2 and 3 times respectively, greater than the control ($p = 5.58 \times 10^{-4}$, 1.55×10^{-9}). Over time, PHOS activity decreased in four-year USB-75 treatments by 39% compared to the one-year samples ($p = 0.02$), however activity in four-year USB-75 treatments was still 2 times greater than the four-year control ($p = 0.04$). In the clay loam, PHOS activity was 39% greater in USB-75 compared to the control ($p = 5.83 \times 10^{-4}$) and 46% greater than USB-25 ($p = 1.55 \times 10^{-4}$).

2.4.3 DOC & TDN

Biochars had negative effects on DOC concentrations in the loamy sand, however they did not significantly affect DOC in the other soil types (**Figure 2.7A**). In the loamy sand treatments, DOC decreased with biochar application by 36% ($p = 7.85 \times 10^{-3}$) and 42% ($p = 7.9$

$\times 10^{-4}$) for CMS-25 and CMS-75, respectively and by 43% for USB-75 ($p = 6.06 \times 10^{-4}$). Additionally, DOC concentration decreased with greater USB application rates ($p = 7.85 \times 10^{-3}$). Four-year USB-25 treatments were 33% lower in DOC than the four-year control (**Figure 2.7B**, $p = 0.05$). Total dissolved N was most strongly affected by biochar in the loamy sand treatments, however response to biochar was not consistent across soil types (**Figure 2.7C**). Total dissolved N decreased in both CMS and USB (all $p < 0.05$) treatments in the loamy sand with larger decreases (34% and 49% for CMS and USB, respectively) in the higher application rate ($p = 4.94 \times 10^{-5}$, 8.4×10^{-8}). In four-year treatments, TDN was greater than one-year samples (**Figure 2.7D**), with control and USB-75 treatments increasing by 86% and 125% respectively compared to their one-year treatments ($p = 0.04$ and 0.01 , respectively). Additionally, TDN in four-year USB-25 treatments was 38% and 64% less than the four-year control and USB-75 respectively (both $p = 0.05$), but this relationship did not exist for one-year samples.

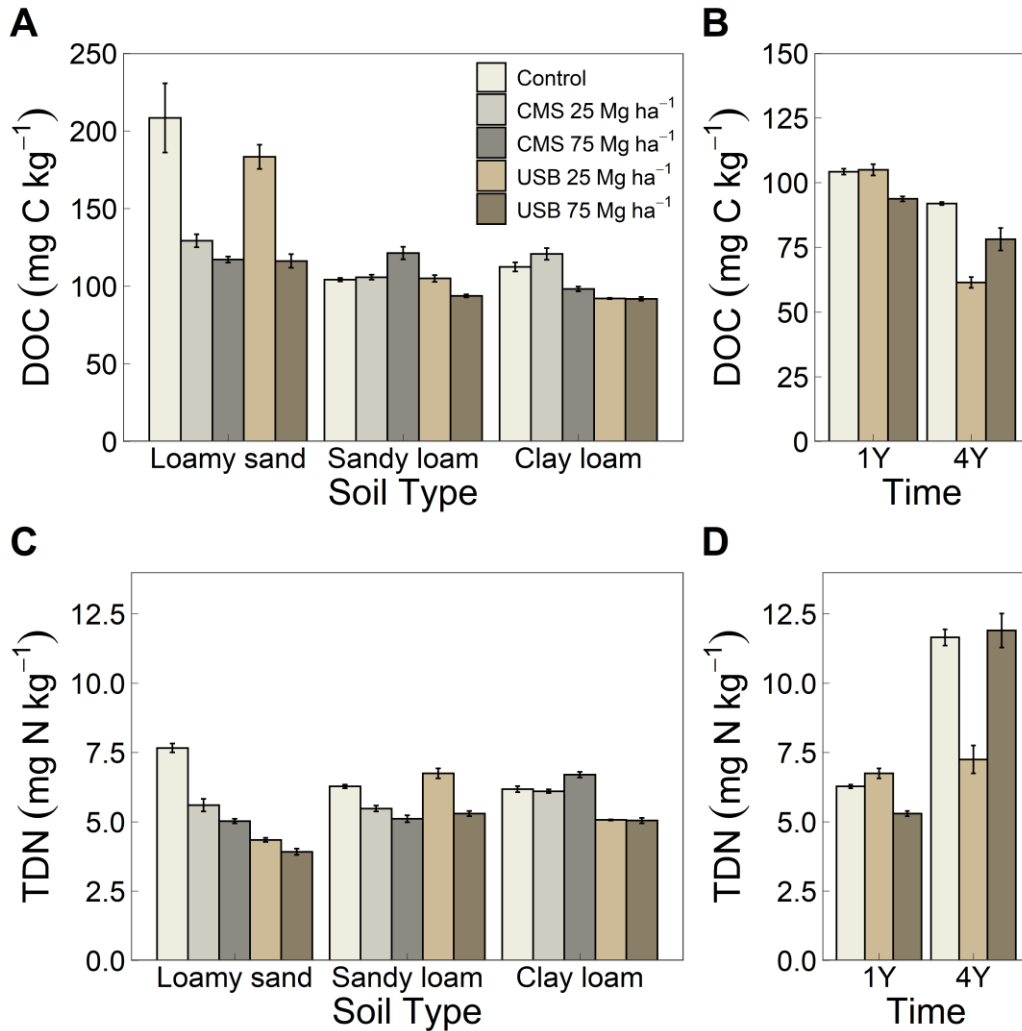


Figure 2.7 Means \pm (SE) of dissolved organic carbon (DOC) (A, B) and total dissolved nitrogen (TDN) (C, D) comparing different soil textures in our one-year samples (A, C) and one-year (1Y) versus four-year (4Y) field exposure of USB biochar in sandy loam soils (B, D) with different biochar treatments indicated by varied colors.

2.4.4 pH

Biochar treatments affected one-year soil pH more strongly in the coarser-textured soils and higher application rates generally led to greater pH (**Figure S2.3**). For example, in the loamy sand, pH was 10% and 25% greater for CMS-25 and CMS-75 when compared to the control ($p = 1.65 \times 10^{-5}$ and 2.94×10^{-14} , respectively). Treatment USB-75 also had greater pH than the control in loamy sand treatments, though not to the same extent as CMS-75 (13% increase, $p =$

1.38×10^{-7}). Additionally, CMS-75 had 14% greater pH than CMS-25 ($p = 9.52 \times 10^{-9}$) and pH in USB-75 was 8% greater than USB-25 ($p = 1.41 \times 10^{-4}$). In the sandy loam, CMS-75 treatment pH was 8% greater than the control treatment and 7% greater than the CMS-25 treatment ($p = 2.87 \times 10^{-5}$ and 3.08×10^{-4} , respectively). There were no significant effects on pH in four-year samples (**Figure S2.3**).

2.4.5 Root biomass

Neither biochar treatment, soil type, nor biochar \times soil type interaction significantly affected one-year root biomass results. However, root biomass in four-year control treatments was 144% greater than the one-year control ($p = 3.7 \times 10^{-3}$, **Figure S2.4**). Additionally, root biomass was 64% lower in four-year USB-25 compared to the four-year control treatments ($p = 6.84 \times 10^{-3}$).

2.4.6 Water-stable aggregates

Soil type consistently affected water stable aggregates with the finer soil texture containing a greater proportion of macroaggregates (> 2 mm) (**Figure 2.8A**) while the coarser soil contained more mesoaggregates (250 $\mu\text{m} - 2$ mm) (**Figure 2.8B**). However, only USB biochar appeared to have any significant effects on aggregate size and only in macroaggregates, large microaggregates (53 – 250 μm), and microaggregates (< 53 μm). Water stable macroaggregates in loamy sands increased with USB application by 2 and 2.5 times for rates 25 Mg ha^{-1} ($p = 0.05$) and 75 Mg ha^{-1} ($p = 0.001$), respectively compared to control treatments, whereas large microaggregates decreased with USB-25 and USB-75 by about 35% each ($p = 2.03 \times 10^{-5}$ and 4.34×10^{-5} , respectively; **Figure 2.8C**). Microaggregate proportion in clay loams increased by 34% in USB-75 compared to the control ($p = 1.69 \times 10^{-3}$), however USB-25 did not differ significantly from the control ($p \geq 0.05$). Over time, macroaggregate proportions increased

and mesoaggregates decreased for both biochar and the control treatments, although the control treatments had the largest changes (**Figure 2.9**). Four-year control treatments increased macroaggregate percentages by 40% and decreased mesoaggregate percentages by 18% ($p = 2.42 \times 10^{-3}$ and 1.48×10^{-4} , respectively). There were no significant effects of biochar or time on MWD (all $p \geq 0.05$), though finer soil textures generally had greater MWDs (**Figure S2.5**).

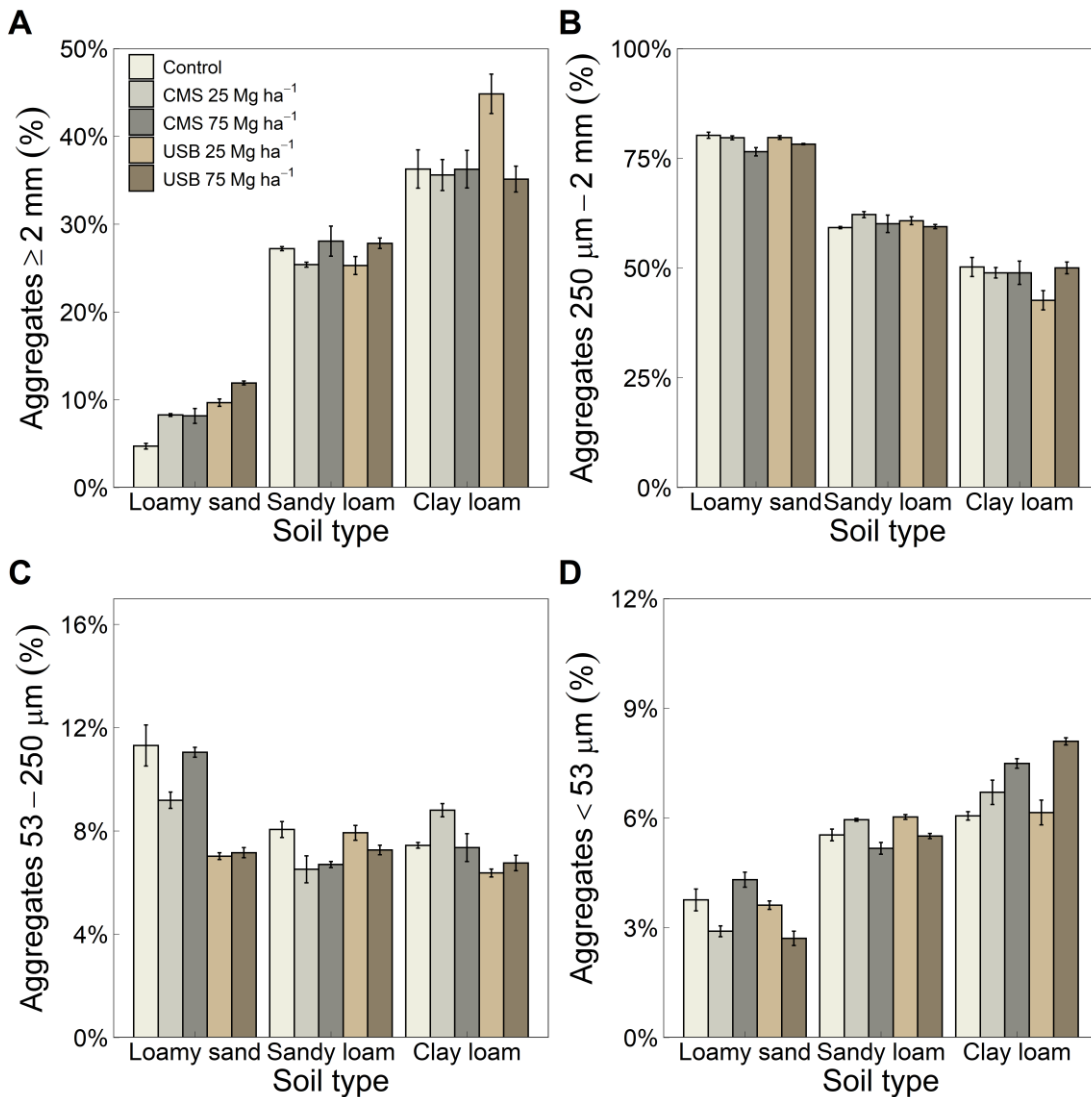


Figure 2.8 Means ± (SE) of water stable aggregate proportions (%) for one-year samples compared across soil textures with macroaggregates (≥ 2 mm) (A), mesoaggregates ($250 \mu\text{m} - 2$ mm) (B), large microaggregates ($53 - 250 \mu\text{m}$) (C) and microaggregates ($< 53 \mu\text{m}$) (D). Biochar treatments are indicated by varied colors.

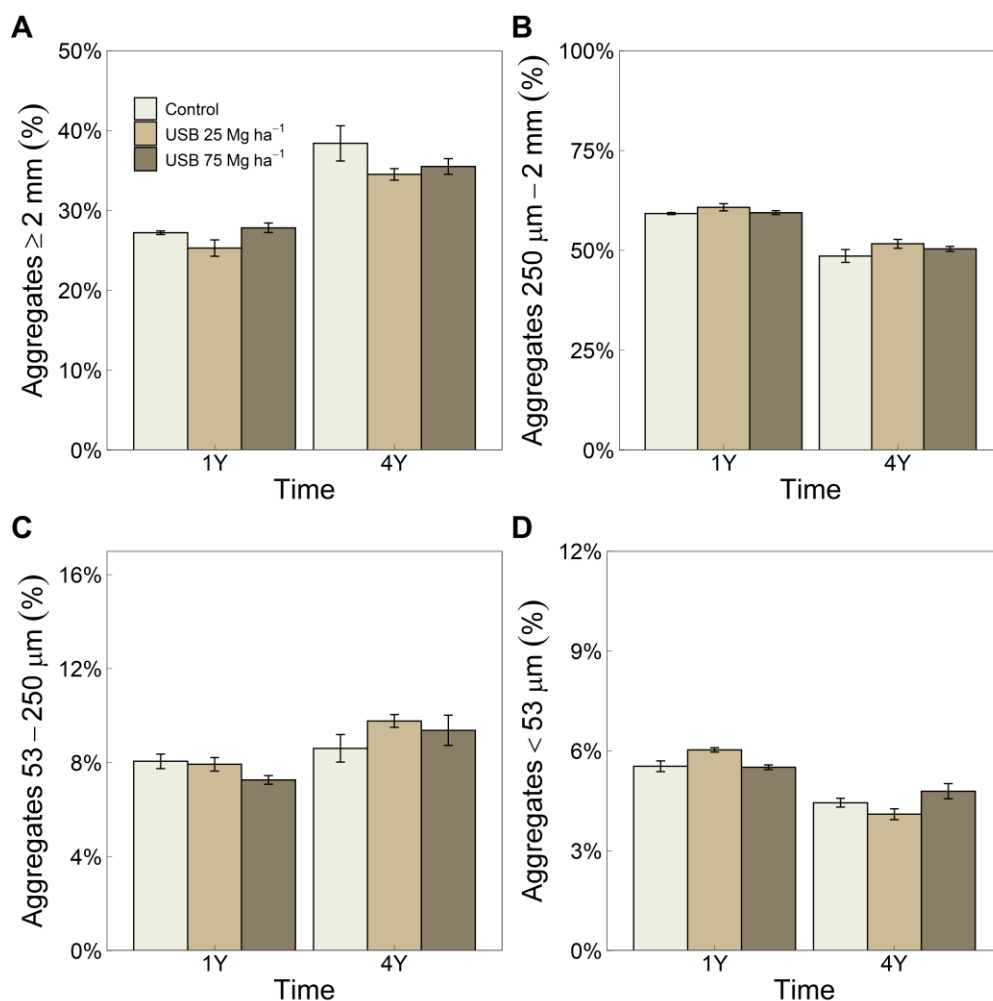


Figure 2.9 Means ± (SE) of water stable aggregate proportions (%) for one-year (1Y) versus four-year (4Y) samples for USB treatments in the sandy loam with macroaggregates (≥ 2 mm) (A), mesoaggregates (250 μm – 2 mm) (B), large microaggregates (53 – 250 μm) (C) and microaggregates (< 53 μm) (D). Biochar treatments are indicated by varied colors.

2.4.7 EDX

USB biochar did not significantly affect C concentrations on soil aggregate surfaces when compared to control treatments (all $p \geq 0.05$). However, C concentrations in four-year USB biochar treatments were 28% less than one-year USB biochar treatments (**Figure S2.6**, $p = 8.61 \times 10^{-3}$). There were no significant effects by biochar or time on silicon, aluminum, or iron concentrations on aggregate surfaces (all $p \geq 0.05$).

2.4.8 Soil porosity + POM

For the intact four-year samples, USB 25 Mg ha⁻¹ treatments had greater soil porosity compared to the control ($p = 0.02$), however the USB 75 Mg ha⁻¹ rate had no significant impact (**Figure S2.8**). For POM, the lower application rate decreased total POM compared to the control ($p = 3.15 \times 10^{-7}$) although the upper application rate increased total POM ($p = 3.24 \times 10^{-3}$). Particulate organic matter decreased with depth for all samples, however it decreased the most (compared to the control and USB 25 Mg ha⁻¹) in the USB 75 Mg ha⁻¹ treatments.

2.4.9 Total soil C & N

In all three soils, biochars increased bulk soil C concentrations, with greater increases for the 75 Mg ha⁻¹ rate and USB biochar (**Figure 2.10B**). Total C increased the most in biochar treatments in the sandy loam; specifically, CMS-75 and USB-75 treatments were 90% and 137% greater in total C compared to the control ($p = 3.21 \times 10^{-4}$ and 3.2×10^{-7} , respectively) and 44% and 77% greater than their respective 25 Mg ha⁻¹ treatments ($p = 0.02$ and 5.04×10^{-5}). Four-year USB-75 treatments increased bulk soil C concentrations by 103% ($p = 3.17 \times 10^{-4}$) compared to the four-year control. Total N in CMS-75 treatments was 44-92% greater than the control in all soil types (all $p < 0.01$), with the largest difference in the sandy loam (**Figure 2.10D**). Although, there were no significant effects of time on total N in biochar treatments (all $p > 0.05$). Based on estimated C concentrations in starting biochar and soil mixtures, substantial C was lost in biochar treatments (**Figure 2.10A, B**). USB treatments accrued the highest C losses, especially in the loamy sand, where both USB treatments lost over 40% of starting soil and biochar C. CMS treatments had minimal C loss in the sandy loam and clay loam, particularly in the 75 Mg ha⁻¹ application rates (< 5% starting C lost). Nitrogen loss was minimal except for the loamy sand,

where biochar treatments lost between 16-46% of starting soil and biochar N (**Figure 2.10C, D**).

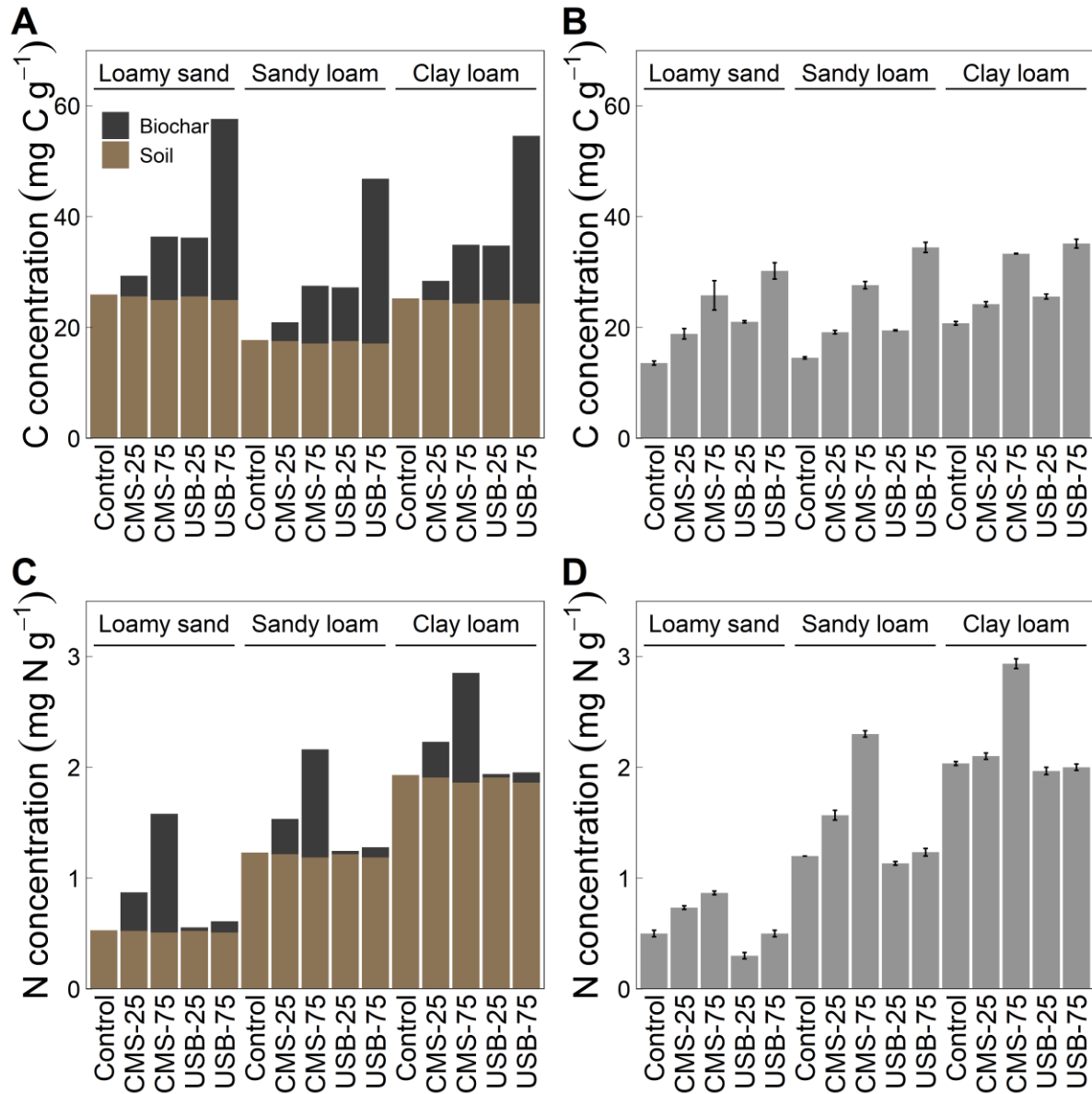


Figure 2.10 Means \pm (SE) of calculated soil C (A) and N (C) when mesocosms were constructed and total C (B) and N concentrations (D) in mesocosm soils after one-year. Soil texture is labeled above the bars, with a line extending across the five treatments in each soil texture, and biochar treatments are labeled across the x-axis. Estimated values for four-year samples were not calculated and thus not shown. Standard errors do not exist for estimated values and thus are not shown. This figure is primarily to show C and N loss over a one-year field incubation.

2.4.10 Soil fractions C

All biochar treatments significantly increased C in CPOM fractions across soil types, with larger increases for the 75 Mg ha⁻¹ application rate (all $p < 0.05$, **Figure 2.11**). While USB treatments generally had larger impact on C in CPOM fractions in the loamy sand and sandy loam, in the clay loam USB and CMS increased C concentrations relatively to the same extent. For example, C in CPOM fractions in the clay loam was about 3.5 times greater in both biochar 25 Mg ha⁻¹ treatments compared to the control (both $p < 1.0 \times 10^{-7}$) and about 8.75 times greater for 75 Mg ha⁻¹ treatments (both $p < 1.0 \times 10^{-12}$). Biochar treatments had the lowest effect size in the loamy sand, although all treatments still increased C concentrations in CPOM fractions by over 2 times (all $p \leq 1.0 \times 10^{-4}$). These trends also continued over time in four-year treatments, however to a lesser extent (**Figure 2.11**). For example, four-year USB-25 and USB-75 treatments increased C concentrations in CPOM fractions by 183% and 415%, ($p = 6.65 \times 10^{-3}$ and 1.63×10^{-4} , respectively) whereas one-year samples increased concentrations by 246% and 943% ($p = 5.57 \times 10^{-8}$ and 2.19×10^{-14}), respectively. While C concentrations in FPOM fractions also increased in biochar treatments, and more so for higher biochar application rates, these differences were not as large as those in CPOM fractions (**Figure 2.11**). Over time, FPOM C concentrations were 92% greater in four-year USB-75 treatments ($p = 5.37 \times 10^{-4}$), which was a slight increase from the one-year samples effect size (83%, $p = 1.89 \times 10^{-10}$). Biochar treatments did not significantly alter C concentrations in the one-year silt + clay fractions (all $p \geq 0.05$); however, four-year USB-75 treatments were 18% greater in C than both one-year USB-75 treatments and the four-year control (both $p < 0.01$).

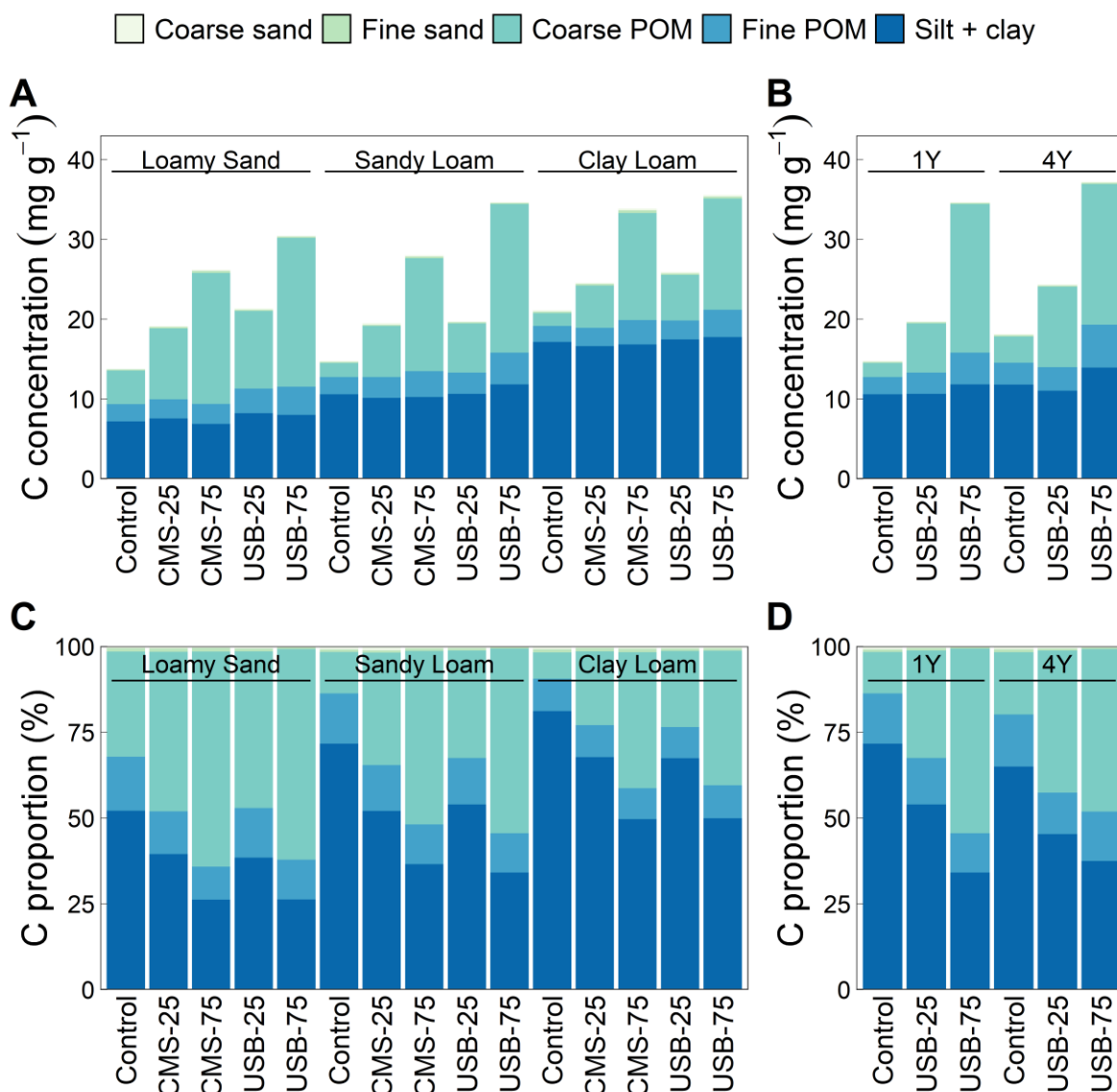


Figure 2.11 Means of soil C concentrations, total and by soil fractions, across different soil textures in one-year samples (A) and one-year (1Y) versus four-year (4Y) field exposure of USB biochar in sandy loam soils (B) or C proportions (%) by soil fractions, across different soil textures in one-year samples (C) and one-year (1Y) versus four-years (4Y) field exposure of USB biochar in sandy loam soils (D). Soil C concentrations (A, B) are measured in mg per C per dry gram of soil, while C proportions (C, D) shows the percentage each fraction contributes to bulk soil C. The different fractions are displayed with varied colors. For one-year treatment panels (A, C), soil texture is labeled above the bars, with a line extending across the five treatments in each soil texture, and biochar treatments are labeled across the x-axis. For one-year versus four-year treatment panels (B, D), time is labeled above the bars and biochar treatments are labeled across the x-axis.

2.4.11 FTIR-DRIFT

In all three soils, biochar treatments had greater aromatic to aliphatic C peak area ratios in both CPOM and FPOM fractions, with greater increases for 75 Mg ha⁻¹ application rates (**Table 2.1**). These increases were greater in CPOM fractions and in sandy loam or clay loam soils. Specifically, the W4:W1 ratio for the CPOM fraction was over 10 times greater in USB-75 and CMS-75 treatments compared to the control in both the sandy loam and clay loam (all $p < 0.01$). Over time, biochar treatments continued to have greater ratios in the CPOM fraction, albeit to a lesser extent compared to one-year samples, and four-year USB-25 treatments had larger increases. This trend was not observed for four-year treatments in the FPOM fraction, which maintained greater ratios for the 75 Mg ha⁻¹ application rate and had greater differences between biochar treatments and the control compared to one-year samples.

Table 2.1 Means \pm (SE) of FTIR-DRIFT peak area ratios of aromatic to aliphatic C compounds for POM fractions. We used W3:W1 and W4:W1 (see Table S2.1 for region assignments) ratios based on Demyan et al., 2012. Bolded values indicate significant statistical differences ($p < 0.05$) from the treatments respective soil type control treatment (i.e., for W3:W1, ratios in the loamy sand CMS-75 treatments are significantly different than those in the loamy sand control).

	Coarse POM		Fine POM	
	W3 : W1	W4 : W1	W3 : W1	W4 : W1
<i>Loamy sand, one-year</i>				
Control	0.99 \pm 0.07	0.62 \pm 0.04	1.02 \pm 0.05	0.59 \pm 0.03
CMS-25	2.38 \pm 0.25	1.82 \pm 0.21	1.25 \pm 0.03	0.75 \pm 0.03
CMS-75	4.43 \pm 0.48	3.66 \pm 0.36	1.77 \pm 0.12	1.18 \pm 0.09
USB-25	1.83 \pm 0.25	1.22 \pm 0.19	1.37 \pm 0.05	0.82 \pm 0.05
USB-75	4.6 \pm 1.22	3.17 \pm 0.92	1.94 \pm 0.18	1.2 \pm 0.11
<i>Sandy loam, one-year</i>				
Control	1.07 \pm 0.02	0.63 \pm 0.02	1.11 \pm 0.04	0.66 \pm 0.03
CMS-25	5.08 \pm 1.51	3.81 \pm 1.14	1.48 \pm 0.04	0.9 \pm 0.03
CMS-75	10.69 \pm 1.22	8.21 \pm 0.58	2.18 \pm 0.03	1.43 \pm 0.02
USB-25	7.22 \pm 2.11	4.8 \pm 1.4	2.04 \pm 0.12	1.24 \pm 0.07
USB-75	8.98 \pm 4.62	5.93 \pm 3.12	2.64 \pm 0.84	1.66 \pm 0.59
<i>Clay loam, one-year</i>				
Control	1.09 \pm 0.04	0.61 \pm 0.03	1.43 \pm 0.14	0.85 \pm 0.1
CMS-25	3.41 \pm 0.65	2.54 \pm 0.49	1.74 \pm 0.23	1.07 \pm 0.16
CMS-75	11.56 \pm 3.02	9.52 \pm 2.35	2.63 \pm 0.37	1.73 \pm 0.23
USB-25	4.45 \pm 0.61	2.96 \pm 0.46	2.54 \pm 0.48	1.59 \pm 0.34
USB-75	12.33 \pm 5.45	8.57 \pm 3.84	3.19 \pm 0.11	2 \pm 0.09
<i>Sandy loam, four-year</i>				
Control	1.32 \pm 0.09	0.75 \pm 0.06	1.31 \pm 0.08	0.79 \pm 0.06
USB-25	11.16 \pm 3.36	7.6 \pm 2.32	3.39 \pm 0.59	2.16 \pm 0.39
USB-75	8.48 \pm 1.57	5.67 \pm 1.03	4.38 \pm 1.05	2.91 \pm 0.76

2.5 DISCUSSION

After a year incubating in the field, biochar treatments affected biological, chemical, and physical soil properties that, in turn, altered C stabilization processes. Soil type influenced biochar treatment effect size and direction (positive/negative) with the loamy sand and sandy loam having more similar responses than the clay loam and the loamy sand having the most significant changes. Higher biochar application rates and USB generally had larger effect sizes

and time both intensified and minimized biochar's effects depending on the response variable. In the following discussion, we describe how biochar treatments may have altered underlying C stabilization processes and how these changes differed across soil types.

2.5.1 Priming effect

Microbes produce extracellular enzymes to breakdown C and other nutrients in organic matter into smaller, more assimilable molecules (Wallenstein and Weintraub, 2008). Adding a new C or nutrient source, such as biochar, to soil can temporarily increase microbial decomposition rates and induce native SOM decomposition, a process called positive priming (Kuzyakov et al., 2000). While biochar can positively prime soils initially, after the labile C is depleted, biochar may decrease microbial decomposition rates (i.e., negative priming) by sorbing DOC, and increasing aggregation and organo-mineral associations (Fang et al., 2015; Maestrini et al., 2015; Cheng et al., 2017). Thus, negative priming evidence in biochar treatments can help explain stabilization processes.

In our loamy sand and sandy loam soils, most one-year biochar treatments did not differ from the controls for CO₂ flux rates or labile C enzyme activity, suggesting that initial positive priming effects may have dissipated after a year in the field. However, after one year, USB-75 treatments still exhibited elevated CO₂ flux rates and labile C enzyme activities in the loamy sand and sandy loam and these trends continued even after four years in the sandy loam (i.e., four-year treatments). In contrast, a recent meta-analysis reported a negative priming effect around 200 days after pyrogenic carbon (i.e., biochar) additions (Maestrini et al., 2015). Additionally, CO₂ flux rates in USB-75 treatments were likely driven by labile-C utilization as the two recalcitrant-C enzyme activities had either a small positive response (PHEN) to USB-75 treatments or a negative response (PER). Although the low impact and opposite PHEN/PER

responses mirror results from another experiment using a bamboo 600°C pyrolyzed biochar (Luo and Gu, 2016), labile C enzyme activity increases are surprising given that lignocellulosic and high pyrolysis temperature biochars typically have low labile C concentrations (Keiluweit et al., 2010; Zhao et al., 2014). Instead, minimal PER/PHEN activity and high BG/CBH activity in USB treatments corresponds with other research which found that initial biochar breakdown, and consequent availability of new C sources, led to aged treatments being dominated by a labile-C cycling microbial community (Zimmermann et al., 2012). Another possibility is that biochar may indirectly positively prime soils by affecting plant growth (Jeffery et al., 2011), as plants can release C sources through root exudates or respiration and trigger SOM decomposition (Bird et al., 2011). However, we did not see significant effects of biochar treatments on root biomass. Ultimately, the positive priming in USB-75 treatments may decrease biochar residence times and C stabilization in our loamy sand and sandy loam soils.

CMS treatments in the clay loam indicated negative priming (e.g., decreased CO₂ flux rates and labile C enzyme activities). Higher temperature biochars can cause negative priming in soils with more clay, possibly due to increased organo-mineral associations (Fang et al., 2015). Other work has found negative soil priming in biochar treatments because of increased C stabilization via organo-mineral associations in biochar treatments as well as sorption of plant-C from root exudates to biochar surfaces (Weng et al., 2017). Additionally, the non-significant trend toward increased lignin-degrading enzyme activities in CMS treatments suggest microbial community shifted towards species which utilize the biochar recalcitrant C sources (Zimmermann et al., 2012). It is also possible that leached heavy metals and polyaromatic hydrocarbons (**Figure S2.7**) from CMS could have negatively impacted microbial processes (Dutta et al., 2017). However, this is unlikely as biochar contaminant bioavailability is generally

thought to be low (Hilber et al., 2017) and original feedstocks leach more than their biochar counterparts (Lu et al., 2016). Thus, negative soil priming in CMS treatments in the clay loam likely indicates soil stabilization processes.

2.5.2 Biochar sorption & leaching

Negative soil priming can arise when biochar pores absorb dissolved organic matter (DOM) (Zimmerman et al., 2011). This process decreases availability of highly mobile C and nutrients and therefore can decrease microbial decomposition rates (Zimmerman et al., 2011). However, the significant decreases in DOC and TDN indicate possible sorption in biochar treatments in the loamy sand, which did not exhibit negative priming. Instead, increased soil pH caused by biochar addition, a common effect in acidic soils (Jeffery et al., 2011; Pandit et al., 2018), may have induced native soil to release DOC/TDN (Andersson and Gahnstrom, 1985; Smebye et al., 2016). Previous work has found biochar to both trigger soil DOM release and also absorb the newly available source (Smebye et al., 2016; Feng et al., 2021), with higher temperature biochars absorbing more (Feng et al., 2021). Pore size typically determines DOM sorption to biochars; specifically micropore (< 2 nm) presence limits sorption (Kasozi et al., 2010; Smebye et al., 2016; Feng et al., 2021). Biochars produced at 500°C have better developed porosity and absorption compared to lower temperature (200°C) biochars, whereas 900°C biochars generally have larger average pore size, but less absorptive capability than 500°C chars (Fu et al., 2009). Thus, both CMS (650°C) and USB (550°C) should have strong adsorptive capabilities, indicated by the similar effect size on DOC/TDN in the loamy sand. However, our study did not assess biochar porosity.

Alternatively, DOM mobility causes leaching (Hussain et al., 2020), and decreases in biochar treatments may instead reflect DOM losses during the one-year incubation. Major et al.,

(2010) found DOC leaching to increase with black carbon (i.e., biochar) additions in a sandy clay loam. While some of the leached DOC came from the black carbon specifically, native DOC leaching from soil sources also increased in black carbon treatments (Major et al., 2010). Although DOM sorption within biochar pores could prevent leaching and thus retain C for microbes within the environment, sorbed DOM stability may not persist long-term. Aging processes can fragment biochar structure (de la Rosa et al., 2018), thereby releasing DOM from pores and consequently increasing microbial activity. This aligns with the extracellular enzyme activity response we observed with four-year USB-75 treatments in the sandy loam.

2.5.3 N sorption & immobilization

Both biochars decreased N mineralization rates while also increasing N-acquiring enzyme activities, and effects increased with application rates. This suggests biochar decreased NO_3^- and NH_4^+ soil concentrations but not organic N breakdown. Such decreases may also be due to sorption processes. While both NO_3^- and NH_4^+ availabilities generally decrease with biochar amendment (Gao et al., 2019), adsorption depends on functional groups present on biochar surfaces, biochar cation and anion exchange capacities, and soil pH (Lehmann et al., 2003; Sarkhot et al., 2013; Lawrinenko and Laird, 2015; Fidel et al., 2018). For example, ammonification rates decreased the most in biochar treatments in the clay loam potentially because NH_4^+ adsorption is maximized at neutral pH (Fidel et al., 2018). Additionally, decreasing N availability has been found to enhance decomposition and microbial biomass (Treseder, 2008), which corresponds with our enzyme activities and CO_2 flux rates. Thus, sorption may allow biochar to act as a N sink by maintaining biological activities and decreasing inorganic N loss over time (Robertson and Groffman, 2006). For agroecosystems, which typically lose N to leaching and runoff, N retention can improve plant health and productivity

(Mobley et al., 2014). This effect may also depend on soil type, as we found little change in total N after a year of biochar treatments in our sandy loam and clay loam, but some decreases in the loamy sand.

Biochar may have also enhanced microbial N immobilization, evidenced by the negative net mineralization rates observed in the clay loam and loamy sand (Lentz et al., 2014). Nitrogen immobilization occurs when organic matter is low in N and therefore microbes retain N in their biomass for their own metabolic processes (Robertson and Groffman, 2006). Substrate additions that are more recalcitrant or have high C:N ratios (greater than 25:1) can trigger N immobilization, as N becomes a limiting factor for microbial processes (Janssen, 1996; Robertson and Groffman, 2006). Thus, biochar has been found to cause N immobilization with prevalence among lignocellulosic and high pyrolysis biochars (Zheng et al., 2013; Lentz et al., 2014; Ameloot et al., 2015; Luo et al., 2016). We found both biochars to potentially induce N immobilization, despite CMS having a C:N ratio lower than 25:1 (~10:1), possibly because biochar N sources were more stable due to high pyrolysis temperatures (Xu et al., 2021). Additionally, the more negative net mineralization rates in treatments with higher biochar application rates were likely caused by increased quantity of a high-C, low-N substrate. However, lower CO₂ flux usually correlates with N immobilization (Lentz et al., 2014), and this was variable for our treatments, suggesting some N mineralization decreases might instead be due to sorption and/or leaching processes. Furthermore, long-term sustained N immobilization is unlikely as biochar effects on N cycling have been found to be transient after initial labile-C sources are depleted and pH changes dissipate (Nelissen et al., 2015). We did not observe N immobilization in our sandy loam after one or four years so we could not determine longer-term

effects. Thus, our results suggest that these potential temporary biochar effects on N cycling can still occur after one year in the field in specific soil types.

2.5.4 Aggregation

Biochar can form larger-sized aggregates in the soil by binding with silt and clay particles (Brodowski et al., 2006; Du et al., 2017). For example, when manure-based biochar was applied to a silt-loam soil, Clark et al. (2019) found macroaggregates (> 2 mm) to increase and the silt + clay fraction (< 53 μm) to decrease which they attributed to biochar binding with clay and silt particles into larger aggregates. They did not observe this for their sandy soil likely because it had less clay and silt (Clark et al., 2019). In our loamy sand, USB increased water stable macroaggregates (> 2 mm) and decreased large microaggregates ($53 - 250$ μm) but did not significantly affect silt + clay sized aggregates (< 53 μm). Thus, macroaggregates may have formed when microbes decomposed fresh biochar residues and produced binding agents (Six et al., 2000), however there was low turnover into large microaggregates due to lower clay content and microbial activity in our sandier soil. The smaller aggregates made within macroaggregates contain older POM and may be more stable (Jastrow et al., 1996; Six et al., 2000), thus macroaggregate turnover is an important process for SOM protection. However, this progression may occur on a longer time scale than our one-year incubation. Therefore, while biochar may have induced large aggregates to form in our loamy sand, we did not observe increased turnover of stabilized smaller aggregates. On the other hand, in our clay loam, USB increased microaggregates (< 53 μm), or the clay + silt size aggregates, similar to other results from soils with more clay and silt (Brodowski et al., 2006; Chen et al., 2020). Therefore, in clay and silty soils biochar may stabilize SOM longer-term by increasing microaggregate presence.

Despite these potential changes to aggregation processes, biochar treatments did not affect aggregate stability (i.e., MWD) after one or four years of aging. Biochar can improve aggregate stability by altering microbial communities and activity and therefore formation and binding of aggregates (Wang et al., 2017). Additionally, biochar can alter soil physical properties such as soil pores and particle surface area which can benefit aggregate stability through increased bond formation and water holding capacity (Ajayi et al., 2016). However, our experimental time length may not be able to observe these effects in the field. For example, Zhang et. al., (2015) did not observe changes to aggregate stability in biochar treatments after one-year, although at the same field-site, four years later, Du et al., (2017) found biochar treatments to increase MWD, with greater values in the higher application rate. After four years in our sandy loam, USB treatments still did not affect MWD. While macroaggregates (> 2 mm) did increase with time, these increases were highest in treatments without biochar, suggesting USB may not improve aggregate stability long-term compared to control treatments. Root biomass was also greater in four-year control treatments, which may have aided macroaggregate formation (Ge et al., 2018). However, macroaggregate surfaces also had lower total C in four-year USB-25 treatments compared to one-year samples. Previous work has suggested these depleted C concentrations may be due to greater decomposition rates on aggregate surfaces (Amelung and Zech, 1996) or surface C transformation and incorporation within aggregates (Bol et al., 2004). Thus, USB at lower application rates (albeit we did not test higher applications) could be increasing C stability, although additional data on C composition within aggregates would be necessary to make further statements on C stabilized in aggregates.

2.5.5 Organo-mineral associations + biochar recalcitrance

Soil organic matter can be protected longer-term by forming chemical interactions with soil minerals, such as clay or silt particles (Lützow et al., 2006). These organo-mineral associations may be enhanced in biochar-amended soils (Liang et al., 2008; Paetsch et al., 2017) because of both direct (e.g., bonding with biochar surface functional groups, Fang et al., 2014) and indirect (e.g., changes to microbial biomass and C breakdown, Fang et al., 2018) biochar effects. For example, the Anthrosols of South America, soils amended with black C (i.e., biochar) up to 7,000 years ago, were found to contain more C in organo-mineral associations with clay particles than soils with no black carbon (Liang et al., 2008). Other work has found aromatic-C location to correlate with clay particle location in biochar-amended soil aggregates (Hernandez-Soriano et al., 2016) and the ways associations form to vary across mineral and biochar types (Yang et al., 2021). For this experiment, we assume C concentrations in the silt + clay fraction represent potential C in organo-mineral associations, however it is possible that fine particles in this fraction are not minerally-associated. Nonetheless, after one year, our biochar additions did not increase C stabilization through organo-mineral associations in any of our soils, however after four years in the sandy loam, there was more C in the silt + clay fraction of four-year USB-75 treatments than the four-year control. In some systems, one year may be adequate time for biochar to increase C in mineral associations; for example, Paetsch et al. (2017) found 5% of clay mineral associated-C to come from biochar (maize-based, 700°C) after one-year. In fact, newly added organic matter can form associations with soil minerals rapidly (e.g., within 30 days) (Kopittke et al., 2020); however, our results indicate that biochar may increase C in mineral associations after a longer time aging. As biochar ages, oxidative processes increase functional groups, such as carboxyls, on biochar particle surfaces, which can then interact with

soil minerals (Brodowski et al., 2005; Liu et al., 2013; Kopittke et al., 2020; Burgeon et al., 2021). Other work showed simulated four-year biochar to have significantly more carboxylic groups on biochar surfaces than biochar incubated in soil for one year (Liu et al., 2013). Thus, longer-term experiments are needed to quantify how biochar aging may lead to enhanced C stabilization via organo-mineral associations. Additionally, we found soils with greater clay content did not enhance associations, possibly because clay types have different C stabilizing capabilities (e.g., surface area, isomorphous substitution, cation exchange capacity) (Sarkar et al., 2018). Therefore, soil type is also an important factor in longer-term studies.

On the other hand, biochar decomposition may initially be controlled by its chemical structure (Liang et al., 2008; Lavalley et al., 2019). For example, in the study by Paetsch et al. (2017), authors found biochar shifted soil C storage from mineral fractions to POM fractions (free-floating and occluded in aggregates) after one year. Similarly, we found biochar-induced increases in total bulk soil C concentrations to mostly stem from greater C in CPOM fractions after one year, and this relationship continued over time (i.e., after four years in USB 75 Mg ha⁻¹ treatments). While we did not differentiate between POM protected in aggregates and free-floating POM, we found minimal biochar effects (only USB treatments) on aggregation processes. Thus, much of this C in POM samples may be free-floating and only protected from mineralization by its chemical recalcitrance. High aromatic to aliphatic C ratios and increases in labile C enzyme activities in USB biochar treatments also suggest biochar-C may be retained because of recalcitrant structure. However, the substantial C losses in biochar treatments over a one-year period suggest biochar-C was not well-protected and was mineralized or translocated offsite (i.e., via rain or DOM leaching, as downward migration within the soil is not possible given our mesocosm design, Major et al., 2010). Interestingly, USB treatments appeared to lose

more C than CMS; for example, CMS-75 treatments had greater total C soil concentrations than USB-25 treatments, despite both treatments adding approximately the same initial total C mass, due to the much lower C concentration in the ash-rich CMS biochar. CMS treatments did not increase aggregation nor C in organo-mineral associations, however these treatments had similar or lower microbial activity (C-acquiring enzyme rates and C flux rates) to the control. Thus, we propose that this low C, high pyrolysis temperature, municipal waste biochar contributed a greater proportion of C in stable forms in a loamy sand, a sandy loam, and a clay loam, which slowed SOM decomposition rates in a one-year period. This may stem from PAHs present in CMS biochar, which were much higher than USB treatments (**Figure S2.7**). Poly-aromatic hydrocarbon concentrations vary based on feedstock type and pyrolysis procedures, with higher concentrations in biochars produced from higher pyrolysis temperatures and fast pyrolysis (Wang et al., 2017). Their persistence in biochar and soil can depend on bioavailability (Wang et al., 2017), however biochar's role in absorbing and/or releasing PAHs is an emerging research question with varying results on its status as a sink or source (Quilliam et al., 2013). Thus, CMS may contain high PAH concentrations, although further work is needed to understand how this impacts C stabilization longer-term.

2.6 CONCLUSIONS

In conclusion, our research examined how different biochars applied at two rates can influence soil properties and therefore C stabilization mechanisms in three contrasting soils. The higher C biochar (i.e., USB) and higher application rate treatments (i.e., 75 Mg ha⁻¹) caused the greatest positive responses, especially in the coarsest-textured and lowest pH soil. While USB treatments did alter aggregation in the loamy sand and clay loam after one year, overall aggregate stability had still not improved after four years. Furthermore, C only increased in clay

+ silt fractions after four years (in USB treatments), indicating that organo-mineral associations with biochar may increase with time. Soil C loss in biochar treatments was substantial in one year, suggesting that initially biochar may be most protected from decomposition through its recalcitrant chemical structure. Interestingly, our low C and higher pyrolysis temperature biochar (i.e., CMS) retained more C compared to USB treatments, possibly through decreased microbial activity and its recalcitrant chemical structure. However, long-term USB treatments may stabilize more C via aggregation and organo-mineral associations.

Our study illustrates how varied management techniques can influence C stabilization mechanisms across different habitats, which is informative for the ongoing efforts to sequester C in soils and mitigate climate change impacts. Initially, our biochars chemical structure appeared to influence decomposition the most, however aggregate C and organo-mineral associations may increase over time. Increasing soil organic C pools can also improve structure and aggregation, water and/or nutrient retention, and rhizospheric processes all of which can impact agricultural productivity and therefore human health (Lal, 2016). Thus, our work has implications for soil health, or a soil system's ability to support plant, animal and human lives by maintaining environmental quality and biological production (Lal, 2016; Bünemann et al., 2018). In fact, many of our measured response variables are soil quality indicators used for assessing soil health (Bünemann et al., 2018). Therefore, by altering soil properties and C stabilization mechanisms, biochar may enhance long-term soil health and encourage sustainable agriculture practices.

APPENDIX

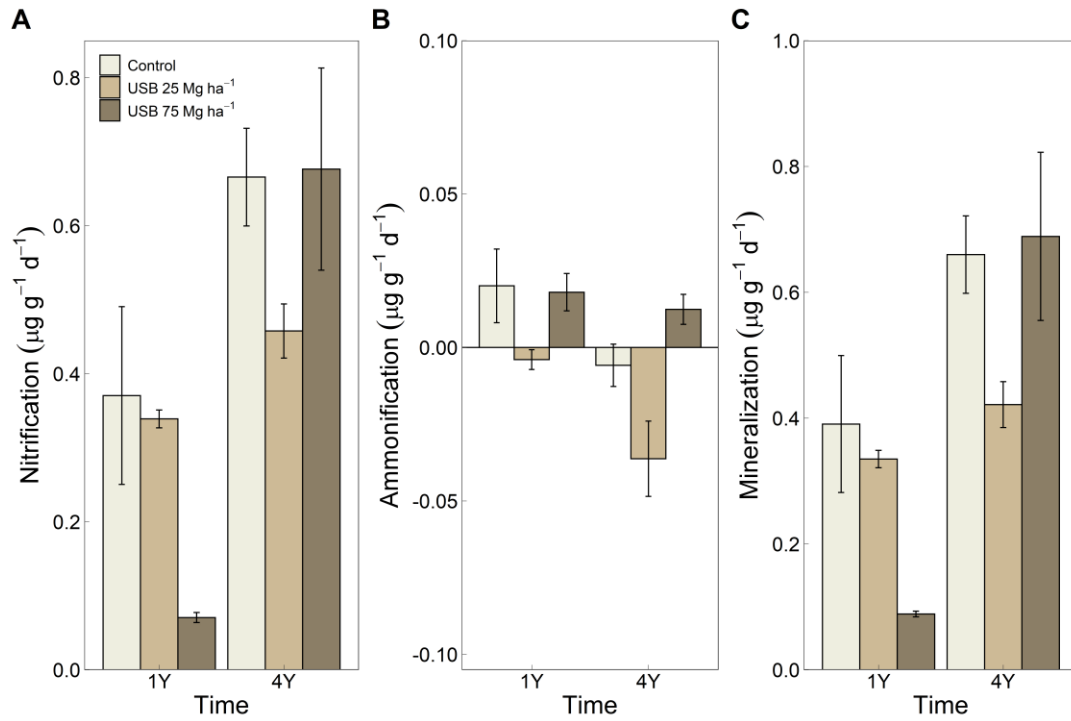


Figure S2.1 Means \pm (SE) of nitrification (A), ammonification (B), and mineralization rates (C) from our 16-day lab incubation comparing one-year (1Y) versus four-year (4Y) samples for USB treatments in the sandy loam soil. Different biochar treatments are indicated by the varied colors.

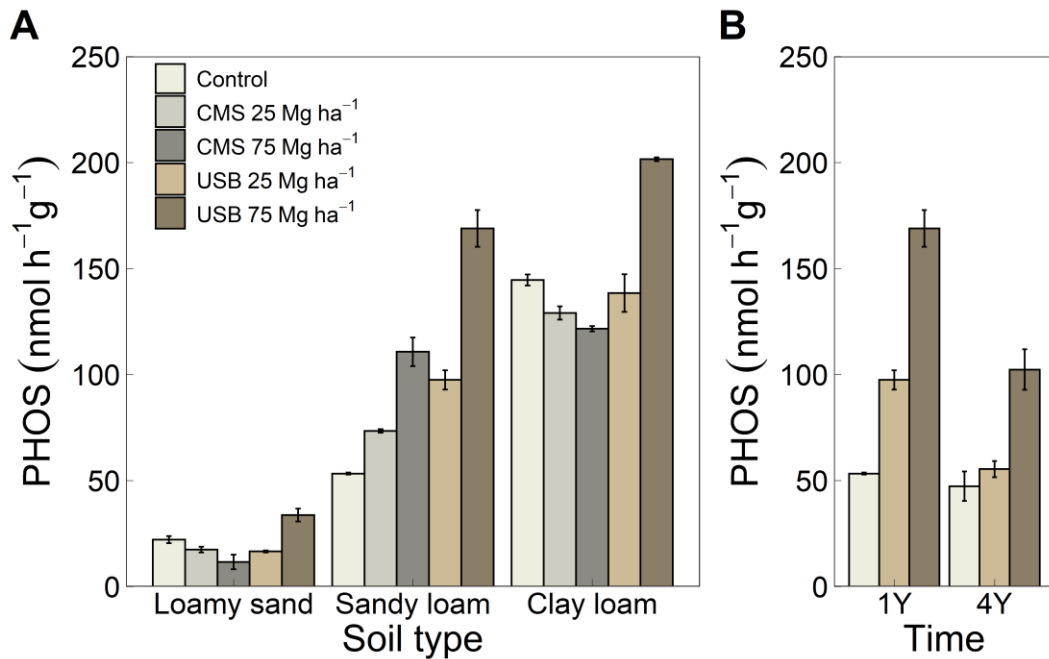


Figure S2.2 Means \pm (SE) of potential enzyme activity rates related to P acquisition across different soil textures in our one-year samples (A) and one-year (1Y) versus four-year (4Y) field exposure of USB biochar in sandy loam soils (B) with different biochar treatments indicated by varied colors.

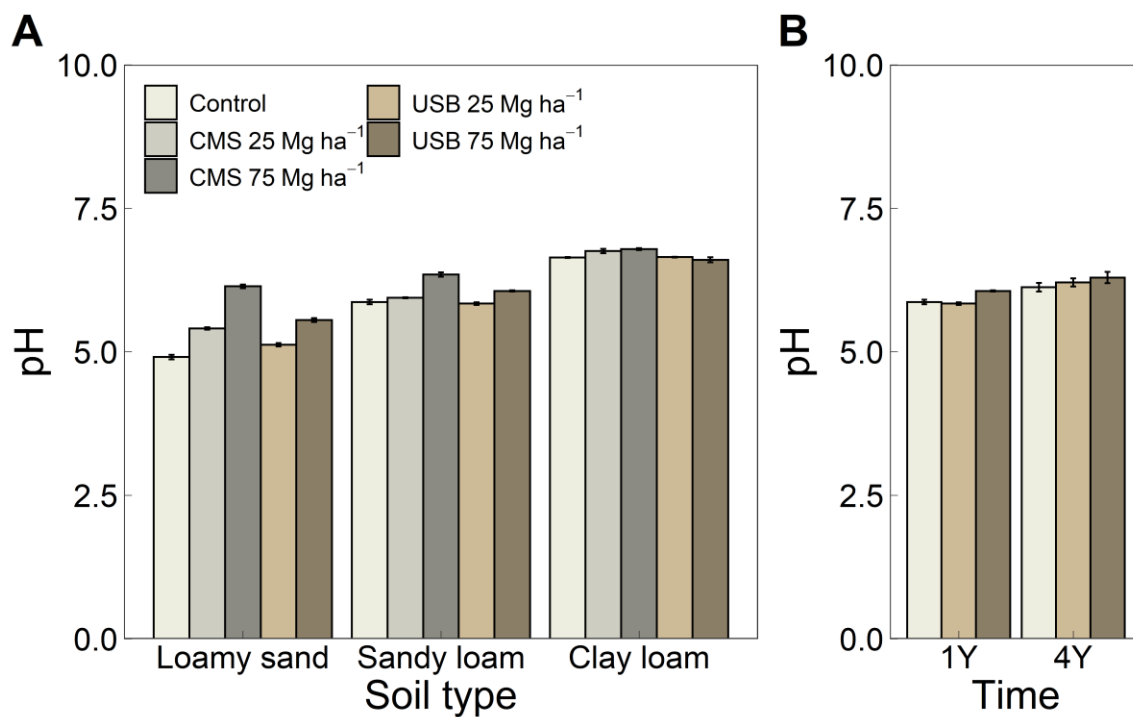


Figure S2.3 Means ± (SE) of soil pH across different soil textures in our one-year samples (A) and one-year (1Y) versus four-year (4Y) field exposure of USB biochar in sandy loam soils (B) with different biochar treatments indicated by varied colors.

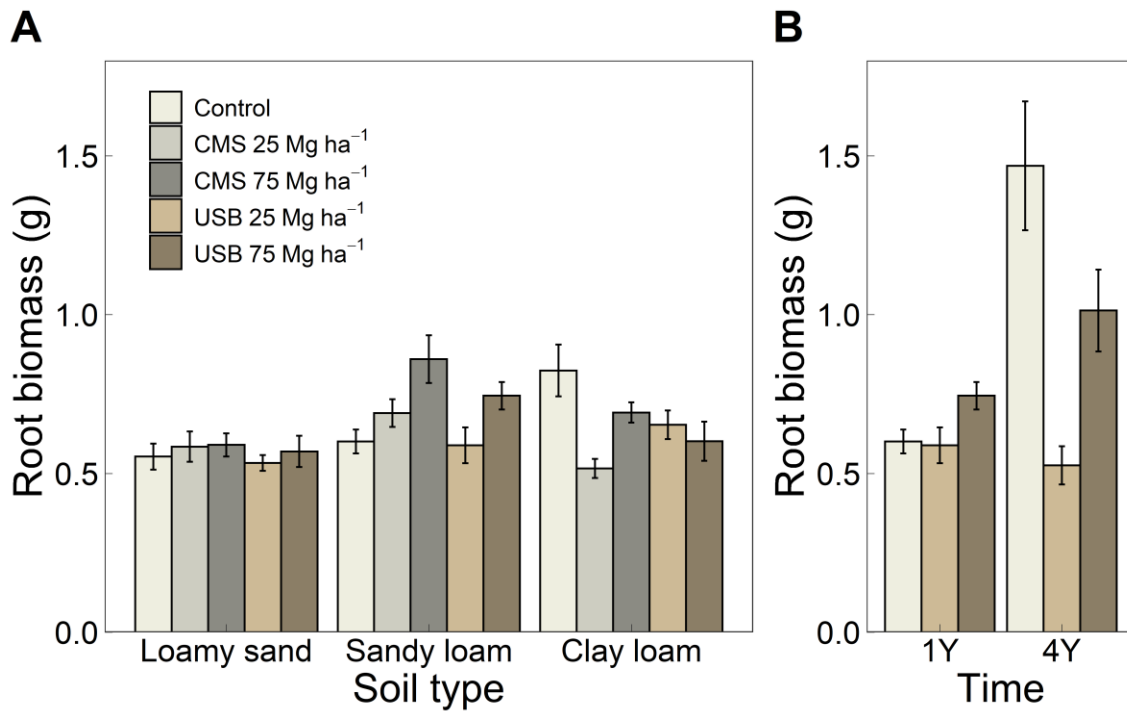


Figure S2.4 Means ± (SE) of root biomass across different soil textures in our one-year samples (A) and one-year (1Y) versus four-year (4Y) field exposure of USB biochar in sandy loam soils (B) with different biochar treatments indicated by varied colors.

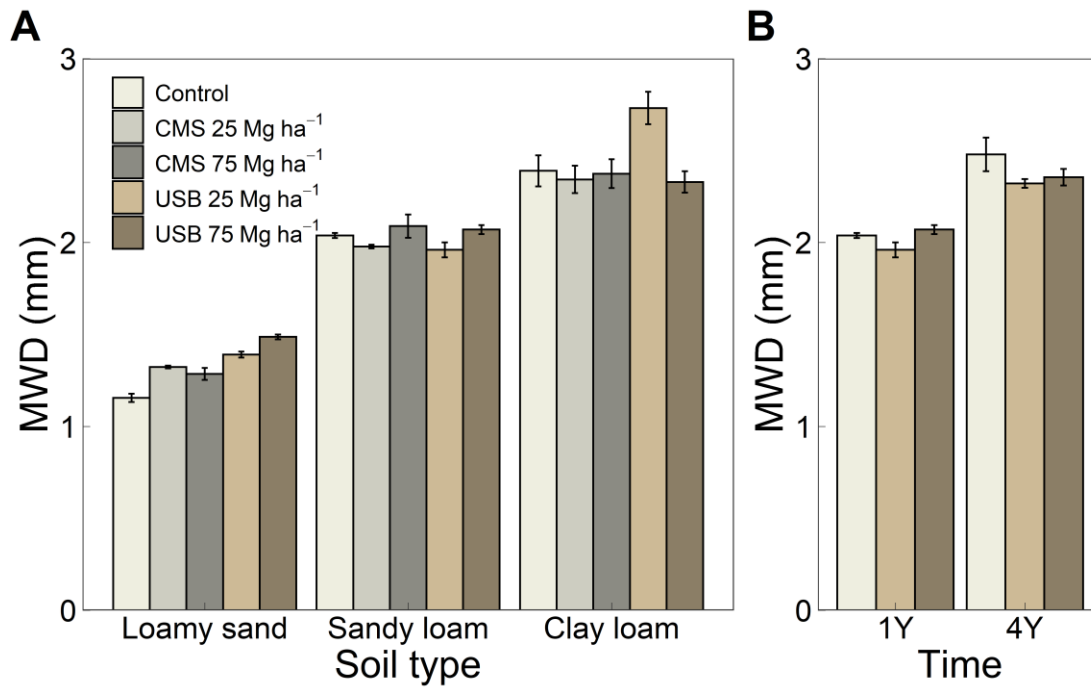


Figure S2.5 Means \pm (SE) of aggregate mean weight diameter (mm) (MWD) across different soil textures in our one-year samples (A) and one-year (1Y) versus four-year (4Y) field exposure of USB biochar in sandy loam soils (B) with different biochar treatments indicated by varied colors.

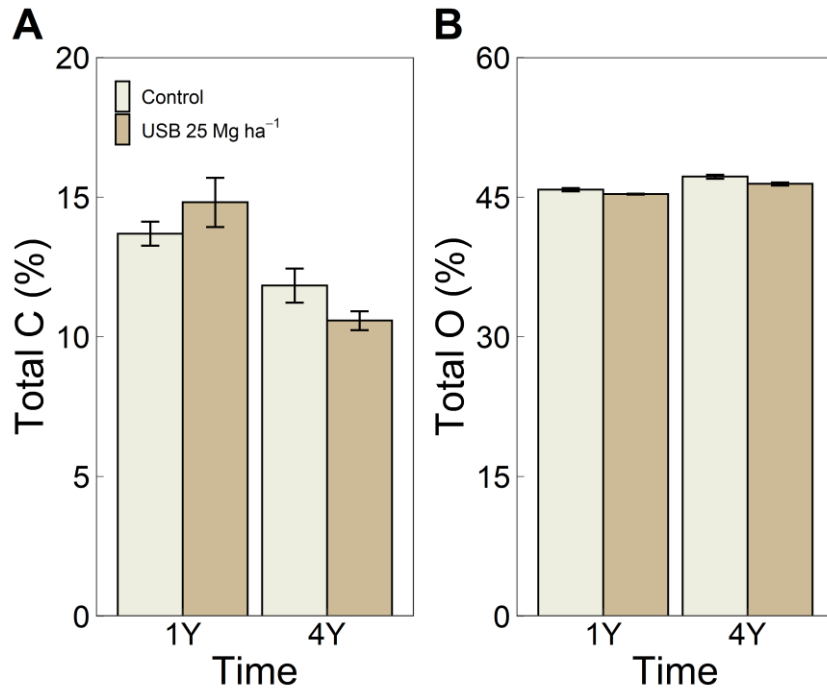
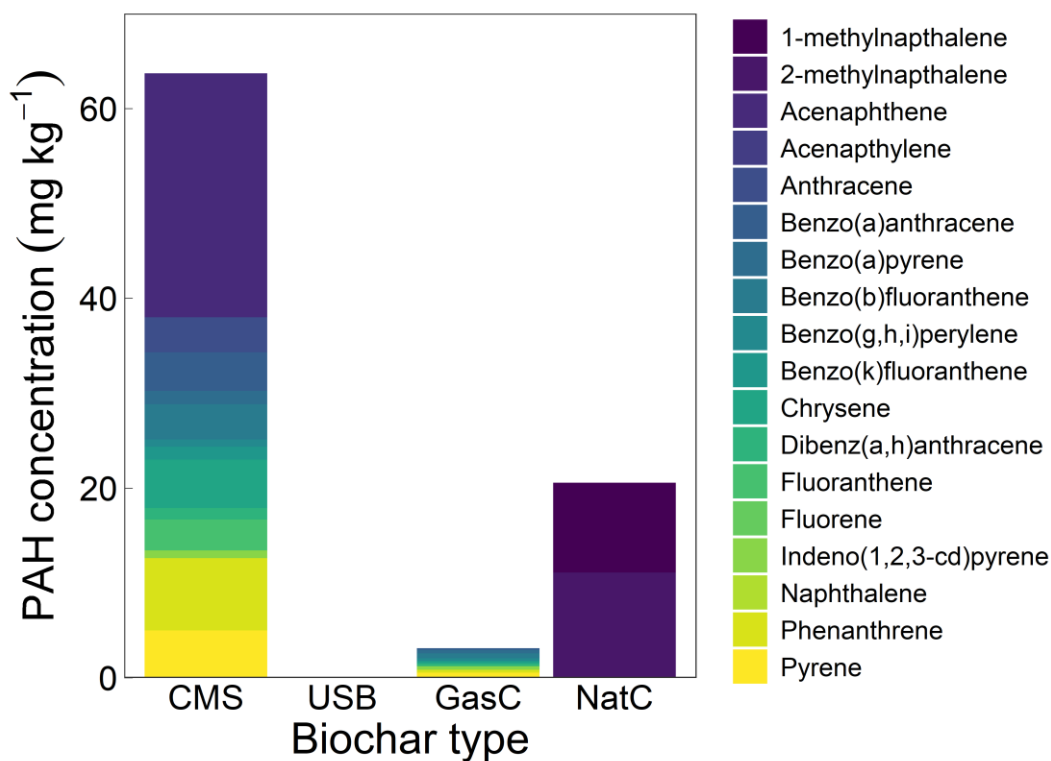
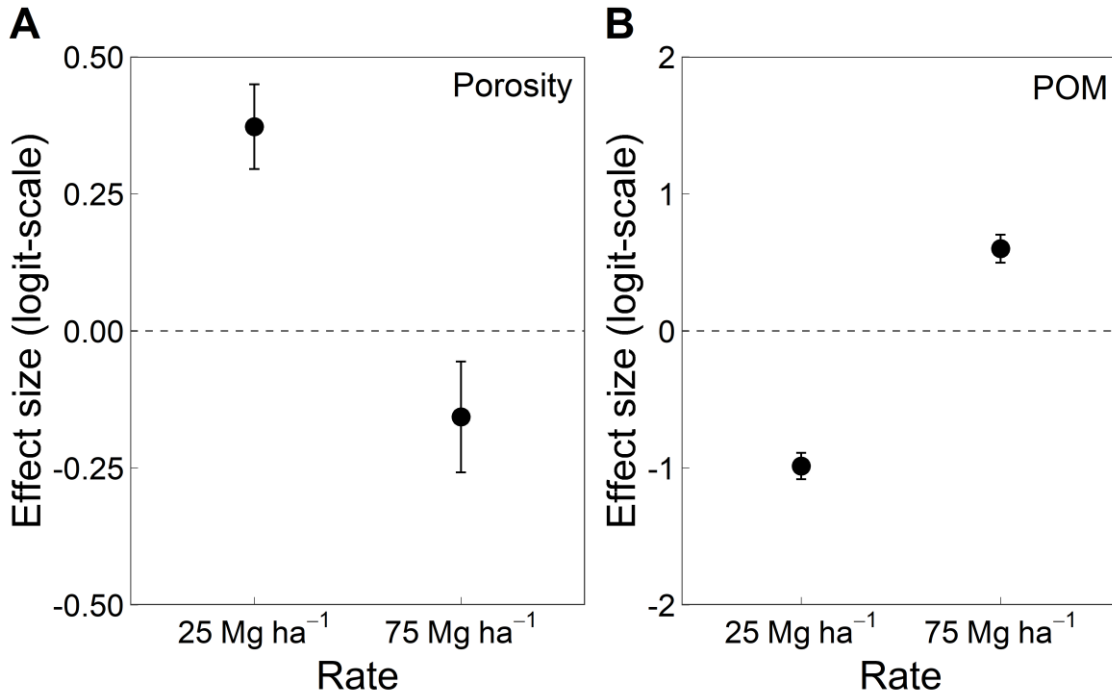


Figure S2.6 Means ± (SE) of total C (%) (A) and total O (%) (B) on aggregate (> 2 mm) surfaces for one-year (1Y) and four-samples (4Y) in the sandy loam. Biochar treatments are indicated by colors.



Figures S2.7 Poly-aromatic hydrocarbons present in CMS, USB and two other biochars.

Biochars were tested for the 16 priority pollutant PAHs and 1-methylnaphthalene and 2-methylnaphthalene. GasC was a gasification biochar (~700°C) and NatC was a biochar produced from a natural fire. USB did test positive for 2-methylnaphthalene, however the concentration was so low (0.0316 mg kg⁻¹) it's not visible on the figure.



Figures S2.8 Effect size (\pm SE) of application rate on soil porosity (A) and total soil POM (B) for intact four-year samples (preliminary data). Application rates are shown across the x-axis with a dotted line at 0 showing the difference from the control treatment (no biochar). Effect sizes are depicted on the logit-scale (beta distribution). Both measurements are taken from soil cores (5 cm diameter \times 15 cm height) using Xray μ CT scanning, thus they estimate porosity and POM from images and differ from lab-based measurements due to pores smaller than the resolution not being accounted for.

Table S2.1 FTIR-DRIFT spectral regions identified from Calderón et al., 2013 for quantifying SOM composition. We gave each region a name (e.g., W1, W2, etc.) for figure simplicity, however due to absorbance issues we only used regions W1, W3, and W4 (bolded) in this thesis to create aromatic to aliphatic C ratios (i.e., W3:W1, W4:W1) (Demyan et al., 2012).

Name	Wavenumber (cm ⁻¹)	Assignment
W1	2930-2870	Stretching C-H
W2	1698-1720	Carboxylic acid
W3	1625-1670	Amide I or phenyl ring stretching C=C, stretching C=O of amide groups and nucleic acids, carboxyl
W4	1570-1600	Ring stretching C=C of phenyl, carboxylate stretching C=O
W5	1480-1560	Amide II band stretching C-N and bending C-N-H, also bending CH in phenyl rings
W6	1400-1450	Bending (CH ₂) in polysaccharides and proteins, also N-H and stretching C-N
W7	1220-1320	Amide III band
W8	1148-1170	C=O
W9	1035-1088	Bending C-O in carbohydrates

REFERENCES

REFERENCES

- Ameloot, N., Sleutel, S., Das, K. C., Kanagaratnam, J., and de Neve, S. (2015). Biochar amendment to soils with contrasting organic matter level: Effects on N mineralization and biological soil properties. *GCB Bioenergy* 7, 135–144. doi:10.1111/gcbb.12119.
- Amelung, W., and Zech, W. (1996). Organic species in ped surface and core fractions along a climosequence in the prairie, North America. *Geoderma* 74, 193–206. doi:10.1016/S0016-7061(96)00063-8.
- Andersson, G., and Gahnstrom, G. (1985). Effects of pH on release and sorption of dissolved substances in sediment-water microcosms. *Ecol. Bull.* 37, 301–318. doi: <https://www.jstor.org/stable/20112960>.
- Angst, G., Mueller, K. E., Kögel-Knabner, I., Freeman, K. H., and Mueller, C. W. (2017). Aggregation controls the stability of lignin and lipids in clay-sized particulate and mineral associated organic matter. *Biogeochemistry* 132, 307–324. doi:10.1007/s10533-017-0304-2.
- Antonangelo, J. A., Zhang, H., Sun, X., and Kumar, A. (2019). Physicochemical properties and morphology of biochars as affected by feedstock sources and pyrolysis temperatures. *Biochar* 1, 325–336. doi:10.1007/s42773-019-00028-z.
- Balesdent, J., Mariotti, A., and Guillet, B. (1987). Natural ¹³C abundance as a tracer for studies of soil organic matter dynamics. *Soil Biol. Biochem.* 19, 25–30. doi:10.1016/0038-0717(87)90120-9.
- Balesdent, J., Pétraud, J.-P., and Feller, C. (1991). Effets des ultrasons sur la distribution granulométrique des matières organiques des sols. *Sci. du sol* 29, 95–106. {hal-02714823}
- Bird, J. A., Herman, D. J., and Firestone, M. K. (2011). Rhizosphere priming of soil organic matter by bacterial groups in a grassland soil. *Soil Biol. Biochem.* 43, 718–725. doi:10.1016/j.soilbio.2010.08.010.
- Bol, R., Amelung, W., and Friedrich, C. (2004). Role of aggregate surface and core fraction in the sequestration of carbon from dung in a temperate grassland soil. *Eur. J. Soil Sci.* 55, 71–77. doi:10.1046/j.1365-2389.2003.00582.x.
- Brodowski, S., Amelung, W., Haumaier, L., Abetz, C., and Zech, W. (2005). Morphological and chemical properties of black carbon in physical soil fractions as revealed by scanning electron microscopy and energy-dispersive X-ray spectroscopy. *Geoderma* 128, 116–129. doi:10.1016/j.geoderma.2004.12.019.

- Brodowski, S., John, B., Flessa, H., and Amelung, W. (2006). Aggregate-occluded black carbon in soil. *Eur. J. Soil Sci.* 57, 539–546. doi:10.1111/j.1365-2389.2006.00807.x.
- Bünemann, E. K., Bongiorno, G., Bai, Z., Creamer, R. E., De Deyn, G., de Goede, R., et al. (2018). Soil quality – A critical review. *Soil Biol. Biochem.* 120, 105–125. doi:10.1016/j.soilbio.2018.01.030.
- Burgeon, V., Fouché, J., Leifeld, J., Chenu, C., and Cornélis, J. T. (2021). Organo-mineral associations largely contribute to the stabilization of century-old pyrogenic organic matter in cropland soils. *Geoderma* 388, 1-14. doi:10.1016/j.geoderma.2020.114841.
- Calderón, F., Haddix, M., Conant, R., Magrini-Bair, K., and Paul, E. (2013). Diffuse-Reflectance Fourier-Transform Mid-Infrared Spectroscopy as a Method of Characterizing Changes in Soil Organic Matter. *Soil Sci. Soc. Am. J.* 77, 1591–1600. doi:10.2136/sssaj2013.04.0131.
- Chen, K., Peng, J., Li, J., Yang, Q., Zhan, X., Liu, N., et al. (2020). Stabilization of soil aggregate and organic matter under the application of three organic resources and biochar-based compound fertilizer. *J. Soils Sediments* 20, 3633–3643. doi:10.1007/s11368-020-02693-1.
- Cheng, H., Hill, P. W., Bastami, M. S., and Jones, D. L. (2017). Biochar stimulates the decomposition of simple organic matter and suppresses the decomposition of complex organic matter in a sandy loam soil. *GCB Bioenergy* 9, 1110–1121. doi:10.1111/gcbb.12402.
- Clark, M., Hastings, M. G., and Ryals, R. (2019). Soil Carbon and Nitrogen Dynamics in Two Agricultural Soils Amended with Manure-Derived Biochar. *J. Environ. Qual.* 48, 727–734. doi:10.2134/jeq2018.10.0384.
- Cotrufo, M. F., Soong, J. L., Horton, A. J., Campbell, E. E., Haddix, M. L., Wall, D. H., et al. (2015). Formation of soil organic matter via biochemical and physical pathways of litter mass loss. *Nat. Geosci.* 8, 776–779. doi:10.1038/ngeo2520.
- de la Rosa, J. M., Rosado, M., Paneque, M., Miller, A. Z., and Knicker, H. (2018). Effects of aging under field conditions on biochar structure and composition: Implications for biochar stability in soils. *Sci. Total Environ.* 613–614, 969–976. doi:10.1016/j.scitotenv.2017.09.124.
- Demyan, M. S., Rasche, F., Schulz, E., Breulmann, M., Müller, T., and Cadisch, G. (2012). Use of specific peaks obtained by diffuse reflectance Fourier transform mid-infrared spectroscopy to study the composition of organic matter in a Haplic Chernozem. *Eur. J. Soil Sci.* 63, 189–199. doi:10.1111/j.1365-2389.2011.01420.x.
- Diacono, M., and Montemurro, F. (2010). Long-term effects of organic amendments on soil fertility. A review. *Agron. Sustain. Dev.* 30, 401–422. doi:10.1051/agro/2009040.

- Du, Z. L., Zhao, J. K., Wang, Y. D., and Zhang, Q. Z. (2017). Biochar addition drives soil aggregation and carbon sequestration in aggregate fractions from an intensive agricultural system. *J. Soils Sediments* 17, 581–589. doi:10.1007/s11368-015-1349-2.
- Dungait, J. A. J., Hopkins, D. W., Gregory, A. S., and Whitmore, A. P. (2012). Soil organic matter turnover is governed by accessibility not recalcitrance. *Glob. Chang. Biol.* 18, 1781–1796. doi:10.1111/j.1365-2486.2012.02665.x.
- Dutta, T., Kwon, E., Bhattacharya, S. S., Jeon, B. H., Deep, A., Uchimiya, M., et al. (2017). Polycyclic aromatic hydrocarbons and volatile organic compounds in biochar and biochar-amended soil: a review. *GCB Bioenergy* 9, 990–1004. doi:10.1111/gcbb.12363.
- Fang, Y., Singh, B. P., Yu, L., Boersma, M., and Zwieten, L. V. (2018). Biochar carbon dynamics in physically separated fractions and microbial use efficiency in contrasting soils under temperate pastures. *Soil Biol. Biochem.* 116, 399–409. doi:10.1016/j.soilbio.2017.10.042.
- Fang, Y., Singh, B., and Singh, B. P. (2015). Effect of temperature on biochar priming effects and its stability in soils. *Soil Biol. Biochem.* 80, 136–145. doi:10.1016/j.soilbio.2014.10.006.
- Fang, Y., Singh, B., Singh, B. P., and Krull, E. (2014). Biochar carbon stability in four contrasting soils. *Eur. J. Soil Sci.* 65, 60–71. doi:10.1111/ejss.12094.
- Feng, Z., Fan, Z., Song, H., Li, K., Lu, H., Liu, Y., et al. (2021). Biochar induced changes of soil dissolved organic matter: The release and adsorption of dissolved organic matter by biochar and soil. *Sci. Total Environ.* 783, 1-8. doi:10.1016/j.scitotenv.2021.147091.
- Fidel, R. B., Laird, D. A., and Spokas, K. A. (2018). Sorption of ammonium and nitrate to biochars is electrostatic and pH-dependent. *Sci. Rep.* 8, 1–10. doi:10.1038/s41598-018-35534-w.
- Fu, P., Hu, S., Xiang, J., Sun, L., Yang, T., Zhang, A., et al. (2009). Effects of pyrolysis temperature on characteristics of porosity in biomass chars. *2009 Int. Conf. Energy Environ. Technol. ICEET 2009* 1, 109–112. doi:10.1109/ICEET.2009.33.
- Gao, S., DeLuca, T. H., and Cleveland, C. C. (2019). Biochar additions alter phosphorus and nitrogen availability in agricultural ecosystems: A meta-analysis. *Sci. Total Environ.* 654, 463–472. doi:10.1016/j.scitotenv.2018.11.124.
- Ge, Z., Fang, S., Chen, H. Y. H., Zhu, R., Peng, S., and Ruan, H. (2018). Soil aggregation and organic carbon dynamics in poplar plantations. *Forests* 9, 1–15. doi:10.3390/f9090508.
- Goh, K. M. (2004). Carbon sequestration and stabilization in soils: Implications for soil productivity and climate change. *Soil Sci. Plant Nutr.* 50, 467–476. doi:10.1080/00380768.2004.10408502.

- Gul, S., Whalen, J. K., Thomas, B. W., Sachdeva, V., and Deng, H. (2015). Physico-chemical properties and microbial responses in biochar-amended soils: Mechanisms and future directions. *Agric. Ecosyst. Environ.* 206, 46–59. doi:10.1016/j.agee.2015.03.015.
- Hernandez-Soriano, M. C., Kerré, B., Kopittke, P. M., Horemans, B., and Smolders, E. (2016). Biochar affects carbon composition and stability in soil: A combined spectroscopy-microscopy study. *Sci. Rep.* 6, 1–13. doi:10.1038/srep25127.
- Hilber, I., Bastos, A. C., Loureiro, S., Soja, G., Marsz, A., Cornelissen, G., et al. (2017). The different faces of biochar: contamination risk versus remediation tool. *J. Environ. Eng. Landsc. Manag.* 25, 86–104. doi:10.3846/16486897.2016.1254089.
- Hussain, M. Z., Robertson, G. P., Basso, B., and Hamilton, S. K. (2020). Leaching losses of dissolved organic carbon and nitrogen from agricultural soils in the upper US Midwest. *Sci. Total Environ.* 734, 139379. doi:10.1016/j.scitotenv.2020.139379.
- Janssen, B. H. (1996). Nitrogen mineralization in relation to C:N ratio and decomposability of organic materials. *Plant Soil* 181, 39–45. doi:https://doi.org/10.1007/978-94-011-5450-5_13.
- Jastrow, J. D., Boutton, T. W., and Miller, R. M. (1996). Carbon Dynamics of Aggregate-Associated Organic Matter Estimated by Carbon-13 Natural Abundance. *Soil Sci. Soc. Am. J.* 60, 801–807. doi: 10.2136/sssaj1996.03615995006000030017x.
- Jeffery, S., Verheijen, F. G. A., van der Velde, M., and Bastos, A. C. (2011). A quantitative review of the effects of biochar application to soils on crop productivity using meta-analysis. *Agric. Ecosyst. Environ.* 144, 175–187. doi:10.1016/j.agee.2011.08.015.
- Kasozi, G. N., Zimmerman, A. R., Nkedi-Kizza, P., and Gao, B. (2010). Catechol and humic acid sorption onto a range of laboratory-produced black carbons (biochars). *Environ. Sci. Technol.* 44, 6189–6195. doi:10.1021/es1014423.
- Keiluweit, M., Nico, P. S., Johnson, M., and Kleber, M. (2010). Dynamic molecular structure of plant biomass-derived black carbon (biochar). *Environ. Sci. Technol.* 44, 1247–1253. doi:10.1021/es9031419.
- Kopittke, P. M., Dalal, R. C., Hoeschen, C., Li, C., Menzies, N. W., and Mueller, C. W. (2020). Soil organic matter is stabilized by organo-mineral associations through two key processes: The role of the carbon to nitrogen ratio. *Geoderma* 357, 1-9. doi:10.1016/j.geoderma.2019.113974.
- Kravchenko, A. N., Guber, A. K., Razavi, B. S., Koestel, J., Quigley, M. Y., Robertson, G. P., et al. (2019). Microbial spatial footprint as a driver of soil carbon stabilization. *Nat. Commun.* 10, 1–10. doi:10.1038/s41467-019-11057-4.

- Kuzyakov, Y., Friedel, J. K., and Stahr, K. (2000). Review of mechanisms and quantification of priming effects. *Soil Biol. Biochem.* 32, 1485–1498. doi:10.1016/S0038-0717(00)00084-5.
- Laghari, M., Mirjat, M. S., Hu, Z., Fazal, S., Xiao, B., Hu, M., et al. (2015). Effects of biochar application rate on sandy desert soil properties and sorghum growth. *Catena* 135, 313–320. doi:10.1016/j.catena.2015.08.013.
- Lal, R. (2009). Challenges and opportunities in soil organic matter research. *Eur. J. Soil Sci.* 60, 158–169. doi:10.1111/j.1365-2389.2008.01114.x.
- Lal, R. (2016). Soil health and carbon management. *Food Energy Secur.* 5, 212–222. doi:10.1002/fes3.96.
- Lavallee, J. M., Conant, R. T., Haddix, M. L., Follett, R. F., Bird, M. I., and Paul, E. A. (2019). Selective preservation of pyrogenic carbon across soil organic matter fractions and its influence on calculations of carbon mean residence times. *Geoderma* 354. doi:10.1016/j.geoderma.2019.07.024.
- Lawrinenko, M., and Laird, D. A. (2015). Anion exchange capacity of biochar. *Green Chem.* 17, 4628–4636. doi:10.1039/c5gc00828j.
- Lehmann, J., Gaunt, J., and Rondon, M. (2006). Bio-char sequestration in terrestrial ecosystems - A review. *Mitig. Adapt. Strateg. Glob. Chang.* 11, 403–427. doi:10.1007/s11027-005-9006-5.
- Lehmann, J., Hansel, C. M., Kaiser, C., Kleber, M., Maher, K., Manzoni, S., et al. (2020). Persistence of soil organic carbon caused by functional complexity. *Nat. Geosci.* 13, 529–534. doi:10.1038/s41561-020-0612-3.
- Lehmann, J., and Kleber, M. (2015). The contentious nature of soil organic matter. *Nature* 528, 60–68. doi:10.1038/nature16069.
- Lehmann, J., Silva Jr, J. P., Steiner, C., Nehls, T., Zech, W., and Glaser, B. (2003). Nutrient availability and leaching an an archaeological Anthrosol and a Ferralsol. *Plant Soil* 249, 343–357. doi: 10.1023/A:1022833116184.
- Lentz, R. D., Ippolito, J. A., and Spokas, K. A. (2014). Biochar and Manure Effects on Net Nitrogen Mineralization and Greenhouse Gas Emissions from Calcareous Soil under Corn. *Soil Sci. Soc. Am. J.* 78, 1641–1655. doi:10.2136/sssaj2014.05.0198.
- Liang, B., Lehmann, J., Solomon, D., Kinyangi, J., Grossman, J., O’Neill, B., et al. (2006). Black Carbon Increases Cation Exchange Capacity in Soils. *Soil Sci. Soc. Am. J.* 70, 1719–1730. doi:10.2136/sssaj2005.0383.

- Liang, B., Lehmann, J., Solomon, D., Sohi, S., Thies, J. E., Skjemstad, J. O., et al. (2008). Stability of biomass-derived black carbon in soils. *Geochim. Cosmochim. Acta* 72, 6069–6078. doi:10.1016/j.gca.2008.09.028.
- Liu, Z., Demisie, W., and Zhang, M. (2013). Simulated degradation of biochar and its potential environmental implications. *Environ. Pollut.* 179, 146–152. doi:10.1016/j.envpol.2013.04.030.
- Lu, T., Yuan, H., Wang, Y., Huang, H., and Chen, Y. (2016). Characteristic of heavy metals in biochar derived from sewage sludge. *J. Mater. Cycles Waste Manag.* 18, 725–733. doi:10.1007/s10163-015-0366-y.
- Luo, L., and Gu, J. D. (2016). Alteration of extracellular enzyme activity and microbial abundance by biochar addition: Implication for carbon sequestration in subtropical mangrove sediment. *J. Environ. Manage.* 182, 29–36. doi:10.1016/j.jenvman.2016.07.040.
- Luo, X., Chen, L., Zheng, H., Chang, J., Wang, H., Wang, Z., et al. (2016). Biochar addition reduced net N mineralization of a coastal wetland soil in the Yellow River Delta, China. *Geoderma* 282, 120–128. doi:10.1016/j.geoderma.2016.07.015.
- Lützw, M. V., Kögel-Knabner, I., Ekschmitt, K., Matzner, E., Guggenberger, G., Marschner, B., et al. (2006). Stabilization of organic matter in temperate soils: Mechanisms and their relevance under different soil conditions - A review. *Eur. J. Soil Sci.* 57, 426–445. doi:10.1111/j.1365-2389.2006.00809.x.
- Maestrini, B., Nannipieri, P., and Abiven, S. (2015). A meta-analysis on pyrogenic organic matter induced priming effect. *GCB Bioenergy* 7, 577–590. doi:10.1111/gcbb.12194.
- Major, J., Lehmann, J., Rondon, M., and Goodale, C. (2010). Fate of soil-applied black carbon: Downward migration, leaching and soil respiration. *Glob. Chang. Biol.* 16, 1366–1379. doi:10.1111/j.1365-2486.2009.02044.x.
- Mobley, M. L., McCulley, R. L., Burke, I. C., Peterson, G., Schimel, D. S., Cole, C. V., et al. (2014). Grazing and No-Till Cropping Impacts on Nitrogen Retention in Dryland Agroecosystems. *J. Environ. Qual.* 43, 1963–1971. doi:10.2134/jeq2013.12.0530.
- Nash, J. A., Miesel, J.R., Bonito, G.M., Sakalidis, M.L., Ren, H., Warnock, D., Tiemann, L.K. (2021). Biochar restructures plant-soil-microbe relationships in a woody cropping system. *Soil Sci. Soc. Am. J.*, 1-21. doi: 10.1002/saj2.20334.
- Nelissen, V., Rütting, T., Huygens, D., Ruyschaert, G., and Boeckx, P. (2015). Temporal evolution of biochar's impact on soil nitrogen processes - a ¹⁵N tracing study. *GCB Bioenergy* 7, 635–645. doi:10.1111/gcbb.12156.

- NRCS (2021). Web Soil Survey. USDA Natural Resources Conservation Service, Washington, DC. Available at: websoilsurvey.nrcs.usda.gov/ (accessed 10 May 2021).
- Obia, A., Mulder, J., Martinsen, V., Cornelissen, G., and Børresen, T. (2016). *In situ* effects of biochar on aggregation, water retention and porosity in light-textured tropical soils. *Soil Tillage Res.* 155, 35–44. doi:10.1016/j.still.2015.08.002.
- Paetsch, L., Mueller, C. W., Rumpel, C., Angst, Š., Wiesheu, A. C., Girardin, C., et al. (2017). A multi-technique approach to assess the fate of biochar in soil and to quantify its effect on soil organic matter composition. *Org. Geochem.* 112, 177–186. doi:10.1016/j.orggeochem.2017.06.012.
- Pandit, N. R., Mulder, J., Hale, S. E., Martinsen, V., Schmidt, H. P., and Cornelissen, G. (2018). Biochar improves maize growth by alleviation of nutrient stress in a moderately acidic low-input Nepalese soil. *Sci. Total Environ.* 625, 1380–1389. doi:10.1016/j.scitotenv.2018.01.022.
- Piash, M. I., Iwabuchi, K., Itoh, T., and Uemura, K. (2021). Release of essential plant nutrients from manure- and wood-based biochars. *Geoderma* 397, 1–12. doi:10.1016/j.geoderma.2021.115100.
- Plaza, C., Courtier-Murias, D., Fernández, J. M., Polo, A., and Simpson, A. J. (2013). Physical, chemical, and biochemical mechanisms of soil organic matter stabilization under conservation tillage systems: A central role for microbes and microbial by-products in C sequestration. *Soil Biol. Biochem.* 57, 124–134. doi:10.1016/j.soilbio.2012.07.026.
- Plaza, C., Giannetta, B., Fernández, J. M., López-de-Sá, E. G., Polo, A., Gascó, G., et al. (2016). Response of different soil organic matter pools to biochar and organic fertilizers. *Agric. Ecosyst. Environ.* 225, 150–159. doi:10.1016/j.agee.2016.04.014.
- Poeplau, C., Don, A., Six, J., Kaiser, M., Benbi, D., Chenu, C., et al. (2018). Isolating organic carbon fractions with varying turnover rates in temperate agricultural soils – A comprehensive method comparison. *Soil Biol. Biochem.* 125, 10–26. doi:10.1016/j.soilbio.2018.06.025.
- Quilliam, R. S., Rangecroft, S., Emmett, B. A., Deluca, T. H., and Jones, D. L. (2013). Is biochar a source or sink for polycyclic aromatic hydrocarbon (PAH) compounds in agricultural soils? *GCB Bioenergy* 5, 96–103. doi:10.1111/gcbb.12007.
- Robertson, G. P., and Groffman, P. M. (2006). "Nitrogen Transformations" in *Soil Microbiology, Ecology and Biochemistry*. Third Edition. Amsterdam: Elsevier Inc. doi:10.1016/b978-0-12-415955-6.00014-1.

- Robertson, G. P., Groffman, P. M., Blair, J. M., Holland, E. A., and Harris, D. (1999). *Standard Soil Methods for Long-term Ecological Research*. First Edition. Oxford: Oxford University Press.
- Saiya-Cork, K., Sinsabaugh, R., Zak, D. (2002). The effects of long term nitrogen deposition on extracellular enzyme activity in an *Acer saccharum* forest soil. *Soil Biol. Biochem.* 34: 1309-1315. doi: 10.1016/S0038-0717(02)00074-3.
- Sarkar, B., Singh, M., Mandal, S., Churchman, G. J., and Bolan, N. S. (2018). "Clay minerals-organic matter interactions in relation to carbon stabilization in soils." in *The Future of Soil Carbon: its conservation and formation*. Amsterdam: Elsevier Inc. doi:10.1016/B978-0-12-811687-6.00003-1.
- Sarkhot, D. V., Ghezzehei, T. A., and Berhe, A. A. (2013). Effectiveness of Biochar for Sorption of Ammonium and Phosphate from Dairy Effluent. *J. Environ. Qual.* 42, 1545–1554. doi:10.2134/jeq2012.0482.
- Schimel, J. P., and Schaeffer, S. M. (2012). Microbial control over carbon cycling in soil. *Front. Microbiol.* 3, 1–11. doi:10.3389/fmicb.2012.00348.
- Schmidt, M. W. I., Torn, M. S., Abiven, S., Dittmar, T., Guggenberger, G., Janssens, I. A., et al. (2011). Persistence of soil organic matter as an ecosystem property. *Nature* 478, 49–56. doi:10.1038/nature10386.
- Singh, N., Abiven, S., Torn, M. S., and Schmidt, M. W. I. (2012). Fire-derived organic carbon in soil turns over on a centennial scale. *Biogeosciences* 9, 2847–2857. doi:10.5194/bg-9-2847-2012.
- Sinsabaugh, R. L., Reynolds, H., and Long, T. M. (2000). Rapid assay for amidohydrolase (urease) activity in environmental samples. *Soil Biol. Biochem.* 32, 2095–2097. doi:10.1016/S0038-0717(00)00102-4.
- Six, J., Conant, R. T., Paul, E. A., and Paustian, K. (2002). Stabilization mechanisms of SOM implications for C saturation of soils. *Plant Soil* 241, 155–176. doi:10.1023/A:1016125726789.
- Six, J., Elliott, E. T., and Paustian, K. (2000). Soil macroaggregate turnover and microaggregate formation: A mechanism for C sequestration under no-tillage agriculture. *Soil Biol. Biochem.* 32, 2099–2103. doi:10.1016/S0038-0717(00)00179-6.
- Smebye, A., Alling, V., Vogt, R. D., Gadmar, T. C., Mulder, J., Cornelissen, G., et al. (2016). Biochar amendment to soil changes dissolved organic matter content and composition. *Chemosphere* 142, 100–105. doi:10.1016/j.chemosphere.2015.04.087.

- Sohi, S., Lopez-Capel, E., Krull, E., and Bol, R. (2009). Biochar's roles in soil and climate change : A review to guide future research. *CSIRO L. Water Sci. Rep.* 1-56.
- Thibault, K., and Stewart, M. (2018). TOS protocol and procedure: plant belowground biomass sampling. NEON.DOC.014038G. NEON (National Ecological Observatory Network).
- Tiemann, L. K., Grandy, A. S., Atkinson, E. E., Marin-Spiotta, E., and Mcdaniel, M. D. (2015). Crop rotational diversity enhances belowground communities and functions in an agroecosystem. *Ecol. Lett.* 18, 761–771. doi:10.1111/ele.12453.
- Treseder, K. K. (2008). Nitrogen additions and microbial biomass: A meta-analysis of ecosystem studies. *Ecol. Lett.* 11, 1111–1120. doi:10.1111/j.1461-0248.2008.01230.x.
- U.S. Weather Service (2018). U.S. Climate Data. Available at: <https://www.usclimatedata.com/climate/lansing/michigan/united-states/usmi0477> (accessed 10 May 2021).
- Wallenstein, M. D., and Weintraub, M. N. (2008). Emerging tools for measuring and modeling the in situ activity of soil extracellular enzymes. *Soil Biol. Biochem.* 40, 2098–2106. doi:10.1016/j.soilbio.2008.01.024.
- Wang, D., Fonte, S. J., Parikh, S. J., Six, J., and Scow, K. M. (2017). Biochar additions can enhance soil structure and the physical stabilization of C in aggregates. *Geoderma* 303, 110–117. doi:10.1016/j.geoderma.2017.05.027.
- Wang, C., Wang, Y., and Herath, H. M. S. K. (2017). Polycyclic aromatic hydrocarbons (PAHs) in biochar – Their formation, occurrence and analysis: A review. *Org. Geochem.* 114, 1–11. doi:10.1016/j.orggeochem.2017.09.001.
- Wang, X., Song, D., Liang, G., Zhang, Q., Ai, C., and Zhou, W. (2015). Maize biochar addition rate influences soil enzyme activity and microbial community composition in a fluvo-aquic soil. *Appl. Soil Ecol.* 96, 265–272. doi:10.1016/j.apsoil.2015.08.018.
- Weil, R. R., and Brady, N. C. (2016). *The Nature and Properties of Soils*. 15th Edition. Columbus, OH: Pearson.
- Weng, Z. H., Van Zwieten, L., Singh, B. P., Tavakkoli, E., Joseph, S., Macdonald, L. M., et al. (2017). Biochar built soil carbon over a decade by stabilizing rhizodeposits. *Nat. Clim. Chang.* 7, 371–376. doi:10.1038/nclimate3276.
- Wittbrodt B.T., Squires D., Walbeck J., Campbell E., Campbell W., Pearce J.M. (2015). Open-source photometric system for enzymatic nitrate quantification. *Plos one.* 10(8): e0134989. doi: 10.1371/journal.pone.0134989.

- Xu, S., Chen, J., Peng, H., Leng, S., Li, H., Qu, W., et al. (2021). Effect of biomass type and pyrolysis temperature on nitrogen in biochar, and the comparison with hydrochar. *Fuel* 291, 1-11. doi:10.1016/j.fuel.2021.120128.
- Yang, F., Xu, Z., Huang, Y., Tsang, D. C. W., Ok, Y. S., Zhao, L., et al. (2021). Stabilization of dissolvable biochar by soil minerals: Release reduction and organo-mineral complexes formation. *J. Hazard. Mater.* 412, 125213. doi:10.1016/j.jhazmat.2021.125213.
- Zhang, Q., Du, Z. L., Lou, Y., and He, X. (2015). A one-year short-term biochar application improved carbon accumulation in large macroaggregate fractions. *Catena* 127, 26–31. doi:10.1016/j.catena.2014.12.009.
- Zhao, L., Zheng, W., and Cao, X. (2014). Distribution and evolution of organic matter phases during biochar formation and their importance in carbon loss and pore structure. *Chem. Eng. J.* 250, 240–247. doi:10.1016/j.cej.2014.04.053.
- Zheng, H., Wang, Z., Deng, X., Herbert, S., and Xing, B. (2013). Impacts of adding biochar on nitrogen retention and bioavailability in agricultural soil. *Geoderma* 206, 32–39. doi:10.1016/j.geoderma.2013.04.018.
- Zimmerman, A. R., Gao, B., and Ahn, M. (2011). Positive and negative carbon mineralization priming effects among a variety of biochar-amended soils. *Soil Biol. Biochem.* 43, 1169–1179. doi:10.1016/j.soilbio.2011.02.005.
- Zimmermann, M., Bird, M. I., Wurster, C., Saiz, G., Goodrick, I., Barta, J., et al. (2012). Rapid degradation of pyrogenic carbon. *Glob. Chang. Biol.* 18, 3306–3316. doi:10.1111/j.1365-2486.2012.02796.x.